UNIVERSITA' DEGLI STUDI DI MILANO-BICOCCA

SCUOLA DI DOTTORATO DI SCIENZE

Facoltà di Scienze Matematiche, Fisiche e Naturali

Corso di Dottorato di Ricerca in Scienze Chimiche XXIV ciclo

New tools in lignocellulosic chemistry

Tutor: Prof. Marco Orlandi

Anika Salanti

Dipartimento di Scienze dell'Ambiente e del Territorio

Anno Accademico 2011-2012

INDEX

INTRODUCTION

1. LIGNOCELLULOSE COMPONENTS INTEGRATION AND MOLECULAR STRUCTURE

2. BIOREFINERY

RESULTS AND DISCUSSION

5. RICE HUSK LIGNIN RECOVERY AND ITS EFFECT AS A FILLER ON THE THERMAL BEHAVIOUR OF POLY(3-HYDROXYBUTYRATE)-BASED BIOCOMPOSITE

6. ARCHAEOLOGICAL WATERLOGGED WOODS CHARACTERIZATION

EXPERIMENTAL SECTION

7. MATERIALS

8. EXTRACTION PROCEDURES

9. DERIVATIZATION PROCEDURES

10. METHODS

SUMMARY

THE PhD PROJECT

The PhD project is inserted within the broad field of lignocellulose chemical characterization and comprehensive utilization, as promoted by the biorefinery approach.

Lignocellulose is an extremely structurated natural material made up of three main biopolymers: cellulose, hemicellulose, and lignin. Cellulose consists of linear chains of β(1-4) linked D-glucopyranose units which, when found in cell wall, is difficult to break down into glucose because of its extensive inter- and intra-molecular H-bonded network and highly organized crystalline structure. Hemicellulose is a carbohydrate heteropolymer composed of several different sugars including five-carbon and six-carbon which is easily broken down into its building blocks. Lignin is a complex and irregular polymer network, composed of randomly cross-linked phenylpropanoid units, and acts as a glue holding cellulose and hemicellulose together.

The biorefinery concept is analogous to today's petroleum refinery that produces multiple fuels, power and chemical products from petroleum. Biorefinery systems generally work by processing a bio-based feedstock input to create fuel, chemicals, feed or power/heat as an output. Lignocellulose biorefinery generally includes three fundamental steps: first, a pretreatment to fractionate the recalcitrant lignocellulose structure; second, an enzymatic hydrolysis of the isolated cellulose moiety to obtain fermentable sugars; and third, the fermentation, to produce cellulosic ethanol or other bio-based chemicals. Because of the resistant structure of crystalline cellulose and natural composite structures of lignocellulosics, efficient pretreatment technologies are needed prior to the enzymatic hydrolysis.

The PhD project found its common thread in the development and application of an integrated analysis protocol - schematically reported below - that enclose different chromatographic and spectroscopic techniques, and the utilization of innovative solvent media (i.e., ionic liquids) for the

functionalization and subsequent chemical analysis of otherwise undetectable substrates such as unprocessed, native lignocellulose. This novel approach requires mild conditions for the derivatization reaction and leaves an overall unaltered substrate, thus avoiding any chemical and structural modification due to components extraction. The only harsh pretreatment required is several hours of milling, needed to reduce the particle size and cellulose crystallinity to help the ionic liquid to diffuse into the interior of the lignocellulose.

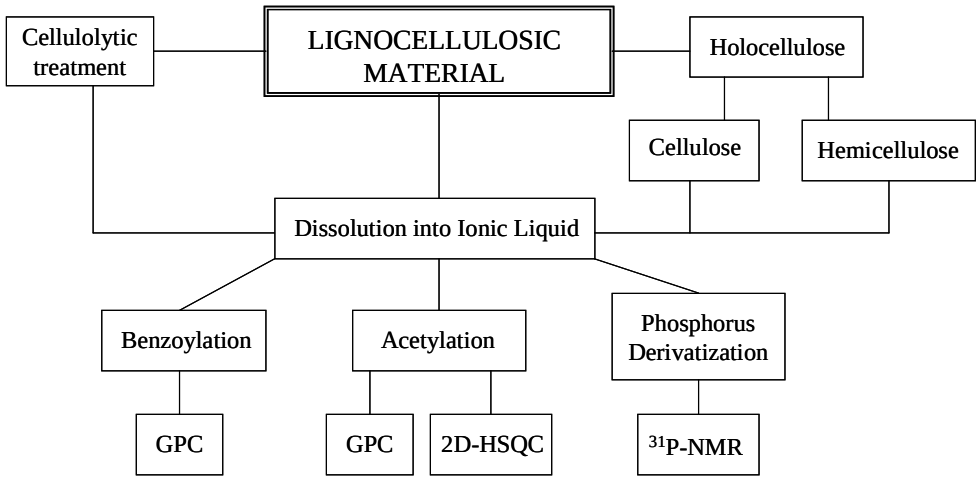

Summarizing, the PhD thesis is based on the following topics:

- ✓ Exhaustive chemical characterization of lignins extracted from different woody and herbaceous materials by chromatographic and spectroscopic analysis.
- ✓ Characterization of unprocessed lignocellulose substrates exploiting the striking solubilizing power of ionic liquids to obtain derivatized specimens subjectable to chromatographic and spectroscopic analysis.
- ✓ Detection of lignin-carbohydrate complexes in native herbaceous plants, again accomplished by solubilization in ionic liquid, appropriate functionalization, and subsequent chromatographic analysis.

- ✓ Optimization of the lignin extraction procedure from husk and its functionalization for the production of value-added fillers addressed to the preparation of novel biocomposites.
- ✓ Thermal, morphological and structural characterization of poly(3-hydroxybutyrate)-based biocomposites prepared by casting from chloroform solution of the polymer and different functionalized lignins.
- ✓ Assessment of the state of conservation of archaeological woods excavated from underwater shipwrecks.

During the PhD research, these different aspects were compenetrated and organized into three different projects, namely:

1. Annual plants: characterization and lignin-carbohydrate complexes detection.
2. Rice husk lignin recovery and its effect as a filler in the thermal behaviour of poly(3-hydroxybutyrate)-based biocomposites.
3. Archaeological waterlogged woods characterization.

The second project has been developed within a joined research activity of the University of Milano-Bicocca, the Italian Pulp and Paper Research Institute (SCCP, Milan) and ISMAC CNR (Milan).

General backgrounds and main conclusions of each topic are reported in the next sections.

Annual plants: characterization and lignin-carbohydrate complexes detection

Lignocellulosic substrates must be pretreated to improve enzymatic saccharification. Among many others, lignin has been shown to be a very influential factor, acting as both a physical barrier and limiting hydrolysis through the adsorption of cellulases. Lignin and related oligomeric and monomeric phenols are possibly found in the lignocellulose structure both as a polysaccharide-linked moiety and as free entity. Lignin is reckoned to be for the most part associated with hemicelluloses through covalent bonds. This type of association is known as lignin-carbohydrate complex (LCC). A number of different approaches have been proposed so far for lignocellulosic pretreatment aimed at the removal of lignin including biological, chemical, physical and thermal processes. However, all of them results in a substantial loss in fermentable sugar content of the residual polysaccharides.

In the last few years, the development of ionic liquids and their application as green solvents for the pretreatment and fractionation of lignocellulosic biomass led to an intensive research which proved the opportunity of selectively extract a chemically unaltered lignin and simultaneously yield an unaltered, highly biodegradable cellulose fraction. Nevertheless, the presence of LCCs could not be avoided due to their intrinsic nature, i.e., a covalent bond connecting a polysaccharide chain to a lignin moiety. Indeed, whereas a fairly large lignin fraction could definitely be solubilized and removed from the lignocellulosic substrate, polysaccharides are regenerated from the ionic liquid solution after the addition of an antisolvent such as water or ethanol. The opportunity for a plain investigation of the presence and amount of lignin-carbohydrate complexes (LCCs) in renewable feedstocks is therefore a major issue in the choice of the most appropriate pretretament.

This study is focused on the chromatographic characterization of lignocellulose from agricultural wastes (rice husk, wheat straw) and

herbaceous energy crops (*Arundo donax*, *Miscanthus sinesis*) and their fractionation products (hemicellulose, cellulose, and lignin). Exploiting alternative chemical derivatizations on the aforementioned samples, which resulted in different instrumental response when submitted for GPC-UV analysis, it was possible to discern the connectivity among the various lignocellulosic components. The acetylation and benzoylation of the milled native substrates in ionic liquid media, and the systematic comparison between their GPC-UV chromatograms has revealed itself as a straightforward technique in the detection of LCCs. Furthermore, the acetylation of the hemicellulosic fractions, along with the benzoylation of the cellulosic fractions in ionic liquid media as well, and the comparison between these molecular weight distributions as opposed to the corresponding chromatograms of functionalized unprocessed starting material, offered a valuable method for the assessment of the LCC-bound polysaccharide nature. Moreover, the method allowed to venture a purely qualitative evaluation of the LCCs molecular weight and composition in terms of hemicellulose to lignin ratio. This novel approach proved the presence of a more or less pronounced connectivity between lignin (or any other aromatic compounds) and the hemicellulosic fraction of the analyzed specimens, whereas the cellulosic fraction was conceived as a substantially unbound moiety, accounting for the sample composition at higher molecular weights.

Moreover, extracted lignin specimens were completely characterized by GPC, 2D-HSQC-NMR, and ^{31}P-NMR revealing a similar structure for all the four samples. It is worth highlighting that the enzymatic digestion of biomass for the production of biofuels leaves as byproduct a large amount of lignin. Therefore, such a similarity surely represents an important feature for a future large-scale production of bio-based chemicals from residual lignin.

Rice husk lignin recovery and its effect as a filler on the thermal behaviour of poly(3-hydroxybutyrate)-based biocomposites

(developed in collaboration with SCCP and ISMAC CNR)

With a production estimated in about 680 million tons/year (FAOSTAT Database, 2008), rice is probably the most important crop with regards to human nutrition worldwide. Rice husk, the outer cover of rice grain, is among the principal processing side-products and accounts for about 20% by weight of rice. Despite its widespread availability, industrial applications of rice husk lignin are rather limited, and it has been reckoned that only 1-2% of it is addressed to the development of innovative bio-based products, such as biocomposites. Biocomposites are novel materials obtained by compounding a biodegradable polymer with biodegradable fillers. In recent years, fillers from renewable source have been increasingly used in the preparation of PHB-based biocomposites. The presence of lignin gives particular properties to the composite: it can act as a stabilizer preventing polymer ageing due to its antioxidant activity, it is able to produce a large amount of char residue upon heating at elevated temperature in an inert atmosphere, a basic aspect of flame retardant additives, and it can also behave as a nucleating agent during the crystallization of different thermoplastic polymers and interfere on their supermolecular structure.

In this work different lignin extraction procedures were tested, but eventually only two of them - namely: acidolysis and alkaline enzymatic - were recognized as viable and thus exhaustively explored varying critical parameters in order to set the more straightforward and feasible extraction process. The lignins thus isolated were fully characterized by means of gravimetric, chromatographic (GPC) and spectroscopic (^{31}P-NMR, 2D-HSQC-NMR) analyses with the aim to define the best method with regard to yield, sample purity and optimal chemical and morphological properties, recognized as key parameters for biocomposites development.

Quantitative ^{31}P-NMR spectroscopy showed that rice husk lignin is mainly formed by guaiacyl and p-hydroxyphenyl units, not depending on the applied extraction procedure. Acidolysis lignin (AL) and alkaline-enzymatic lignin (AEL) specimens were further analyzed by 2D-HSQC-NMR spectroscopy to identify the principal intermonomeric bonds and to evaluate any significant differences in the two polyphenols connectivity. Comprehensively, spectroscopic analyses were consistent with an AEL sample still rich in carbohydrates, even after the cellulolytic treatment, and also containing a large amount of oxidized functionalities, originated either by cellulose degradation or lignin side chains oxidation (or both). The best results with regard to gravimetric analyses (yield, purity, ash) were identified in the AL sample, which showed an appreciable lignin recovery, high purity, a reduced carbohydrates fraction, and low ash content.

Subsequently, biocomposites of poly(3-hydroxybutyrate) (PHB) and acetylated acidolysis and alkaline-enzymatic lignin were prepared by casting from chloroform solution and thoroughly tested with the aim to establish a relationship between the biocomposite properties and the ligno-derivatives characteristics. Preliminary investigations by TGA and DSC showed that the interference on PHB thermal stability and crystallization behaviour was stronger for the AL sample than for the AEL one. Therefore, a second part of the study was dedicated to the structural and morphological characterization of PHB/AL composites and to the evaluation of the influence of various lignin contents on the thermal properties of PHB/AL composites. A decrease of PHB crystallization rate and an increase in thermal stability was observed as a function of the lignin amount in the PHB/AL biocomposite series. The morphological characterization pointed out the presence of AL particles having dimensions ranging from some tens of nm to some μm, confirming the accomplishment of an effective dispersion of the filler into the polymer

matrix to which the enhancement of the thermal stability of the composites could be ascribed.

Summarizing, the addition of AL causes a decrease of the overall crystallization rate and the spherulite radial growth of PHB. The depression of the crystallization rate was ascribed to the increased energy required for the transport of PHB macromolecules through the melt, caused by the presence of lignin domains.

Archaeological waterlogged woods characterization

Anaerobic erosion bacteria can slowly degrade waterlogged wood, causing a loss of cellulose and hemicellulose. During this process, lignin can also be altered. For this reason, the chemical characterization of waterlogged archaeological wood is crucial for both the elucidation of the degradation processes and also the development of consolidation and conservation procedures. The limit of the present approach is that the diagnostic of archaeological wooden objects is still based on lignin isolation which may result in some extent of chemical and structural modification, even if mild conditions are applied to the extraction procedure.

The complex structure of lignocellulose makes it practically impossible to dissolve wood in its native form in conventional molecular solvents. Ionic liquids can provide a homogenous reaction medium for wood-based lignocellulosic materials. Highly substituted lignocellulosic esters and phosphite esters can be obtained under mild conditions by reacting pulverized wood dissolved in ionic liquid with either acyl chlorides or dioxaphospholanes in the presence of pyridine. As a result, the functionalized wood develops an enhanced solubility in molecular solvents, allowing for a complete characterization by means of spectroscopic and chromatographic techniques. The use of innovative solvent system as the ionic liquid [amim]Cl and complementary techniques based on NMR and GPC enabled to highlight

chemical and morphological changes of lignin in native wood avoiding further handling and potential alteration thereof.

In this study, archaeological woods and reference sound woods of the same *taxa* (*Quercu*s and *Arbutus Unedo*), along with the corresponding extracted lignin, were exhaustively characterized by means of ^{31}P-NMR spectroscopy, two dimensional NMR spectroscopy (2D-HSQC-NMR) and GPC analysis. The samples were collected from the Site of the Ancient Ships of San Rossore (Pisa, Italy), where many shipwrecks dating from 2nd century BC to 5th century AD have been discovered.

The results highlighted a limited degradation of the extracted lignin fractions. The chemical structure of archaeological lignins is still very similar to the one of lignin specimens isolated from reference sound wood of the same *taxa*.

Analyses on the unprocessed woods under examination pointed out a deeper and faster consumption of the polysaccharide matrix and confirmed a limited degradation of the polyphenolic fraction. Furthermore, on the basis of this approach it was possible to assess the presence of lignin-carbohydrate complexes which may have been otherwise altered to some extent during the lignin extraction procedure. Altogether, chromatographic, spectroscopic and Klason analyses demonstrated a severe degradation concerning the archaeological *Arbutus Unedo* wood. Ancient *Quercus* wood, instead, showed an overall recalcitrant behaviour towards chemical and/or biological degradation which could be related to the pronounced LCC content highlighted by GPC and quantitative ^{31}P-NMR analyses for both the archaeological and the reference sound wood.

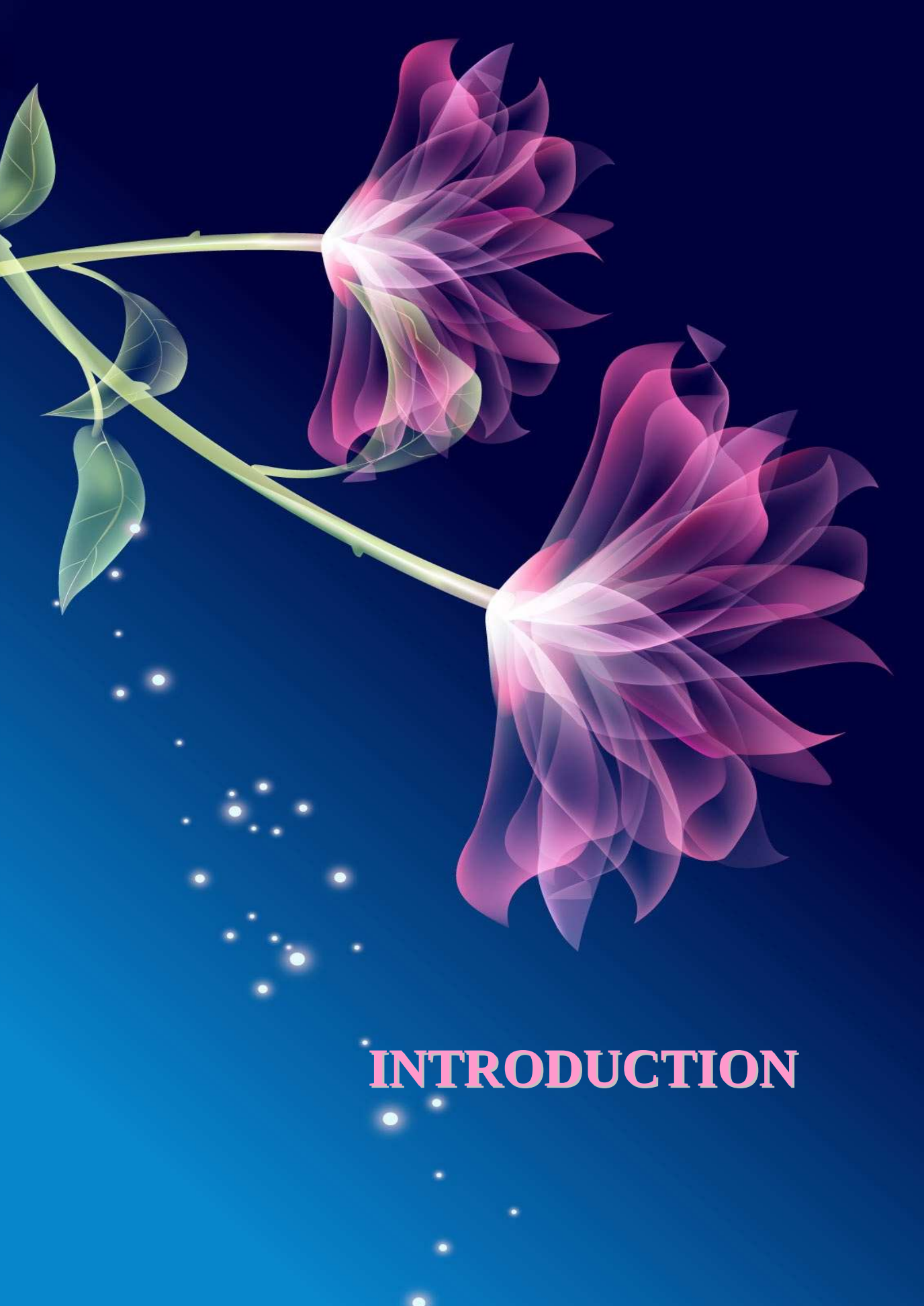

INTRODUCTION

1. LIGNOCELLULOSE: COMPONENTS INTEGRATION AND MOLECULAR STRUCTURE

1.1 Cell wall structure

Green plants constitute about half of the living matter on Earth and have a diversity ranging from simple green algae to flowering plants.

Limited and unstable resources of oil have sparked a renewed interest in the use of plant cell wall carbohydrates. Constituting the most abundant reservoir of polysaccharides structures in nature, cell wall carbohydrates are envisaged as primary source of biomass for biofuel production.

The cell wall is the extracellular matrix of the plant cell. It must be strong enough to support the plant and withstand the internal turgor pressure of the cell. It must also be able to extend during cell growth and participate in interactions with the environment.

Plant cells use two types of cell walls to perform their functions, termed the primary and secondary walls. Typical primary plant cell walls are composed of cellulose microfibrils (9-25%) and an interpenetrating matrix of hemicelluloses (25-50%), pectins (10-35%) and proteins (10%) (*1-4*). Cellulose forms the framework of the cell wall while hemicelluloses cross-link non-cellulosic and cellulosic polymers. Pectins provide cross-links and structural support to the cell wall, whereas proteins can function either structurally (extensin) or enzymatically.

As a definition, secondary walls are derived from primary walls by thickening and inclusion of lignin into the cell wall matrix (*5*) and occur inside the primary wall. Secondary cell walls of plants contain cellulose (40-80%), hemicellulose (10-40%), and lignin (5-25%) (*6,7*). The arrangement of these components results in a network of strong rod-like molecules of cellulose tethered together by cross-linked glycans and embedded in a matrix of lignin. The relevance of secondary cell wall structure to different fields has urged the scientific

community to structurally analyze components of the secondary cell wall structure.

1.2 Cellulose (*8*)

Cellulose is the major consistuent of plants cell wall. Its function is always mechanical, and it occurrs either in pure form as in the seed hair of cotton, or mixed with other polysaccharides and lignin, as in wood. The role of cellulose in this composite is to work as an enforcing fibre.

The primary structure, i.e., its covalent bond pattern, of cellulose is very simple: a linear unbranched polymer of β-glucopyranoside residues connected by β (1→4) glycosidic bonds. The degree of polymerization of cellulose chains is around 2,000-25,000 glucose residues, making cellulose one of the longest polysaccharide known. The fact that the glucopyranose units are in the form of β-anomers makes the polysaccharide straight and extended, in opposition to the 1→4 glucan of α-anomers, amylose, which is helicoidally shaped. Nevertheless, the cellulose chain is not totally straight: theoretical calculations indicate that a cellulose chain form a very extended helix. If this has some biological significance is not known. Every second glucose residue is “turned upside down” compared to the previous, i.e., the residues are rotated 180° towards each other. Thus, the repeating unit in cellulose is a cellobiose residue rather than a glucose residue.

However, the properties of cellulose that have made it such a biological and technical interesting polysaccharide are dependent on its secondary structure (*Figure 1*). Two hydrogen bonds - between the C6 hydroxyl and the C2 hydroxyl, and between the C5 oxygen and the C3 hydroxyl - stabilize the glycosidic bond and make the structure stiff. There are also hydrogen bonds between cellulose chains forming sheets. These hydrogen bonds are located between the hydroxyls at C6 and C3.

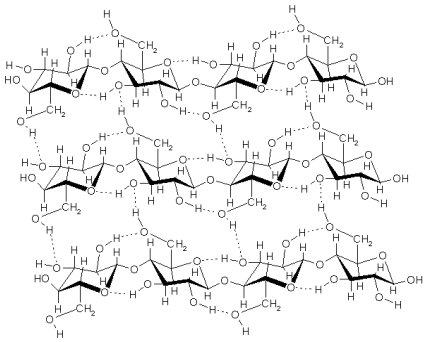

Figure 1. Representation of intra- ed inter-molecular hydrogen bonds pattern in a cellulose sheet. Hydrogen bonds between the C6 hydroxyl and the C2 hydroxyl, and between the C5 oxygen and the C3 hydroxyl stabilize the glycosidic bond and make the cellulose chain structure stiff. Hydrogen bonds located between the C6 and the C3 hydroxyls result in the formation of a sheet.

Cellulose sheets are stocked over each other and interact by van der Waals bonds and χ-interaction, i.e., hydrophobic interactions. Surprisingly, hydrophobic forces are important in the cellulose structure. Even if both glucose and cellulose are considered to be very hydrophilic, the chair conformation of glucose can be described as a discus with the hydroxyl groups pointing outwards. Thus the top and the bottom of anhydrous glucose is actually rather hydrophobic. Furthermore, the hydroxyl groups are locked in hydrogen bonds in the structure.

When the cellulose sheets bind to each other, they can afford two different crystal forms, cellulose I_α and I_β. This is due to the glucose residues of different sheets that do not stack directly over each other, causing a displacement in the position of the chains in the adjacent cellulose sheet. The third layer can be dispaced in the same direction as the second, forming cellulose I_α, or in the opposed direction, forming cellulose I_β. There are also differences in the hydrogen bonding pattern of cellulose I_α and I_β. As a result, these two different type of cellulose are described by different unit cell. Both crystal forms are thought to co-exist in cellulose: cellulose I_α is meta-stable and can be transformed in the more stable cellulose I_β at high temperature and pressure in alkaline or acidic solution.

Upgrading its complexity, long and relatively narrow sheets of cellulose chains forms highly organized bundles called microfibrils. Their size varies among different organism, as well as in different tissues; the size can even vary among cell wall layers. A cellulose chain may be 5-7 μm long, but a fibril can be much longer, probably at least 40 μm due to several chains overlapping each other. Each cellulose microfibril has approximately 36 glucose chains, and every elementary fibrils are further associated into larger units, called fibrils aggregates, by means of non-cellulosic polymers, i.e., hemicelluloses and pectines (*Figure 2)*. Furthermore, cellulose microfibrils contains both highly ordered (crystalline) and less ordered (semi-crystalline or amorphous) structures, with the less ordered cellulose suggested to be located either on the fibrilar surface or in amorphous segments of the fibril.

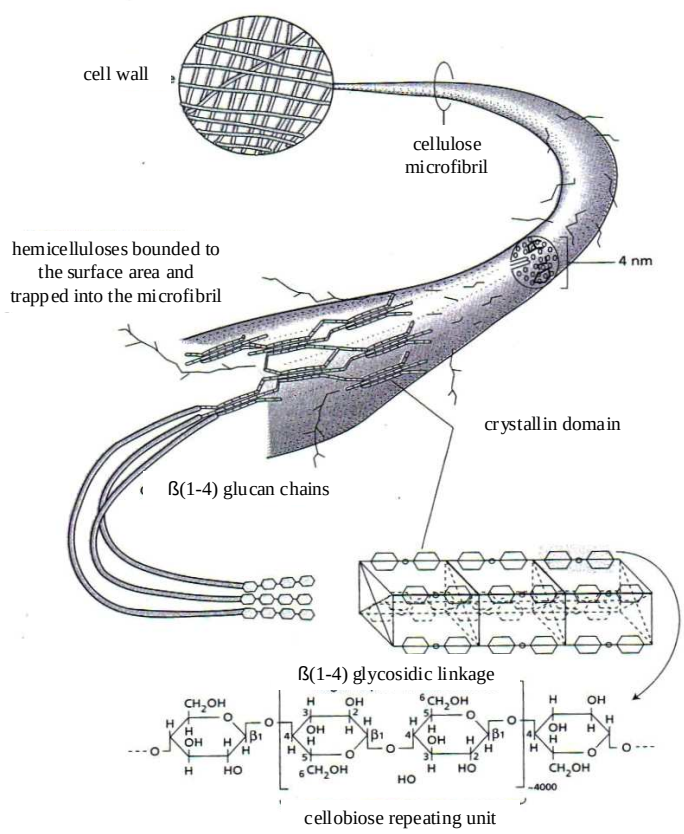

Figure 2. Representation of a cellulose microfibril showing its organization.

1.3 Hemicellulose *(9,10)*

A hemicellulose is any of several heteropolymers present along with cellulose in almost all plant cell walls. It consists of short, highly branched chains of sugars. In contrast to cellulose, which is a homopolymer of glucose, a hemicellulose is a heteropolymer containing different sugars. It contains five-carbon sugars (usually D-xylose and L-arabinose), six-carbon sugars (D-galactose, D-glucose, and D-mannose) and uronic acids. The sugars are highly substituted with acetic acid. The branched nature of hemicellulose renders it amorphous and relatively easy to hydrolyze to its constituent sugars compared to cellulose.

Hemicelluloses have β-(1→4)-linked backbones with an equatorial configuration. They include xylan, xyloglucan, arabinoxylan, glucomannan, glucuronoxylan, and β-(1→3,1→4)-glucans. These types of hemicelluloses are present in the cell walls of all terrestrial plants, except for β-(1→3,1→4)-glucans, which are restricted to Poales (the order to which Gramineae belong). The detailed structure of the hemicelluloses and their abundance vary widely between different species and cell types. The most important biological role of hemicelluloses is their contribution to strengthening the cell wall by interaction with cellulose and lignin. In addition, hemicelluloses may be cross-linked to lignin by ester and ether linkages, giving what is referred to as a lignin-carbohydrate complex (LCC).

Xylans are the dominant hemicelluloses in hardwood and non-woody biomass. They are known as heteropolymeric substrates consisting of a repeating β-(1→4)-linked xylose backbone branched with acetyl groups, arabinofuranosyl residues, and glucuronic acid or its 4-O-methyl ether (*Figure 3*). Xylans from different sources differ in composition; the frequency and composition of branches are dependent on the source of xylan. Xylans can be categorized as linear homoxylan, arabinoxylan, glucuronoxylan, and glucuronoarabinoxylan.

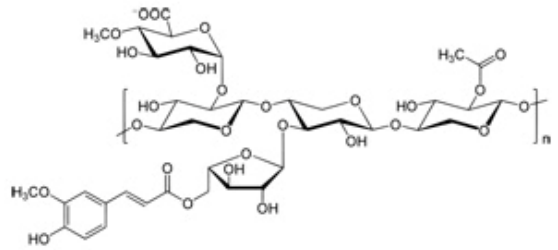

Figure 3. Basic structure of a xylan in grasses. The O-5 position of arabinofuranosyl residues is able to ester bound to ferulic acid, a phenolic bridge between hemicellulose and lignin.

Glucomannans and galactoglucomannans are the major hemicellulosic components of the secondary cell walls of softwoods (*Figure 4*). Glucomannan is a water-soluble hemicellulose polysaccharide, mainly a straight-chain natural polymer, with a small amount of branching. The component sugars are β-(1→4)-linked D-mannose and D-glucose in a ratio of 1.6:1. The degree of branching is about 8% through β-(1→6)-glucosyl linkages. Glucomannan with α-(1→6)-linked galactose units in side branches is called galactoglucomannan. Glucomannans and galactoglucomannans show some variations in structural features depending on the plant species and stage of development. The extent of galactosylation governs their association tendency to cellulose microfibrils and, hence, their extractability from the cell wall matrix.

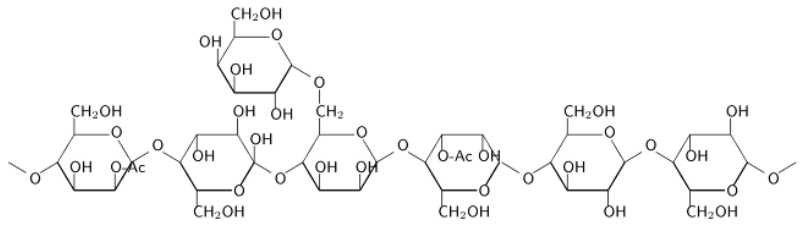

Figure 4. Structure of a galactoglucomannan

1.4 Lignin

The word “lignin” is derived from the Latin term *lignum*, which means wood. Anselme Payen, in 1838, was the first to recognize the composite nature of wood and referred to a carbonrich substance as the “encrusting material”

which embedded cellulose in the wood. Later, in 1865, Schulze defined this encrusting material as lignin.

Lignin is the second most abundant biological material on the planet, exceeded only by cellulose and hemicellulose, and comprises 15-25% of the dry weight of woody plants. This macromolecule plays a vital role in providing mechanical support to bind plant fibers together and also plays an important function in the plant natural defense against degradation by impeding the penetration of destructive enzymes through the cell wall *(11*).

Lignin monomers originate from the action of phenylalanine ammonia lyase, tyrosine ammonia lyase and other phenylpropanoid-related enzymes directing metabolites to, among other things, lignin biosynthesis (*2,12*). The shikimic acid pathway and phenylpropanoid metabolism lead to the synthesis of the following lignin monomers: para-coumaric acid, ferulic acid, diferulic acid, sinapic acid, cinnamic acid, and *p*-hydroxybenzoic acid. Enzymes subsequently catalyze the formation of three alcohols, also known as monolignols - para-coumaryl, coniferyl, and sinapyl alcohol (*Figure 5*) - which interact and polymerize to form lignin in the secondary cell wall.

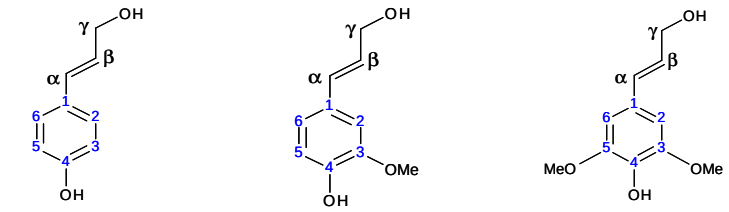

Para-coumaryl alcohol | Coniferyl alcohol | Sinapyl alcohol

Figure 5. para-hydroxycinnamic alcohols involved in lignin biosynthesis.

Lignin has been described as a random, three-dimensional network polymer comprised of variously linked phenylpropane units. Plant lignins can be broadly divided into three classes: softwood (gymnosperm), hardwood

(angiosperm) and grass or annual plant (graminaceous) lignin (*13*). Guaiacyl lignin is composed principally of coniferyl alcohol units, while guaiacyl-syringyl lignin contains monomeric units from coniferyl and sinapyl alcohol. In general, guaiacyl lignin is found in softwoods while guaiacyl-syringyl lignin is present in hardwoods. Graminaceous lignin is composed mainly of para-coumaryl and coniferyl alcohol units, but even sinapyl alcohol is well represented.

The lignification process, which accompanies secondary cell wall formation, arises from generation of free radicals that react spontaneously to form lignin and even some linkages to wall polysaccharides (*14*). Indeed, lignin is always associated with carbohydrates (in particular with hemicelluloses) via covalent bonds at two sites: the α-carbon in the propanoid chain and the C4 in the benzene ring, and this association is called lignin-carbohydrate complex (LCC). Polymerization of monomeric free radicals results in highly condensed core lignin, while free radical linkages between lignin monomers and polysaccharides may produce what is referred to as non-core lignin. Non-core lignin is typical of the Graminae family and its components include: p-cumaric, ferulic, p-hydroxybenzoic, sinapic, and cinnamic acids.

Lignin polymerization is initiated by oxidation of the phenylpropane phenolic hydroxyl groups. Freudenberg has shown that lignin precursors undergo dimerization through enzymatic dehydrogenation, which is initiated by an electron transfer and yields resonance-stabilized phenoxy radicals (*15*). A monolignol free radical can then undergo radical coupling reactions at any of the positions of the unpaired electron, producing a variety of dimers, termed dilignols. Branching of the polymer may take place through subsequent nucleophilic attack by water, alcohols or phenolic hydroxyl groups on the benzyl carbon of the quinone methide intermediate. The dilignols then undergo further endwise polymerization, instead of combining with one another.

After many years of study, the structure of native lignin still remains unclear. However, the dominant structures in lignin have been elucidated as the methods for the identification of the degradation products and for the synthesis of model compounds have improved. The results from these numerous studies have yielded what is believed to be an accurate representation of the structure of lignin. Examples of the elucidated structural features of lignin include the dominant linkages between the phenylpropane units and their abundance, as well as the abundance and frequency of some functional groups. *Figure 6* shows some of the most common linkages found in lignin. The dominant is the β-O-4 linkage. In 1995, Karhunen *et al*. (*16,17*) discovered a new 8-membered ring linkage in softwood lignin called dibenzodioxocin. This linkage is now proposed to be the main branching point in softwood lignin (*18*).

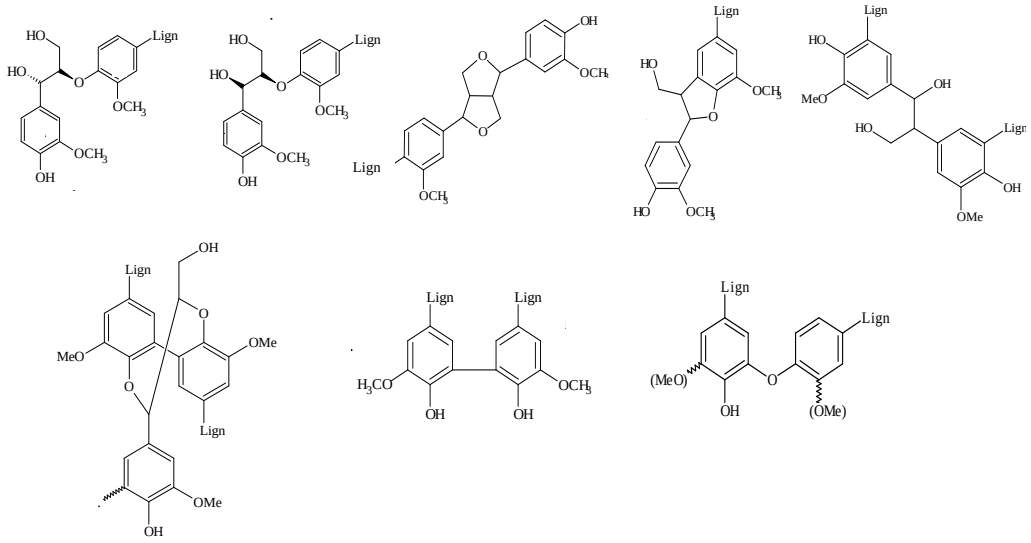

Figure 6. Intermonomeric linkages found in lignin. Top, left to right: arylglycerol-β-arylether (β-O-4) erythro and threo form, pinoresinol (β–β), phenylcoumaran (β-5), and β-1 unit. Bottom: condensed phenols, left to right: dibenzodioxocine (5-5'-O-4), biphenyl (5-5'), and diaryl ether (4-O-5').

The lignin macromolecule also contains a variety of functional groups that have an impact on its reactivity, such as methoxyl groups, phenolic hydroxyl groups, and few terminal aldehyde groups.

The nature of lignin polymerization reactions results in the formation of a three-dimensional, hydrophobic, racemic, highly-branched, interlocking network of high molecular weight. *Figure 7* pictures a tentative representation of a softwood lignin proposed by Adler (*19*) and later modified by Karhunen *et al*. It is important to note that the model proposed does not depict the actual structure of lignin. Instead, it serves as a tool to visualize the linkages and functional groups believed to occur in lignin.

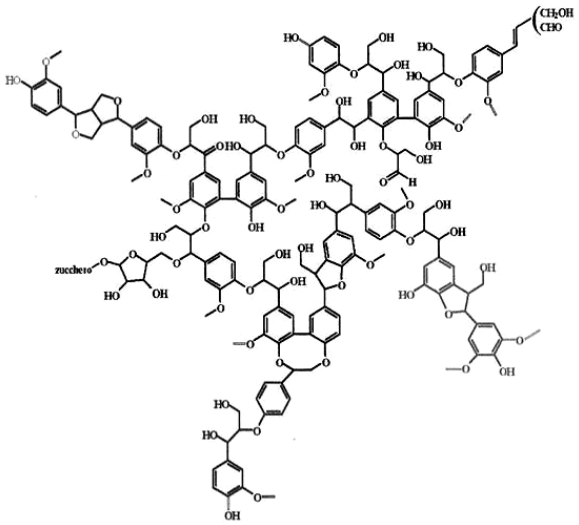

Figure 7. Tentative representation of a softwood lignin

1.5 Lignin-carbohydrate complexes (LCCs)

As mentioned in the previous section, lignin does not exist in plant tissue as an independent entity but it is bonded with other polymers forming complexes with them. Lignin is always associated with hemicelluloses, not only as physical admixtures, but through covalent bonds (*11*). This type of association represents the so-called lignin–carbohydrate complexes (LCCs). Because of these associations, it is practically impossible to extract lignins in pure form. The diverse and complex nature of lignin monomers and hemicellulosic moieties in ligno-hemicellulosic bonds make stereotypic conceptualizations of secondary cell wall structures for all plants extremely difficult. For this reason,

a general distinction between wood and grasses LCCs features is broadly accepted.

The lignin–carbohydrate complexes were first extracted with hot water from poplar wood in 1953. After this work, a wide range of organic solvents, alkaline solutions and enzymes were used.

Lignin and carbohydrates in wood are attached to each other via benzyl ether, benzyl ester, and glycosidic type bonds (*20*) (*Figure 8*).

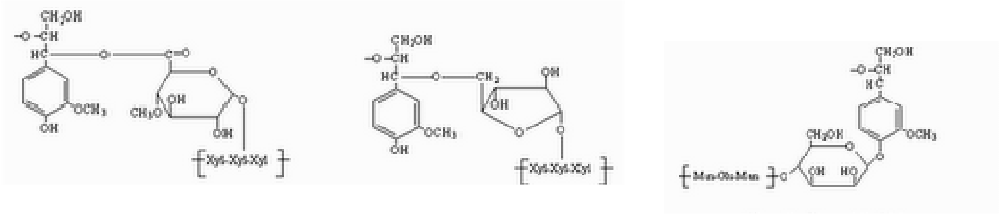

Figure 8. Typical LCCs found in woody materials. Left to right: benzyl ester, benzyl ether, and glycosidic linkage.

Ester linkages occur between the free carboxy group of uronic acids in hemicellulose and the benzyl groups in lignin. Others are present as acetyl side groups on hemicellulose, and still others occur between hemicellulose chains. Alkali-stable ether linkages occurr between the benzyl groups in lignin and the O-6 position of the hexoses side chain of glucomannan. The direct evidence for the existence of these LCCs is obtained with oxidative cleavage of benzyl ether and benzyl ester bonds, reduction, methylation analysis, chromatography, spectroscopy and electron microscopy (*21*). LCCs in wood contain mainly lignin (85%), acetyl groups (3%) and carbohydrates (15%). These carbohydrates consist mainly of xylose (80%), and varying amounts of other sugars such as galactose, glucose, mannose and arabinose (*22*).

In herbaceous plants, hydroxycynnamic acids are attached to lignin and hemicelluloses via ether and ester bonds as bridges between them forming lignin/phenolics–carbohydrate complexes (*23*,*24*). Researches, mostly directed towards the understanding of ligno-hemicellulosic linkages in grasses, has

been performed on a variety of Gramineae (*25-29*). As already discussed, two types of lignin, namely core and non-core, are encountered for this family: the non-core portion of lignin binds to the hemicellulosic fraction of the secondary cell wall, and the core lignin forms an amorphous matrix. Moreover, core lignin is bounded to non-core lignin by both ester and ether bonds, and non-core lignin is in turn connected to hemicellulose which is hydrogen-bonded to cellulose. These studies have shown that an ester bond connecting arabinose to non-core lignin is the major ligno-hemicellulosic linkage in plant secondary cell walls (*Figure 9*).

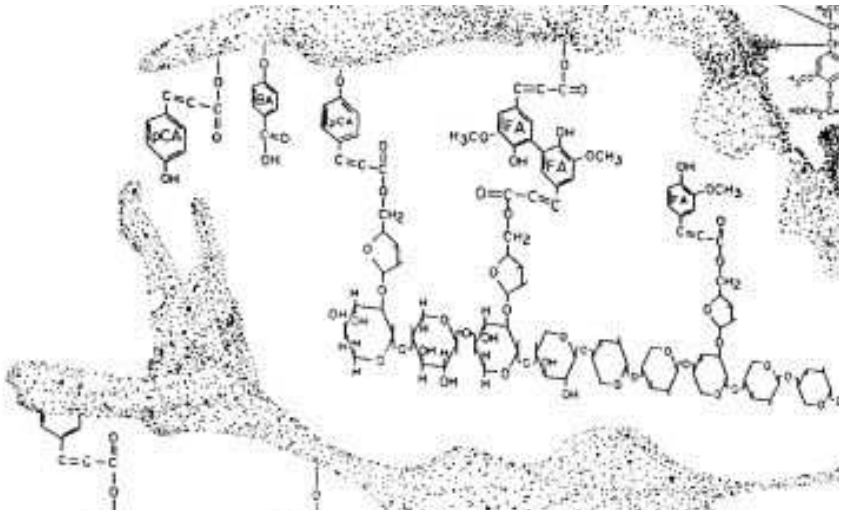

Figure 9. Secondary cell wall structure of a typical grass. Core lignin is presented as a dotted area embedding hemicellulose and cellulose microfibrils (not shown) while individual non-core components are shown in molecular form bound to hemicellulose. Ester bonds between hemicellulose and non-core lignin are mainly represented by linkages between the O-5 position of arabinose in arabinoxylan and p-coumaric, ferulic, and diferulic acids. Some of these lignin monomers, such as ferulic acid, may be so intimately associated with the hemicellulosic fraction that they fail to cross-link to lignin.

Ferulic and p-coumaric acids are the major non-core lignin monomers that link hemicellulose and core lignin (*30*) although diferulic, sinapic, cinnamic, and p-hydroxybenzoic acid constituents can also be found. The phenolic bridge is attached to lignin via ether bonds and to carbohydrates via ester bond. In the

Gramineae, these alkali-labile ester linkages involving arabinose predominate over alkali-stable bonds such as phenyl glycosidic and benzylether linkages (*31*) found in wood. Because of this difference, half of the total phenolics in herbaceous plants are removed with sodium hydroxide at ambient temperature (*32*,*33*).

References

1. Esau, K. Cell Wall. In: Plant Anatomy; John Wiley & Sons, New York, NY 1977, 43-60.
2. Goodwin, T.W.; Mercer, E.I. The Plant Cell Wall. In: Introduction to Plant Biochemistry; Pergamon Press, New York, NY, 1983, 55-91.
3. Keegstra, K.; Talmadge, K.W.; Bauer, W.D.; Albersheim, P. The structure of plant cell walls III. A model of the walls of suspension-cultured sycamore cells based on the interconnections of the macromolecular components. *Plant Physiol*., **1973**, *51*, 188-196.
4. Preston, R.D. Polysaccharide Conformation and Cell Wall Function. *Ann. Rev. Plant Physiol*. **1979**, *30*, 55-78.
5. Theander, O.; Aman, P. Anatomical and Chemical Characteristics. In: Straw and Other Fibrous By-Products as Feed; Sundstol, F.; Owen, E. Eds., Elsevier, Amsterdam, Holland, 1984, 45-78.
6. Bidlack, J.E., Cell-Wall Components and Lignin Biosynthesis in Forages. Ph.D. Dissertation, Iowa State Univ., Ames, IA, 1990.
7. Salisbury, F.B.; Ross, C.W. Plant Physiology and Plant Cells. In: Plant Physiology, Wadsworth, Inc., Belmont, CA, 1992, 3-26.
8. Henriksson, G.; Lennholm, H. Cellulose and carbohydrate chemistry. In: Wood Chemistry and Wood Biotechnology; Ek M.; Gellerstedt, G.; Henriksson, G. Eds.; de Gruyter GmbH & Co., Berlin, 2009, 71-100.
9. Saha, B.C. Hemicellulose bioconversion. J. Ind. Microbiol. Biotechnol. 2003, 30, 279-291.
10. Scheller, H.V.; Ulvskov, P. Hemicelluloses. Annu. Rev. Plant Biol. 2010, 61, 263-289.
11. 1 Sarkanen, K.V.; Ludwig, C.H. Lignin: Occurrence, Formation, Structure and Reactions. Sarkanen K.V.; Ludwig, C.H. Eds. Wiley-Interscience, New York, NY, 1971.
12. Hahlbrock, K., and Grisebach, H. Enzymatic Controls in the Biosynthesis of Lignin and Flavonoids. *Ann. Rev. Plant Physiol*. **1979**, *30*, 105-130.
13. Lewis, N.G.,; Yamamoto, E. Lignin: Occurrence, Biogenesis and Biodegradation. *Ann. Rev. Plant Physiol*. **1990**, *41*, 455-496.
14. Pearl, I.W. The Chemistry of Lignin. Marcel Dekker, Inc.; New York, NY, 1967.
15. Freudenberg, K.; Neish, A.C. Constitution and Biosynthesis of Lignin. Springer, G.F.; Kleinzeller, A. Eds., Springer-Verlag: New York, NY, 1968.
16. Karhunen, P.; Rummakko, P.; Sipilä, J.; Brunow, G. and Kilpeläinen, I.; Dibenzodioxocins: a novel type of linkage in softwood lignins. *Tetrahedron Letters*, **1995**, *36 (1)*, 167-170.
17. Karhunen, P.; Rummakko, P.; Sipilä, J.; Brunow, G. and Kilpeläinen, I.; The formation of dibenzodioxocin: structures by oxidative coupling. A model for lignin biosynthesis. *Tetrahedron Letters*, **1995**, *36 (25)*, 4501-4504.

18. Karhunen, P.; Mikkola, J.; Pajunen, A.; Brunow, G. The behavior of dibenzodioxocin structures during alkaline pulping processes. *Nordic Pulp and Paper Research Journal*, **1999**, *14 (2)*, 123-128.
19. Adler, E. Wood chemistry - past present and future. *Wood Sci. Technol*. **1977**, *11*, 169-218.
20. Watanabe, T. Structural studies on the covalent bonds between lignin and carbohydrate in lignin-carbohydrate complexes by selective oxidation of the lignin with 2,3-dichloro-5,6-dicyano-1,4-benzoquinone. *Wood Res*., **1989**, *76*, 59-123.
21. Choi, J.-W.; Faix, O.,. Investigation on residual lignins and residual carbohydrates and the covalent bonds between them. In: Proc. 10th Int. Symp., Wood Pulp Chem. 1, 1999, 368-373.
22. Koshijima, T.; Watanabe, T. In: Association Between Lignin and Carbohydrates in Wood and Other Plant Tissues. Timell, T.E. Ed., Springer-Verlag, Berlin, Germany, 2003.
23. Baucher, M.; Monties, B.; Van Montagu, M.; Boerjan, W. Biosynthesis and genetic engineering of lignin. *Crit. Rev. Plant Sci*., **1998**, *17*, 125–197.
24. Sun, R.; Tomkinson, J. Comparative study of lignins isolated by alkali and ultrasound-assisted alkali extractions from wheat straw. *Ultrason. Sonochem*., **2002**, *9 (2)*, 85–93.
25. Hartley, R.D. p-Coumaric and Ferulic Acid Components of Cell Walls of Ryegrass and Their Relationships with Lignin and Digestibility. *J. Sci. Food Agric*. **1972**, *23*, 1347-1354.
26. Morrison, I.M., Structural Investigations on the Lignin-Carbohydrate Complexes of Lolium perenne. *Biochem. J*. **1974**, *139*, 197-204.
27. Atsushi, K.; Azuma, J.; Koshijima, T. Lignin-Carbohydrate Complexes and Phenolic Acids in Bagasse. *Holzforschung*, **1984**, *38*, 141-149.
28. Scalbert, A.; Monties, B.; Lallemand. J.Y.; Guittet, E.; Rolando, C. Ether linkage Between Phenolic Acids and Lignin Fractions from Wheat Straw. *Phytochemistry* **1985**, *24*, 1359-1362.
29. Mueller-Harvey, I.; Hartley, R.D. Linkage of p-Coumaroyl and Feruloyl Groups to Cell-Wall Polysaccharides of Barley Straw. *Carbohydrate Res*. **1986**, *148*, 71-85.
30. Jung, H.G. Forage Lignins and Their Effects on Fiber Digestibility. *Agron. J*. **1989**, *81*, 33-38.
31. Ford, C.W. Borohydride-soluble lignin–carbohydrate complex esters of p-coumaric acid from the cell walls of a tropical grass. *Carbohydr. Res*. **1990**, *201*, 299–310.
32. Chesson, A.; Murison, S.D. Biochemical evaluation of straw as a feedstuff for ruminants. In: Evaluation of Straw in Ruminant Feeding. Appl. Sci. Publ., Chenost, M., Reiniger, P. (Eds.), London, UK, 1989, 124–133.

33. Hartley, R.D.; Morrison, W.H. Monomeric and dimeric phenolic acids released from cell walls of grasses by sequential treatment with sodium hydroxide. *J. Sci. Food Agric*. **1991**, *55*, 265–375.

2. BIOREFINERY

2.1 Basic biorefinery concepts (*1)*

The markets for bio-based products are expected to grow globally over the next few years due to four irreversible trends. First, the economics of fossil-based products are deteriorating since conventional crude oil resources are getting scarce. Second is the growing need for national energy security and geopolitical security. Third, public pressure for environmental sustainability is increasing due to an increasing environmental awareness. Last, but not least, rapid demographic growth will drive demand supported by rising economic aspirations of developing countries.

These fundamental trends triggered a vast interest in bio-based products and placed them high on the strategic agenda of most players in a variety of industries. In agriculture, for example, new economic opportunities will emerge from the rising demand for biomass. In the chemicals industry, bio-based innovative products outside the conventional petroleum-based product family trees will confer an advantage to players who manage to find the right molecules and insert them into existing or new value chains. In the automotive and aviation industries, corporations are looking at biofuels as an important means to reduce the greenhouse gas emissions of their fleets to comply with regional or national regulations, while utilities are making high investments in the expansion of their renewable power generation assets, with biomass coming third after solar and wind investments. Despite the great relevance of bio-based products for many industries, experts still see numerous technical, strategic and commercial challenges that need to be overcome before any large-scale commercialization of the industry can succeed.

2.1.1 Definition

Biorefineries are facilities that convert biomass – biological materials from living or recently living organisms – into bio-based products.

The term "bio-based products" refers to three different product categories: biofuels (e.g. biodiesel and bioethanol), bio-energy (heat and power) and bio-based chemicals and materials (e.g. succinic acid and polylactic acid). They are produced by a biorefinery that integrates the biomass conversion processes. The biorefinery concept is thus analogous to today's petroleum refineries that produce multiple fuels, power and chemical products from petroleum. Biorefinery systems generally work by processing a bio-based feedstock input to create fuel, chemicals, feed or power/heat as an output (*Figure 1*). Biorefineries thus use a wide variety of different inputs/feedstocks and conversion technologies.

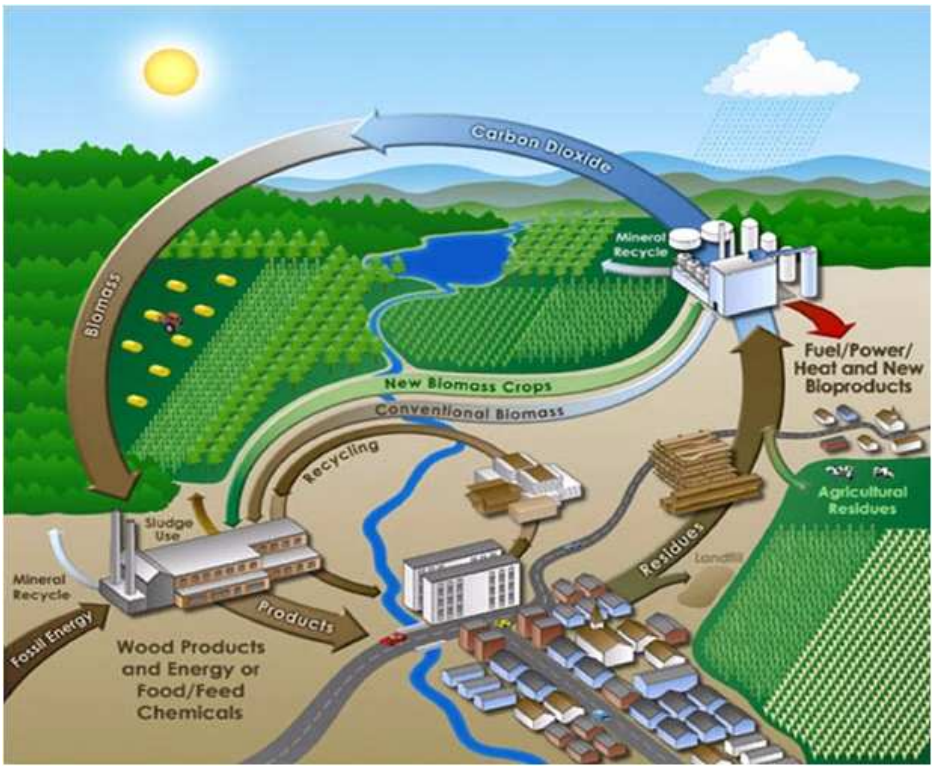

Figure 1. The biorefinery concept. Any number of conversion processes can take place within one biorefinery, analogous to today's oil refinery.

2.1.2 Biomass feedstock

Bio-based products can be manufactured from various feedstocks. However, at present there is no feedstock or process that would make these a clear alternative to fossil-based products. There are many options available, each with advantages and disadvantages. Two categories of feedstock dominate research: first and second generation.

First-generation products are manufactured from edible biomass such as sugar- rich, starch-rich, and oily plants:

- The most common type of biorefinery today uses sugar- or starch-rich crops. Sugar-rich crops such as sugar cane store large amounts of saccharose, which can easily be extracted from the plant material for subsequent fermentation to ethanol or bio-based chemicals. Starch-rich crops such as corn, wheat and cassava can be hydrolyzed enzymatically to deliver a sugar solution, which can subsequently be fermented and processed into fuels and chemicals.
- Vegetable oil is mainly used for the production of biodiesel by transesterification. There are two categories: pure plant oil and waste vegetable oil. Pure plant oil stems from dedicated oil crops such as palm, soybean, rapeseed and sunflower seeds. Use of waste vegetable oil, for example cooking oil or animal fat, is an effective method of recycling our daily wastes; however, it does need refinement as well as hydrogenation to become usable biodiesel.

Major issues in relation to first-generation feedstocks are the need for extensive and dedicated land-use, significant land-use change and related sustainability issues.

Fuels derived from sugar- or starch-rich crops and vegetable oil are widely used; however, their use is likely to be most effective as a supplement to other energy forms, not as a primary source. Second-generation products utilize biomass consisting of the residual non-food parts of current crops or

other non-food sources, such as perennial grasses or algae. These are widely seen as possessing a significantly higher potential to replace fossil-based products.

- The Jatropha Curcas tree from Central and South America contains 27-40% inedible oil, which can be converted to biodiesel via transesterification. An assessment of *j.curcas* sustainability reveals a positive effect on the environment and greehouse gas emissions, provided cultivation occurs on wasteland or degraded ground.
- Micro-algae are a large and diverse group of unicellular photo- and hetero-trophic organisms that have attracted much attention in recent years due to their potential value as a renewable energy source. Focus has been on storage lipids in the form of triacylglycerols, which can be used to synthesize biodiesel via transesterification. The remaining carbohydrate content can also be converted to bioethanol via fermentation. The advantages of using algae-derived fuels as an alternative are numerous. First, they can provide between 10 and 100 times more oil per acre than other second-generation biofuel feedstock and the resulting oil content of some micro-algae exceeds 80% of the dry weight of algae biomas. They are safe, biodegradable, highly productive, quick to cultivate and simply require CO_2, sunlight and water to grow. However, numerous barriers remain to be overcome before the large-scale production of micro-algae-derived biofuels can become a commercial reality.
- Lignocellulosic biomass refers to inedible plant material mainly composed of cellulose, hemicellulose and lignin. It is deemed likely that this type of second-generation feedstock will be used for the production of biofuels and bio-based chemicals in the future using different conversion technologies. However, it is more difficult to convert lignocellulosic biomass into a usable output than other types

of biomass; the main reason for this is that the protective shield of hemicellulose and lignin that surrounds cellulose has to be broken down, which is a highly energy intensive process. Nevertheless, cellulosic ethanol is ready for deployment due to recent significant breakthroughs in the enzymatic conversion process *(2*). On the pro side, lignocellulose feedstocks can be derived from many different sources, including forestry waste, agricultural waste, paper and municipal waste, as well as dedicated energy crops such as switchgrass, miscanthus or short-rotation poplar. These feedstocks exclude direct land-use and minimize indirect land-use change.

2.1.3 Conversion platforms

Adapted from the National Renewable Energy Laboratory (NREL), a simple biorefinery concept has been devised that is built on three different platforms to promote different product routes: the Biochemical, the Thermochemical, and the Microorganism Platform.

- The Biochemical Platform is currently based on biochemical conversion processes and focuses on the fermentation of sugars extracted from biomass feedstocks. The production of bioethanol requires three main steps: fermentation of the sugars, distillation to remove the bulk of the water and dehydration to further remove water from the remaining azeotropic water/ethanol mixture. Starch-based feedstock requires saccharification to produce fermentable sugars. When using lignocellulosic biomass, feedstock processing needs to separate the cellulosic and hemicellulosic material from the non-fermentable lignin, which are strongly bonded by covalent cross-links. This is usually done mechanically, followed by acid, alkali and/or steam treatment. While the lignin is currently mostly combusted to deliver energy, the cellulosic and hemicellulosic

components are hydrolyzed enzymatically to deliver sugar solutions, followed by fermentation.

- The Thermochemical Platform is currently based on thermochemical conversion processes and focuses on the gasification of biomass feedstocks and resulting by-products. Where gasification of carbonaceous materials is widely used (e.g. syngas production from coal), gasification of lignocellulosic biomass is still a developing technology.
- Algae biofuels occupy a third Microorganism Platform, where cultivation and extraction occur on the same site. Photobioreactors provide a greater oil yield per hectare due to their higher volumetric biomass productivity. In addition to oils, micro-algal biomass contains significant quantities of proteins, carbohydrates and other nutrients. A micro-algal biorefinery can simultaneously produce biodiesel, animal feed, biogas and electrical power. The cost of producing micro-algal biodiesel can be reduced substantially by using a biorefinery based production strategy, improving capabilities of micro-algae through genetic engineering, designing new synthetic microorganisms and advances in engineering of photobioreactors (*3*).

2.2 Conversion of lignocellulosic biomass (*4*)

In lignocellulose biorefineries, biological conversion of lignocellulose generally has three main steps:

(1) lignocellulose pretreatment, which converts the recalcitrant lignocellulose structure to reactive cellulosic intermediates;

(2) enzymatic cellulose hydrolysis, by which cellulases hydrolyze reactive intermediates to fermentable sugars (e.g., glucose);

(3) fermentation, which produces cellulosic ethanol or other bio-based chemicals (e.g., lactic acid, succinic acid).

2.2.1 Factors affecting the saccharification yield

Because lignocellulose is water insoluble, the heterogeneous reactions involved in biomass conversion processes require direct physical contact between enzymes and substrates (i.e., cellulose and hemicellulose). Mechanical pretreatments are always necessary to enhance biomass digestibility by reducing particle size and partially disgregating the highly organized and cemented structure of lignocellulose, but a number of different chemical and physical structural features have been recognized as crucial for the yield in enzymatic saccharification as well. The interference of cellulose crystallinity, its accessible surface area, and lignin content on the enzymatic digestion is among the most studied and debated issue, however the role of other lignocellulose constituents, such as hemicelluloses, lignin-carbohydrate complexes, and ashes has been recently deemed as relevant as well.

- Cellulose. The cellulose microfibrils have both crystalline and amorphous regions. The major part of cellulose (around 2/3 of the total cellulose) is in the crystalline form. It was shown that cellulase readily hydrolyzes the more accessible amorphous portion of cellulose, while the enzyme is not so effective in degrading the less accessible crystalline portion. It is therefore expected that high-crystallinity cellulose will be more resistant to enzymatic hydrolysis, and it is widely accepted that decreasing the crystallinity increases the digestibility of lignocelluloses (*5*). However, this is not the only factor in effective enzymatic hydrolysis of these materials since other features as the polymerization degree, the pore volume, and the surface area play an important role.
- Lignin. Cellulose and hemicellulose are cemented together by lignin. Lignin is responsible for integrity, structural rigidity, and prevention of swelling of lignocelluloses. Thus, lignin content and distribution constitute the most recognized factor which is responsible for the

recalcitrance of lignocellulosic materials to enzymatic degradation by limiting the enzyme accessibility; therefore the delignification processes can improve the rate and extent of enzymatic hydrolysis (*6*). However, in most delignification methods, part of the hemicellulose is also hydrolyzed, and hence the delignification does not show the sole effect of lignin. Several mechanisms have been suggested about how lignin limits enzymatic hydrolysis:

1- steric hindrance caused by lignin-polysaccharide linkages (LCCs) that limit access of fibrolytic enzymes to specific carbohydrate moieties. For example, the degradation rate of xylan is said to depend on the number and location of side branches and their lignin associations.

2- lignin as a hydrophobic filler that displaces water in the cell wall matrix. As a result of the hydrophobicity of lignin, water cannot approach internal polymers of the cell wall. Hence, the action of hydrophilic enzymes may be limited by this hydrophobic environment.

3- adsorption of enzymes, which increases the loading but decreases the effects, and toxic effects to the enzymes for simple phenolic compounds.

- Hemicellulose. Hemicellulose removal substantially enhances cellulose digestion despite of high lignin content (*7,8*). It is believed that hemicellulose in biomass blocks the contact of cellulolytic enzymes with cellulose by adsorbing enzyme and by physically blocking access of the cellulase to the cellulose surface (*9*). As a result, hemicellulose removal alone can increase the surface area and the pore volume making cellulose more accessible to cellulase.
- Cellulose accessible surface area. Several studies have shown a good correlation between the pore volume and the enzymatic digestibility

of lignocellulosic materials. The main reason for the improvement in enzymatic hydrolysis by removing lignin and hemicellulose is related to the cellulose accessible surface area. The effect of this area may correlate with crystallinity or lignin protection or hemicellulose presentation or all of them (*10*). The first part of enzymatic hydrolysis consists of: adsorption of cellulase enzymes from liquid phase onto the surface of cellulose (solid), biodegradation of cellulose to simple sugars, mainly cellobiose and oligomers, and desorption of cellulase to the liquid phase. Thus, the reaction is a heterogeneous catalytic reaction and direct physical contact between the cellulytic enzymes and cellulose is a prerequisite for enzymatic hydrolysis. As a result, the accessibile surface area in lignocellulosic material and its interaction with the enzymes can be limiting in enzymatic hydrolysis (*5*,*11*,*12*).

- Lignin-carbohydrate complexes (LCCs). Lignin and hemicelluloses are always covalently associated in lignocellulosic biomass. The advantages in the removal of LCCs (*13*) are stricly related to those of lignin and hemicellulose removal, already discussed.
- Ashes. Large ashes content is counterproductive to the enzymes activity. Ashes may adhere to cellulose chains, shielding the substrate from the approaching enzyme.

It is clear that effectively overcoming the recalcitrance structure of lignocellulose and releasing the locked polysaccharides is one of the most important and urgent R&D priorities for the emerging biofuel and biobased product industry, because lignocellulose pretreatment is among the most costly steps and has a major influence on the costs of both prior operation (i.e., lignocellulose particle size reduction) and subsequent operations (e.g., enzymatic hydrolysis and fermentation).

2.2.2 Lignocellulose biomass pretreatment

The efficient, cost-effective depolymerization of polysaccharides in biomass to monosaccharides remains a key challenge in the utilization of this bioresource for fermentation to ethanol. To date, effective utilization through biological routes is predicated on pretreatment technologies that can reduce lignocellulose recalcitrance. The objective of pretreating lignocellulosics is to alter the structure of biomass and to make the cellulose and hemicelluloses more accessibile and amenable to hydrolytic enzymes (*14)*. The lignin shield and the crystalline structure of cellulose have to be broken to increase the accessibility and porosity of cellulose. Effective pretreatment technologies need to address several important criteria, including: minimization of hemicellulose degradation products, limiting the formation of by-products that inhibit ethanol fermentation, reducing energy/water use and lowering environmental impacts, capital and operating costs. Some of the most promising pretreatments include steam explosion, hot water/auto-catalyzed pretreatment, dilute acid, aqueous lime or NaOH pretreatment, ammonia, and organosolv pretreatment.

- Steam explosion involves rapidly heating biomass with steam at elevated temperatures (190-240 °C) with residence times of 3-8 minutes followed by explosive decompression. This treatment promotes hemicellulose hydrolysis and opens up the plant cell structure, although enhanced digestibility of cellulose is only weakly correlated with the physical effects (*15,16*).
- Hot water or auto-catalyzed pretreatment can result in extensive hemicellulose hydrolysis but high residual lignin content in biomass reduces subsequent cellulase hydrolysis (*17)*. The generation of furfural and 5-hydroxymethyl furfural has been reported to be detrimental to subsequent fermentation operations.

- Dilute acid pretreatment has been extensively studied and typically employs 0.4-2% H_2SO_4 at temperatures of 160–220 °C to remove hemicelluloses and enhance cellulase digestion of cellulose (*18, 19*).
- Aqueous lime or NaOH pretreatment has been shown to be effective for wheat straw and sugarcane bagasse at lower temperatures than acid treatments; however, the treatment times are in some cases on the order of hours (*20*). The use of an alkaline treatment also incurs additional capital cost, as the recovery of salts requires a lime kiln to regenerate the base.
- Ammonia pretreatment involves pretreating biomass with an aqueous ammonia solution causing depolymerization and cleavage of lignin–carbohydrate bonds. Agricultural residues and herbaceous plants treated in this manner exhibit an excellent response to cellulase (*21, 22*). However, woody biomass is often not efficiently treated by this technology, and in all cases, ammonia recovery is an additional cost and an important consideration.
- Organosolv pretreatment of biomass resides on the use of an organic solvent system (*23-26*) with enhanced lignin solubilizing properties. Usually, the resultant cellulosic fraction is highly susceptible to enzymatic hydrolysis, generating very high yields of glucose that can be readily converted to ethanol.

Ionic liquid pretreatment has recently emerged as a valuable alternative to traditional pretreatments strategies (*see section 3.4*). Once the ionic liquid has dissolved the lignocellulose biomass into its components, the subsequent addition of an anti-solvent, such as water or ethanol, results in the sugars being precipitated out while a fairly large fraction of the lignin remains in solution. The resulting regenerated cellulose can then be separated by filtration or centrifugation while the ionic liquid can be recovered through distillation of the antisolvent. The recovery of ionic liquids still requires

much more research, although studies on biphasic systems in regards to the recovery have already been performed. The regenerated cellulose can differ from the native cellulose in both the macro- and microstructure while the degree of crystallinity can be changed due to the changes in the regeneration conditions. Most important, the regenerated cellulose demonstrated improved enzymatic hydrolysis kinetics (*27).*

After pretreatment, the remaining pretreated material is reacted with cellulase to hydrolyze cellulose to glucose, which is then fermented to ethanol. An important consideration during the hydrolysis process is to minimize formation of compounds that inhibit the fermentation (*28*). The nature, composition, and concentration of these compounds are dependent on the hydrolysis conditions and have a profound influence on the fermentation production rate of biofuels from the hydrolyzate. For optimal process economics, all available sugars need to be converted to biofuel. The microorganisms that are able to ferment sugars to ethanol can be either yeasts or bacteria. Over the past decades, new methods in molecular biology, protein chemistry and genetic engineering have led to an increasing number of new strains, exhibiting improved characteristics to ferment the full spectrum of sugars available in hydrolyzates (*29, 30*).

2.2.3 Lignin side stream

Most biomass pretreatments release some simple sugars from the hemicelluloses, which are directly fermented to ethanol. The pretreated solid material is reacted with cellulase to hydrolyze cellulose to glucose, which is then fermented to ethanol (*31*). Regardless of the exact bioprocessing technology employed, almost all biological processing platforms for the conversion of plant polysaccharides to bioethanol result in the formation of a vast lignin process stream (*32*). This material is frequently utilized as an energy source for power generation, in part because there are few efficient

chemical conversion processes available that can convert lignin into transportation biofuels or higher value chemical substrates. Although a fraction (nearly 40%) of the dried lignin-rich solid stream after ethanol production is necessary to meet the thermal requirements of bioethanol production, which includes pretreatment and ethanol distillation (*33, 34*), modern biological cellulosic processing plants will have almost 60% excess of lignin that could be utilized as a feedstock for biogasoline/green diesel and/or green chemicals, thus offering a significant opportunity for enhancing the operation of a lignocellulosic biorefinery.

With currently available technologies, it is often not readily feasible to purify the fermentation residue to a form suitable for the production of lignin-based biomaterials. It should be noted that among current pretreatment technologies, the organosolv pretreatment produces a relatively pure lignin stream as a by-product, which can be converted to biomaterials. For most other acidic pretreatments, which do not extract lignin during pretreatment, the conversion of the residue to liquid fuels is presently a more viable option.

2.3 Ionic liquids in lignocellulose chemistry

The crystalline structure of cellulose and the three-dimensional lignin network that binds lignocellulosic components together makes it practically impossible to dissolve lignocellulosic materials in their native form in conventional molecular solvents. Thus, it is important to find a non-derivatizing solvent to provide efficient dissolution and stability to varius reagent in order to achieve a homogeneous reaction environment to preserve the native structure of lignocellulose. Ionic liquids (ILs) have arisen as such solvent. They are defined as organic salts that melt below 100°C entirely composed of ions, typically large organic cations and small inorganic anions. Compared with conventional molecular solvents, they emit no volatile compounds to pollute the atmosphere and their properties can be tuned to

match the end use application by varying anions and cations (*35,36*). They are therefore considered as a potential alternative for green chemistry (*37*). In recent years, there have been lots of reports on dissolution of cellulose in ILs and its application (*38,39*), but solubilization of native lignocellulosic materials is far more complicated due to their complex structure from the three-dimensional lignin network. In ILs, both the cation and the anion of the salt play a crucial role in the dissolution of lignocellulose. Kilpelainen et al. (*40*) pointed out that wood dissolution in ILs is not only needed to disrupt the H-binding interactions present in crystalline cellulose but also to solvate the aromatic character of lignin by means of aromatic π-π interaction. The most promising cations are butyl or allyl derivatives of imidazolium salts whose electronrich aromatic π-system creates stronger interactions for polymers which undergoes π-π stacking i.e., lignin. Counter chloride anions, whereas, are usually the most effective in disrupting the extensive inter- and intra-molecular H-bonding interactions mainly present in the cellulosic fraction of the material (*41-43*) allowing the IL to diffuse into the interior causing the swelling to disruption of hydrogen bonding between cellulose fibrils and lignin (*Figure 2*).

Figure 2 *(44).* Fluorescence images of a stem of switchgrass treated with ionic liquid ([emim]Ac). Left to right: the section before treatment, 20 minutes after treatment, 50 minutes after treatment, and two hours after treatment. The organized plant cell wall structure has been completely broken down.

2.3.1 Ionic liquids in the pretreatment and characterization of lignocellulose

As a result of the complex and elusive nature of the interactions of the various lignocellulose components, traditional industries utilizing wood as a

renewable resource have resorted to selective degradation of one or more components, usually lignin, for the production of higher value purified materials such as wood pulp (for paper) or cellulose. As the connectivity between the individual plant components (cellulose, hemicelluloses and lignin) is crucial for their structural integrity, development of novel fractionation processes for the complete utilization of woody materials as renewable resources requires detailed structural analysis to thoroughly characterize the material, including revealing details of the connectivity between components.

Dissolution in ILs has definitely opened an entire new perspective in lignocellulosic research and its efficient utilization in the following topics:

- Analysis of biomass components and structure
- Pretreatment of biomass wastes for the production of chemical feedstocks and biofuels
- Extraction of cellulose from agro-industrial wastes
- Preparation of biomasses derivatives and composites
- Production of valuable chemicals such as vanillin, ferulic acid and lignans

With regard to the analysis of biomass components and structure, ILs can provide a homogenous reaction medium for both unprocessed lignocellulose and its fractionation products. Highly substituted lignocellulosic esters can be obtained under mild conditions by reacting the lignocellulose dissolved in ionic liquid with a number of reactives in the presence of pyridine**.** As a result, the functionalized material develops an enhanced solubility in molecular solvents, allowing a complete characterization by means of spectroscopic and chromatographic techniques.

Biomass pretreatment and fractionation represent a major challenge as well as an essential need in the efficient conversion of lignocellulose into biofuels and chemicals. Because of its natural composite structure, lignocellulose

must be pretreated prior to addition of hydrolytic enzymes for saccharification of cellulose or hemicelluloses, as yields are otherwise too low (*45*). These pretreatments can be mechanical, chemical, thermochemical, and/or biological in nature, and currently represent some of the most costly steps in the lignocellulosic biorefining process.

The pretreatment of lignocellulose with a variety of ionic liquids produced an enhancement of cellulase saccharification yields due both to the extraction of lignin (*46*) and the dissolution of cellulose microfibrils (*47*). Once the ionic liquid had dissolved the lignocellulose biomass into its components, the subsequent addition of an anti-solvent, such as water or ethanol (*48*), results in the sugars being regenerated and precipitated out while a fairly large fraction of the lignin remains in solution. The regenerated cellulose has almost the same degree of polymerization and polydispersity as the initial one, but its morphology is significantly changed and its microfibrils are fused into a relatively homogeneous macrostructure. By changing the regeneration process, the regenerated cellulose can be in a range of structural forms, such as powder, fiber and film. The regeneration processes also have an impact on the regenerated cellulose microstructure. The degree of crystallinity of the cellulose can be modified during its regeneration and the cellulose with micro-crystallinity varying from amorphous to crystalline can be obtained under different regeneration conditions. The increase of the cellulose surface area accessible to water, which in turn provides more exposed enzyme binding sites, results in greater accessibility of the polysaccharide chains to cellulases, and thus more facile hydrolysis. This confirms that the ionic liquid pretreatment effectively disrupts the recalcitrance of the lignocellulose biomass and helps liberate the fermentable sugars. In comparison to untreated biomass, ionic liquid pretreated biomass produces cellulose that is efficiently hydrolyzed with commercial cellulase cocktail and provides sugar yields over a relatively short time interval.

2.4 Biocomposites *(49-51)*

A biocomposite is a material formed by a matrix and a reinforcement of natural fibers. Polymer blending quite often is a very convenient industrial process since it provides tailoredmade materials excluding any synthetic stage.

2.4.1 Lignocellulose-based fillers

Natural fibers have been used to reinforce materials for over 3,000 years. Significant examples include the use of reinforcing mud walls in houses with bamboo shoots, glued laminated wood by Egyptians (1500 BC) and laminated metals in the forging of swords (1800 AD). More recently they have been employed in combination with plastics as renewable and cheap reinforcement for composite materials.

Many types of natural fibers have been investigated for use in plastics including flax, hemp, jute, straw, wood fiber, rice husks, wheat, barley, oats, rye, cane (sugar and bamboo), grass reeds, kenaf, ramie, oil palm empty fruit bunch, sisal, etc. It is worth noticing that plant fibers are composite materials themselves, designed by nature. The fibers are basically a rigid, crystalline cellulose microfibril reinforced by an amorphous lignin/hemicellulose matrix. The properties of the constituents contribute to the overall properties of the fiber. Hemicellulose is responsible for the biodegradation, microabsorption and thermal degradation of the fiber as it shows the least resistance, whereas lignin is thermally stable but prone to UV degradation. The percentage composition of each of these components varies for different fibers. The cell wall of the fibers undergoes pyrolysis with increasing processing temperature and contributes to char formation. These charred layers help to insulate the lignocellulose from further thermal degradation.

Lignin is one of the most abundant naturally occurring polymers and is often obtained as a byproduct in the industry. Most of it is burned as an energy

source, but there are some other potential uses for lignin, including applications as a filler, as a prepolymer, and as a nucleating agent for poly(hydroxyalkanoates), PHA. Lignin powder with fine particle size meets several requirements as a nucleating agent in that it possesses many polar functional groups that can interact with PHA carbonyl groups and it has no melting point with a high glass-transition temperature.

The use of natural fiber for the reinforcement of composites has received increasing attention both by the academic sector and the industry because of their advantages over other established materials. They are environmentally friendly, fully biodegradable, abundantly available, renewable, cheap and have low density. Plant fibers are light compared to glass, carbon and aramid fibers. The biodegradability of plant fibers can contribute to a healthy ecosystem while their low cost and high performance fulfils the economic interest of industry. When natural fiber-reinforced plastics are subjected, at the end of their life cycle, to combustion process or landfill, the released amount of CO_2 of the fibers is neutral with respect to the assimilated amount during their growth.

Natural fiber-reinforced plastics, if biodegradable polymers are used as matrices, are the most environmental friendly materials which can be composed at the end of their life cycle.

2.4.2 Poly(3-hydroxybutyrate) (PHB)

Poly(3-hydroxybutyrate), PHB, is a member of the poly(hydroxyalkanoates) family, PHA. It is an environmental friendly bacterial polyester behaving as conventional thermoplastic materials that was first isolated and characterized in 1925. PHB is produced by microorganisms as a form of energy storage molecule to be metabolized when other common energy sources are not available. The most advantageous characteristic of this material is its

biocompatibility and biodegradability, presenting microbial degradation in climatic/landscapes environmental.

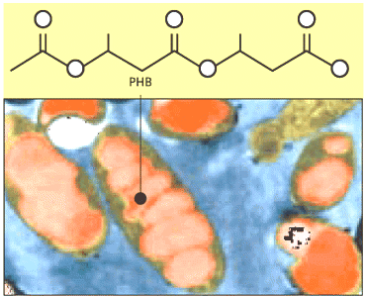

Figure 3. Microbial biosynthesis of PHB starts with the condensation of two molecules of acetyl-CoA to give acetoacetyl-CoA which is subsequently reduced to hydroxybutyryl-CoA. This latter compound is then used as a monomer to polymerize PHB.

PHB tends to be more brittle than conventional thermoplastics, limiting its fields of application, even though mechanical properties of this biodegradable material can be compared with those of the commercially used thermoplastic isopolypropylene. Other drawbacks of PHB, besides fragility, are thermal degradability at temperatures near to the range of the melting point (T_m = 175°C). Indeed, above 170 °C this polyester undergoes a decrease of molecular weight proportional to the time. The mechanism of the thermal degradation follows a random scission at the ester groups according to a β-hydrogen elimination.

PHB homopolymer also crystallizes slowly when is cooled down from the melting temperature and consequentially it suffers from an increase of the embrittlement when is subjected to an aging process. The storage at or above room temperature induces in the polymer a logarithmic increase in crystallinity with time. PHB also suffers of scarce impact resistance due both to its relatively high glass transition temperature (T_g = 9°C) and its characteristic to form very large spherulites. Because bacterially synthesized PHB is a completely isotactic stereoregular polyester, it has a high tendency to crystallize. However, the nucleation density of bacterial PHB is too low to

initiate efficient crystallization. As a result, it forms spherulites of extremely large size. The large-size spherulite and secondary crystallization promote interspherulitic cracking during storage of the polymer at room temperature, which is commonly known to impair the mechanical properties of the materials.

These disadvantageous properties, along with its high price, limit widely the application of PHB. Many studies have been devoted to modifying the brittleness of PHB. Copolymerization and blending are used as common methods to overcome the brittleness of PHB. Especially, blending of PHB with other compatible polymers of either synthetic or natural origin may occur in diverse advantages to the composite:

- they can decrease of the melting temperature of the polymer, which imply the possibility to process the material at lower temperature, avoiding or limiting its thermal degradation;
- they can improve the physico-mechanical properties as a consequence of the establishment of intermolecular interactions;
- they can act as nucleating agents, affecting the crystallization processes and thus improving the mechanical properties of the material.

References

1. King, D. The future of industrial biorefineries, white paper for the World Economic Forum 2010.
2. Naik, S.N. Production of first and second-generation biofuels: A comprehensive review. *Renewable and Sustainable Energy Reviews*, **2010**, *14 (2)*, 578-597.
3. Chisti, Y. Biodiesel from microalgae. *Biotechnology Advances*, **2007**, *25 (3)*, 294-301.
4. Sannigrahi, P.; Pu, Y.; Ragauskas, A. Cellulosic biorefineries – unleashing lignin opportunities. *Current Opinion in Environmental Sustainability*, **2010**, *2*, 383-393.
5. Fan, L.T.; Lee, Y.; Beardmore, D.H. Mechanism of the enzymatic hydrolysis of cellulose: Effects of major structural features of cellulose on enzymatic hydrolysis. *Biotechnol. Bioeng*. **1980**, *22*, 177-199.
6. Yu, Z.; Jameel, H.; Chang, H.M.; Park, S. The effect of delignification of forest biomass on enzymatic hydrolysis. *Bioresour. Technol*., **2011**, *102 (19)*, 9083-9089.
7. Grohmann, K.; Torget, R.; Himmel, M. Optimization of dilute acid pretreatment of biomass. *Biotechnol. Bioeng. Symp*., **1985,** *15*, 59–80.
8. Grohmann, K.; Torget, R.; Himmel, M. Dilute acid pretreatment of biomass at high solid concentrations. *Biotechnol. Bioeng. Symp*., **1986**, *17*, 135–151.
9. Yoon, H.H. Pretreatment of lignocellulosic biomass by autohydrolysis and aqueous ammonia percolation. *Korean J. Chem. Eng*., **1998**, *15 (6)*, 631–636.
10. Wyman, C.E. Handbook on bioethanol: production and utilization; Taylor & Francis; Washington DC, USA, 1996.
11. Sun, Y.; Cheng, J. Hydrolysis of lignocellulosic materials for ethanol production: A review. *Bioresource Technol***. 2002**, *83*, 1-11.
12. Stone, J.E.; Scallan, A.M.; Donefer, E.; Ahlgren, E. Cellulases and their Applications. Hajny, G.J., Reese, E.T., Eds.; American Chemical Society: Washington DC, USA, 1969.
13. Balan, V.; da Costa Sousa, L.; Chundawat, S. P. S.; Marshall, D.; Lansing, E.; Sharma, L. N.; Chambliss, C. K.; Dale, B. E. Enzymatic Digestibility and Pretreatment Degradation Products of AFEX-Treated Hardwoods (Populus nigra). *Biotechnol. Prog.*, **2009**, *25 (2)*, 365-375.
14. Mosier, N.; Wyman, C.; Dale, B.; Elander, R.; Lee, Y.Y.; Holtzapple, M.; Ladisch, M. Features of promising technologies for pretreatment of lignocellulosic biomass. *Bioresour Technol*, **2005**, *96*, 673-686.
15. Glasser, W.G.; Wright, R.S. Steam-assisted biomass fractionation. II. Fractionation behavior of various biomass resources. *Biomass Bioenerg.*, **1998**, *14*, 219-235.

16. Negro, M.J.; Manzanares, P.; Oliva, J.M.; Ballesteros, I.; Ballesteros, M. Changes in various physical/chemical parameters of Pinus pinaster wood after steam explosion pretreatment. *Biomass. Bioenerg*., **2003**, *25*, 301-308.
17. Liu, C.; Wyman, C.E. Impact of fluid velocity on hot water only pretreatment of corn stover in a flow through reactor. *Appl Biochem Biotechnol*, **2004,** *113 (116)*, 977-987.
18. Brunecky, R.; Vinzant, T.B.; Porter, S.E.; Donohoe, B.S.; Johnson, D.K.; Himmel, M.E. Redistribution of xylan in maize cell walls during dilute acid pretreatment. *Biotechnol Bioeng*, **2009**,*102*, 1537-1543.
19. South, C.R.; Wyman, C.E.; Martin, R.L. Two-stage method for pretreatment of lignocellulosic biomass. PCT Int. Appl. 2008.
20. Chang, V.S.; Nagwani, M.; Holtzapple, M.T. Lime pretreatment of crop residues bagasse and wheat straw. *Appl Biochem Biotechnol*, **1998**, *743*, 135-159.
21. Kim, T.H.; Lee, Y.Y. Pretreatment and fractionation of corn stover by ammonia recycle percolation process. *Bioresour Technol*, **2005**, *96*, 2007-2013.
22. Teymouri, F.; Laureano, L.; Alizadeh, H.; Dale, B.E. Optimization of the ammonia fiber explosion AFEX, treatment parameters for enzymatic hydrolysis of corn stover. *Bioresour Technol*, **2005,** *96*, 2014-2018.
23. Arato, C.; Pye, E.K.; Gjennestad, G. The lignol approach to biorefining of woody biomass to produce ethanol and chemicals. *Appl Biochem Biotechnol*, **2005,** *121 (124)*, 871-882.
24. Pan, X.; Kadla, J.F.; Ehara, K.; Gilkes, N.; Saddler, J.N. Organosolv ethanol lignin from hybrid poplar as a radical scavenger: relationship between lignin structure extraction conditions and antioxidant activity. *J Agric Food Chem*, **2006,** *54*, 5806-5813.
25. Hasegawa, I.; Tabata, K.; Okuma, O.; Mae, K. New pretreatmentmethods combining a hot water treatment and water/acetone extraction for thermo-chemical conversion of biomass. *Energy Fuels*, **2004,** *18*, 755-760.
26. Bozell, J.J.; Black, S.K.; Myers, M. Clean fractionation of lignocellulosics—a new process for preparation of alternative feedstocks for the chemical industry. In Proceedings of 8th International Symposium on Wood and Pulping Chemistry, vol. 1. 1995, 697-704.
27. Xie, H.; Zhao, Z.K. Selective break down of lignocellulose in ionic liquids. In: Ionic Liquids: Applications and Perspectives; Kokorin, A. Ed.; Intech, Rijeka, Croatia, 2011.
28. Palmqvist, E.; Hahn, B.; Fermentation of lignocellulosic hydrolysates. I: inhibition and detoxification. *Bioresour Technol*., **2000**, *74*, 17-24.
29. Helle, S.S.; Murray, A.; Lam, J.; Cameron, D.R.; Duff, S.J.B. Xylose fermentation by genetically modified Saccharomyces cerevisiae 259ST in spent sulfite liquor. *Bioresour Technol*, **2004**, *92*, 163-171.

30. Lawford, H.G.; Rousseau, J.D. Performance testing of zymomonas mobilis metabolically engineered for cofermentation of glucose xylose and arabinose. *Appl Biochem Biotechnol*, **2002**, *98*, 100:429-448.
31. Sheehan, J.; Himmel, M. Enzymes energy and the environment: a strategic perspective on the US Department of Energy's Research and Development Activities for Bioethanol. *Biotechnol. Prog*., **1999**, *15*, 817-827.
32. Wyman, C.E. What is and is not, vital to advancing cellulosic ethanol. *Trends Biotechnol*, **2007**, *254*, 153-157.
33. Sassner, P.; Galbe, M.; Zacchi, G. Techno-economic evaluation of bioethanol production from three different lignocellulosic materials. *Biomass Bioenerg*., **2008,** *32*, 422-430.
34. Schmer, M.R.; Vogel, K.P.; Mitchell, R.B.; Perrin, R.K. Net energy of cellulosic ethanol from switchgrass. *Proc Natl Acad Sci USA*, **2008,** *105*, 464-469.
35. Rogers, R.D.; Seddon, K.R.; Volkov, S. Green Industrial Applications of Ionic Liquids, 2003, Springer, Germany.
36. Liebert, T.; Heinze, T. Interaction of ionic liquids with polysaccharides 5. Solvents and reaction media for the modification of cellulose. *BioResources*, **2008**, *3(2)*, 576-601
37. Ke, M.; Zhou, A.; Song, Z.; Jiang,Q. Prog. Chem, 2007, 19(5), 671-679
38. Zhu, S.; Wu, Y.; Chen, Q.; Yu, Z.; Wang, C.; Jin, S.; Ding, Y.; Wu, G. Dissolution of cellulose in ionic liquids and its application: a mini-review, *Green Chem*., **2006**, *8*, 325-327.
39. Zhang, H.; Wu, J.; Zhang, J.; He, J. 1-allyl-3-methylimidazolium chloride room temperature ionic liquid: a new and powerful non-derivatizing solvent for cellulose, *Macromolecules*, **2005**, *38*, 8272-8277.
40. Kilpelainen, H.; Xie, A.; King, M.; Granstrom, S.; Argyropoulos, D.S. Dissolution of wood in ionic liquids, *J. Agric. Food. Chem*., **2007**, *55*, 9142-9148.
41. Swatloski, R.P.; Spear, S.K.H.; Rogers, R.D. Dissolution of cellulose with ionic liquids, *J. Am. Chem. Soc*., **2002**, *124*, 4974–4975.
42. Phillips, D.M.; Drummy, L.F.; Conrady, D.G.; Fox, D.M.; Naik, R.R.; Stone, M.O.; Trulove, P.C.; De Long, H.C.; Mantz, R.A. Dissolution and regeneration of Bombyx mori silk fibroin using ionic liquids. *J. Am. Chem. Soc*., **2004,** *126*, 14350–14351.
43. Remsing, R.C.; Swatloski, R.P.; Rogers, R.D.; Moyna, G. Mechanism of cellulose dissolution in the ionic liquid 1-n-butyl-3-methylimidazolium chloride: a 13C and 35/37Cl NMR relaxation study on model systems. *Chem. Commun*., **2006**, *12*, 1271–1273.
44. Singh, S.; Simmons, B.A.; Vogel, K.P. Visualization of biomass solubilisation and cellulose regeneration during ionic liquid pretreatment of switchgrass. *Biotechol. Bioeng*. **2009**, *104 (1)*, 68-75.

45. Yang, B.; Wyman, C.E. Pretreatment: The key to unlocking low-cost cellulosic ethanol. *Biofuels Bioproducts Biorefining*, **2008**, *2 (1)*, 26–40.
46. Lee, H.S.; Doherty, T.V.; Linhardt, R.J.; Dordick, J.S. Ionic liquid-mediated selective extraction of lignin from wood leading to enhanced enzymatic cellulose hydrolysis. *Biotechnol Bioeng*, **2009,** *102 (5)*, 1368–1376.
47. Kamiya, N.; Matsushita, Y.; Hanaki, M.; Nakashima, K.; Narita, M.; Goto, M.; Takahashi, H. Enzymatic in situ saccharification of cellulose in aqueous-ionic liquid media. *Biotechnol Lett***, 2008,** *30*, 1037–1040.
48. Swatloski, R.P.; Holbrey, J. D.; Spear, S.K.; Rogers, R. D. Ionic Liquids for the dissolution and regeneration of cellulose. In Molten Salts XIII, Proceedings of the thirteenth international symposium on molten salts. De Long, H. C.; Bradshaw, R. W.; Matsunaga, M.; Stafford, G. R.; Truelove, P. C. eds. 2002, 155-165.
49. Taj, S.; Munawar, M.A.; Khan, S. Natural fiber-reinforced polymer composites. *Proc. Pakistan acad. Sci*., **2007**, *44 (2)*, 129-144
50. Avella, M.; Martuscelli, E.; Raimo, M. Review. Properties of blends and composites based on poly(3- hydroxy)butyrate (PHB) and poly(3-hydroxybutyrate-hydroxyvalerate) (PHBV) copolymers. *J. Mat. Sci.*, **2000**, *35*, 523-545.
51. Luckachan, G.E.; Pillai, C.K.S. Biodegradable polymers – a review on recent trends and emerging perspectives. *J. Polym. Environ*., **2011**, *19*, 637-676.

3. ARCHAEOLOGICAL WATERLOGGED WOODS

3.1 Changes through deterioration in the constituent components of wood cell walls

The study of archaeological woods is to date focusing an increasing interest due to a novel awareness of the relevance of the valorization of cultural heritage. As broadly discussed in section 2, cell walls of wood are mainly composed of cellulose, hemicelluloses and lignins. In addition, several percent of ash and extractives are included.

In the constituent analysis of wood, when lignin is selectively removed, what is obtained is holocellulose. Holocellulose can be thought of as the total of cellulose and all hemicelluloses and represents the polysaccharide fraction that is easily decomposed and metabolized by wood-rot fungi. While the wood is buried under the ground, the holocellulose is considerably decomposed and tends to disappear. In contrast to the polysaccharides, the quantitative decomposition and disappearance of lignin is substantially less, and as a result its content increases relatively. In recent wood, holocellulose content is about 70% and lignin content is about 30%. In excavated wood, the holocellulose content drops to about 20% while lignin increases relatively to about 80%. Although the quantitative decrease is small, it is clear that lignin actually decomposes and decreases under the ground.

Archaeological waterlogged woods are actually in a completely different state if compared to archaeological woods excavated in dry environments. Under favorable conditions of low temperature and low oxygen, wooden artefacts can survive underwater in a surprisingly good condition, as happened in the case of the Vasa ship conserved in the Vasa Museum in Stockholm (Sweden) (*1*,*2*), or for the Roman and Etruscan shipwrecks recovered in the San Rossore harbor in Pisa (Italy) (*3*). When the structure of waterlogged woods is observed under a microscope, it can be seen to be surprisingly well preserved. Regardless of the substantial decomposition and

disappearance of constituents of the cell walls, the structural characteristics are well enough preserved that the type of wood can be identified. This reflects the fact that the components of the cell wall have decomposed and lisciviated away without changing the size of the cell wall itself. New voids are formed in the parts of the cell wall where components have disappeared, immediately filled by water that provides a powerful aid to the maintenance of the original wood shape.

Nevertheless, it has been shown that bacteria can slowly degrade waterlogged wood even under near anoxic conditions eroding mainly the cellulosic components as source of nutrients (*4*). As a consequence, expensive and technically difficult consolidation treatments are required. Therefore, chemical characterization of waterlogged archaeological wood is of fundamental importance not only for understanding the degradation processes of wood in archaeological objects but also in the development of consolidation and conservation procedures.

3.2 Diagnostic and related opportunities with ionic liquids

In degraded wood the content of cellulose is generally very low compared to lignin, especially after long exposure to wet environments. Due to the almost complete loss of cellulosic components, the chemical characterization of lignin is an aspect of primary importance in the diagnosis and conservation of waterlogged wood artefacts.

Traditionally, lignin contents are determined by the standard Klason UV lignin content method (*5*). This involves extensive chemical modification of the lignocellulosic substrate and provides no structural information. Gel permeation chromatography (GPC) is useful to define the molecular weight distribution and related molecular weight indexes of residual lignin but, again, no chemical features are elucidated by this technique. Further information about specific lignin structures has been provided by the advent

of ^{1}H-NMR, although the limited ppm range causes a significant overlap of signals (*6*). ^{13}C-NMR offers a wider ppm range and resolution between individual polymer backbone resonances (*7*). Nevertheless, the low sensitivity of the ^{13}C nuclei often requires some extent of compromise on acquisition conditions to achieve adequate sensitivity, reducing the quantitative viability of the analysis. Two- and three-dimensional ^{1}H and ^{13}C NMR have emerged as powerful tools in the elucidation of lignin structure, especially in regard to phenylpropanoids units and interunit linkages. However, one major drawback of multidimensional techniques is the reduction in quantitivity.

In the last few years, the use of phosphorus-containing derivatizing reagents for lignin analysis has grown in importance (*8*). Phosphorus-31 is a nucleus that is 100% naturally abundant. The sensitivity of a ^{31}P-NMR experiment is only 15 times less than that of a proton NMR experiment and the range of ^{31}P chemical shifts is more than 1000 ppm. Various types of organophosphorus compounds give signals within narrow ranges, characteristic of the oxidation state of the phosphorus nuclei. All of these factors make ^{31}P-NMR an ideal tool in the study of labile groups in lignin.

On the other hand, the studies dealing with the analysis of intact ancient wood have been mainly focused on the use of scanning electron microscopy (SEM), FT-IR spectroscopy, pyrolysis GC-MS spectrometry (PY/GC/MS) of volatile wood extractives and X-ray diffraction. SEM of wood allows the identification of the nature of microbiological attack that occurred by the characterization of the different morphological characteristics of the residual cell walls (*9*). FT-IR spectroscopy with the aid of deuterium exchange method allows to clarify the ageing process of archaeological wood as a change in the state of order on a macromolecular structural level (*10*). X-ray diffraction is a technique that can identify the presence of heteroatoms. It was applied at the determination of sulfates and sulphides and sulfur accumulated

in waterlogged wood (*11*). GC-MS pyrolysis allows the identification of volatile species after thermal degradation in ancient wood (*12–14*). However, these techniques are not able to elucidate the chemical structure of intact wood, which in turn means the characterization of an unaltered lignin.

At present GPC, 2D-HSQC-NMR, and ^{31}P-NMR are the only experimental techniques that enable to gain detailed information on the chemical structure of native lignin, by analyzing the whole lignocellulose sample after a suitable dissolution and functionalization in an ionic liquid media.

The following paragraphs describe the basic advances in each of the aforementioned analytical techniques.

3.2.1 GPC

Gel permeation chromatography is a commonly used method of measuring the size of macromolecules. Depending on their size, the macromolecules can diffuse in varying proportions into the porous gel.

To break the highly organized structure of lignocellulose down to analyzable fractions, bonds must be broken, and random scission of linkages will lead to a wide range of molecular sizes. It is typical of isolated lignin samples to be very polydisperse, and the measured molecular size range is very much dependent on the isolation procedure.

An important limitation of the study of wood polymers is that properties such as molecular mass and molecular shape have been investigated almost exclusively with isolated samples, and these characteristics of the wood polymers in situ can be deduced only by inference.

Among other advantages, solubilization in ionic liquids opened new perspectives in the chromatographic study of native lignocellulosic materials (*15*). A novel approach, reported by Zoia et al. (*16*), is based on the dissolution of the ball-milled samples in the ionic liquid 1-allyl-3-methylimidazolium chloride, [amim]Cl, and their functionalization. During

this procedure, essentially all lignocellulose hydroxyl groups (from both polysaccharides and lignin) are functionalized as benzoyl esters, facilitating the visualization of all components by GPC with UV detection. Using comparative GPC analyses of benzoylated intact wood and correspondent benzoylated holocellulose and lignin fractions, it is possible to obtain valuable information on the molecular weight distributions and, in particular, arrive at information pertaining to the elusive lignin-carbohydrate linkages.

3.2.2 2D-HSQC-NMR

2D-NMR provides information about the structure of the whole macromolecole and is a powerful tool for lignin structural characterization, particularly in the identification of different units and in the unambiguous demonstration of their presence (*17-21*). Heteronuclear single quantum coherence (HSQC) NMR spectra of lignin show three regions corresponding to aliphatic, side-chain, and aromatic ^{13}C-^{1}H correlations. The aliphatic (non-oxygenated) region includes signals with no structural information. The aliphatic side chain region yields information about the relative abundance of interunit linkages in the whole polymer. Side chains absorbances show for all lignins a predominance of β-O-4 ether linkages (66-72% of total side-chains), followed by β-β resinol-type linkages (16-19%) and lower amounts of β-5 phenylcoumaran-type (3-7%) and β-1 spirodienone-type linkages (1-4%). Aromatic regions of the HSQC spectra highlight the differences in the p-hydroxyphenyl, guaiacyl, syringyl and related monomers distributions in the lignins. Simple guaiacyl : syringyl (G : S) and even p-hydroxyphenyl : guaiacyl : syringyl (H :G: S) integral ratios can be obtained readily by integrating the contours.

Polymer isolation approaches at best fractionate the polymer of interest, not always representatively, and at worst alter that polymer. It is clear how a structural analysis to thoroughly characterize the material, including

revealing details of the connectivity between components, would be of considerable use in the elucidation of the complex and elusive nature of the interactions among the various wood components. Recent advances in dissolution of cell wall materials, even if currently still limited to severely ball-milled walls, have allowed fractionated walls to be examined without the need for component isolation. Most of nowadays knowledge about 2D-NMR analysis of intact cell wall should be ascribed to the pioneristic work by Ralph et al. (*22-26*). Solution-state NMR techniques, coupled with appropriate dissolution or gelling solvents (DMSO-d_6/N-methylimidazole-d_5; DMSO-d_6/pyridine-d_5) have been proven to be powerful tools for characterizing lignocellulosic biomass without the need for isolation and purification of individual components. The incredible complexity of the cell wall naturally results in complex spectra, but the considerable dispersion provided by 2D-NMR methods, such as $^{13}C–^{1}H$ correlation spectroscopy, allows for at least some key resonances from many of the components to be sufficiently resolved to allow substantive interpretation.

3.2.3 ^{31}P-NMR

Early works on ^{31}P-NMR of lignin preparations focused on the phospholanes produced after derivatization of hydroxyl groups with 2-chloro-1,3,2-dioxaphospholane. In a series of paper by Argyropoulos et al. *(27,28,29*) the potential of this technique was evaluated by investigating a large variety of model compounds with structures likely to occur in lignins. This research showed that the technique could distinguish not only some forms of phenolic hydroxyls but also primary and secondary aliphatic hydroxyls and erythro- and threo-forms of β-O-4 structures. However, signal overlap between the syringyl phenolic structures and those belonging to condensed phenolic groups limited its capacity for distinction and accurate determination of these moieties. Another phosphitylation reagent was then developed: 2-chloro-

4,4,5,5-tetramethyl-1,3,2-dioxaphospholane, which was found to be particularly good at resolving this region at the expense of fine resolution between primary and secondary aliphatic hydroxyls (*30*). The ^{31}P-NMR signals were now well resolved for the free phenolic hydroxyls belonging to guaiacyl (G, originating from coniferyl alcohol monomer), syringyl (S, originating from the sinapyl alcohol monomer or ferulate), p-hydroxyphenyl (H, originating from p-coumaryl alcohol monomer or p-coumarate), and most C5 and C6 related condensed phenolic forms. In addition, signals due to carboxylic acids were well separated from all other signals, allowing a direct access to this important information related to the fundamental changes occurring within lignins under oxidative conditions (*31*). Background informations about ^{31}P spin-lattice and spin-spin relaxation behaviour of phosphitylated lignin were then used to design an experimental protocol for obtaining quantitative ^{31}P-NMR spectra (*32*). As a result, the phosphitylated hydroxyls in lignin can be quantitatively assessed against an internal standard (endo-N-hydroxy-5-norbornene-2,3-dicarboximide) demonstrating adequate stability and satisfactory resolution from other lignocellulosic functionality regions, in the ^{31}P-NMR spectra after phosphitylation.

Although this provides an expedient technique for the determination of lignin functionalities in purified lignins, the insolubility of wood in traditional molecular solvents does not allow for quantification of hydroxyl functionalities from fully representative and potentially artifact free native lignin, in minimally treated lignocellulose samples. This requires a solvent capable of solvating the carbohydrate portion of the samples in addition to the lignin. These characteristics were met by the ionic liquids. Ionic liquids such as [amim]Cl and [bnmim]Cl have been shown to dissolve wood to such a state that it can be chemically modified (*33, 34*). With the appropriate conditions determined for formation and solubilization of the lignin phosphite esters, this technique can now be applied to wood (*35*).

References

1. Hafors, B. Conservation of the Swedish warship Vasa from 1628. Vasa Studies 18, 2001.
2. Sandstrom, M.; Fors, Y.; Persson, I. The Vasa's new battle: sulphur, acid and iron, Vasa Studies 19, 2003.
3. Giachi, G.; Bettazzi, F.; Chimichi, S.; Staccioli, G. Chemical characterization of degraded wood in ships discovered in a recent excavation of the Etruscan and Roman harbour of Pisa. *Journal of Cultural Heritage*, **2003**, *4*, 75–83.
4. Blanchette, R.A.; Nilsson, T.; Daniel, G.F.; Abad, A. In: Archaeological Wood, R.M. Rawell, R.J. Barbour Eds., , Adv. in Chem. Series, Am. Chem. Soc., 1990, vol. 225.
5. Determination of Acid-Insoluble (Klason) Lignin, Tappi standard Method, T222; Technical Association of the Pulp and Paper Industry, August 2nd, 2002.
6. Lundquist, K. Methods in lignin chemistry. In: Proton 1H Spectroscopy; Lin, S.Y.; Dence, C.W. Eds.; Springer: Berlin, Germany, 1992, 242-249.
7. Robert, D. Methods in lignin chemistry. In: Carbon-13 Nuclear Magnetic Resonance Spectrometry; Lin, S.Y.; Dence, C.W. Eds.; Springer: Berlin, Germany, 1992, 250-273.
8. Argyropoulos, D.S. Hetronuclear NMR spectroscopy of lignins. In: Lignin and Lignans: Advances in Chemistry; Heitner, C.; Dimmel, D.R.; Schmidt, J.A. Eds.; CRC Press, Taylor & Francis Group, Bova Raton, FL, 2010, 245-265.
9. Nilsson, T.; Daniel, G. Structure and aging process of dry archaeological wood. In: Archaeological wood, Advances in Chemistry series; Rowell, R.M.; Barbour, R.J. Eds., vol. 255, ACS, Washington DC, 1990, 67–86.
10. Tsuchikawa, S.; Yonenobu, H.; Siesler, H.V. Near-infrared spectroscopic observation of the ageing process in archaeological wood using a deuterium exchange method. *Analyst***, 2005**, *130*, 379–384.
11. Schuster, I.; Pecaut, J.; Tran, K. X-ray diffraction for serving in the preservation of water gorged archaeological wood. *J. Phys. IV Proc*., **2004**, *118*, 377–384.
12. Saiz-Jimenez, C.; Boon, J.J.; Hedges, J.I.; Hessels, J.K.C.; de Leeuw, J.W. Chemical characterisation of recent and buried wood by analytical pyrolysis. Comparison of pyrolysis data with 13C NMR and wet chemical data. *J. Anal. Appl. Pyrolysis*, **1987**, *11*, 437-450.
13. Ucar, G.; Meier, D.; Faix, O.; Wegener, G. Analytical pyrolysis and FT-IR spectroscopy of fossil Sequoiadendron giganteum (Lindl.) wood and MWLs isolated hereof. *Holz Roh- Werkst*., **2005**, *63*, 57–63.
14. Shedrinsky, A.M.; Indictor, N.; Baer, N.S. Application of analytical pyrolysis to problems in art and archaeology: a review, *J. Anal. Appl. Pyrolysis*, **1989**, *15*, 393–412.

15. Xie, H.; Zhao, Z.K. Selective breakdown of lignocellulose in ionic liquids. In: Ionic Liquids: Applications and Perspectives; Kokorin A. Ed., InTech, Rojeca, Croatioa, 2011, 61-80.
16. Zoia, L.; King A. W. T.; Argyropoulos, D. S. Molecular weight distributions and linkages in lignocellulosic materials derivatized from ionic liquid media. *J.Agric. Food Chem.* **2011**, *59 (3)*, 829-838.
17. Ralph, J.; Marita, J.M.; Ralph, S.A.; Hatfield, R.D.; Lu, F.; Ede, R.M.; Peng, J.; Quideau, S.; Helm, R.F.; Grabber, J.H.; Kim, H.; Jimenez-Monteon, G.; Zhang, Y.; Jung, H.-J.G.; Landucci, L.L.; MacKay, J.J.; Sederoff, R.R.; Chapple, C.; Boudet, J.; Rencoret, A.M. et al. Solution-state NMR of lignin. In: Advances in Lignocellulosics Characterization. Argyropoulos, D.S. Eds., Tappi Press, Atlanta, GA, 1999, 55–108.
18. Ralph, S. A.; Ralph, J.; Landucci, L. L. NMR database of lignin and cell wall model compounds, 2004; available at http://www.dfrc.ars.usda.gov/software.html.
19. Capanema, E.A.; Balakshin, M.Y.; Kadla, J.F. A comprehensive approach for quantitative lignin characterization by NMR spectroscopy. *J. Agric. Food Chem*., **2004**, *52*, 1850–1860.
20. Capanema, E.A.; Balakshin, M.Y.; Kadla, J.F. Quantitative characterization of a hardwood milled wood lignin by nuclear magnetic resonance spectroscopy. *J. Agric. Food Chem*., **2005**, *53*, 9639–9649.
21. Balakshin, M.Y.; Capanema, E.A.; Chen, C.-L.; Gracz, H.S. Elucidation of the structures of residual and dissolvedpine kraft lignins using an HMQC NMR technique. *J. Agric.Food Chem*., **2003**, *51*, 6116–6127.
22. Lu, F.; Ralph, J. Non-degradative dissolution and acetylation of ball-milled plant cell walls: high-resolution solution-state NMR. *The Plant Journal*, **2003**, *35*, 535-544
23. Yelle, D.J.; Ralph, J.; Frihart, C.R. Characterization of non derivatized plant cell walls using high-resolution solution-state NMR spectroscopy. *Magn Reson Chem*., **2008**, *46*, 508–17
24. Hedenstrom, M.; Wiklund-Lindstrom, S.; Oman, T.; Lu, F.; Gerber, L.; Schatz, P.; Sundberg, B.; Ralph, J. Identification of lignin and polysaccharide modification in Populus wood by chemometric analysis of 2D NMR spectra from dissolved cell walls. *Mol. Plant*, **2009**, *2 (5)*, 933-942.
25. Kim, H; Ralph, J. Solution -state 2D NMR of ball-milled plant cell wall gels in DMSO-d6/pyridine-d5. *Org. Bimol. Chem*., **2010**, *8*, 576–91.
26. Lu, F.; Ralph, J. Solution-state NMR of lignocellulosic biomass. *J. of Biobased Materials and Bioenergy*, **2011**, *5 (2)*, 169-180.
27. Argyropoulos, D.S. ^{31}P NMR in wood chemistry: a review of recent progress. *Research on chemical intermediates*, **1995**, *21 (3-5)*, 373-395.

28. Archipov, Y.; Argyropoulos, D.S.; Bolker, H.I.; Heitner, C. ^{31}P NMR spectroscopy in wood chemistry. Part I. Lignin model compounds. J. *Wood Chem. Technol*., **1991**, *11 (2)*, 137-157.
29. Argyropoulos, D. S.; Bolker, H. I.; Heitner, C.; Archipov, Y. 31P NMR Spectroscopy in Wood Chemistry. Part V, Qualitative Analysis of Lignin Functional Groups. *J. Wood Chem. Technol*. **1993**, *13 (2)*, 187-212.
30. Granata, A.; Argyropoulos, D.S. 2-Chloro-4, 4, 5, 5-tetramethyl-1, 3, 2-dioxaphospholane, a reagent for the accurate determination of the uncondensed and condensed phenolic moieties in lignins. *J. Agric. Food Chem.* **1995**, *43*, 1538-1544.
31. Sun, Y.; Argyropoulos, D.S. Fundamentals of high pressure oxygen and low pressure oxygen-peroxide delignification of softwood and hardwood kraft pulps: a comparison. *J. Pulp Paper Sci*., **1995**, *21 (6)*, 185-190.
32. Argyropoulos, D.S. Quantitative phosphorus-31 NMR analysis of lignin: a new tool for the lignin chemist. *J. of Wood Chemistry and Technology*, **1994**, *14 (1)*, 45-63.
33. Helm, R. F. Lignin: Properties and Materials. In: Lignin-Polysaccharide Interactions in Woody Plants; Schultz, T. P., Ed.; American Chemical Society: Washington, DC, 2000; Vol. 742,161-171.
34. Koshijima, T.; Watanabe, T. Association between Lignin and Carbohydrates in Wood and Other Plant Tissues. In: Wood Science; Springer: Heidelberg, Germany, 2003, Vol. 1, 298.
35. King, A.W.T.; Kilpelainen, I.; Heikkinen, S.; Jarvi, P.; Argyropoulos, D. S. Hydrophobic interactions determining functionalized lignocellulose solubility in dialkylimidazoliumchlorides, as probed by ^{31}PNMR. *Biomacromolecules*, **2009**, *10*, 458–463.

RESULTS AND DISCUSSION

4. ANNUAL PLANTS: CHARACTERIZATION AND LIGNIN-CARBOHYDRATE COMPLEXES DETECTION (*1*)

4.1 Background, objectives, and strategies

Traditionally, two types of materials are regarded as renewable feedstock: woody-based biomass and agricultural biomass. In recent years, lignocellulosic biomass from agricultural residues and herbaceous energy crops are under intense investigation due to its annual renewability and large annual biomass stock (*2*). As replacement for fossil fuels, lignocellulosic biomass, especially from herbaceous plants, represents a promising alternative for the production of biofuels due to its naturally high content of fermentable reducing sugars (*3*, *4*).

Lignocellulose is an extremely structurated natural composite made up of three main biopolymers: cellulose, hemicellulose, and lignin. Cellulose consists of linear chains of β(1-4) linked D-glucopyranose units which, when found in cell wall, is difficult to break down into glucose because of its extensive H-bonded network and highly organized crystalline structure. Hemicellulose is a carbohydrate heteropolymer composed of several different sugars including six-carbon and five-carbon sugars and is easily broken down into its building blocks. Lignin is a complex and irregular polymer network, composed of randomly cross-linked phenylpropanoid units, that acts as a glue holding cellulose and hemicellulose together.

Lignocellulose biorefinery generally includes three fundamental steps: pretreatment to fractionate the recalcitrant lignocellulose structure; enzymatic hydrolysis of the isolated cellulose moiety, by which cellulases hydrolyze reactive intermediates to fermentable sugars; and fermentation, which produces cellulosic ethanol or other bio-based chemicals (*5*).

Because of the resistant structure of crystalline cellulose and natural composite structures of lignocellulosics, efficient pretreatment technologies are needed prior to the enzymatic hydrolysis. The recalcitrance of

lignocellulosic materials to enzymatic hydrolysis is substantially attributed to the low accessibility of crystalline cellulose fibers, which restricts cellulase activity (*6,7*). The presence of lignin and hemicellulose on the surface of cellulose prevents cellulase from accessing the substrate and it is recognized that enzymes performance is reduced during lignocellulose hydrolysis by interaction with lignin and, especially, lignin-carbohydrate complexes (LCCs) (*8)*. A number of different approaches have been proposed so far for lignocellulosic pretreatment aimed at the removal of lignin (either in the form of LCCs or free polyphenols) including biological, chemical, physical and thermal processes. However, all of them results in a substantial loss in fermentable sugar content of the residual polysaccharides (*9*).

In the last few years, the development of ionic liquids and their application as green solvents for the pretreatment and fractionation of lignocellulosic biomass led to an intensive research which proved the opportunity of selectively extract a chemically unaltered lignin and simultaneously yield an unaltered, highly biodegradable cellulose fraction (*10-13*). Ionic liquids (ILs) are defined as organic salts that melt below 100°C, entirely composed of ions, typically large organic cations and small inorganic anions. The most promising cations in the dissolution of lignocellulose are derivatives of imidazolium salts, which are able to solvate the aromatic character of lignin by means of aromatic π-π interaction, whereas counter chloride anions are usually the most effective due to their hydrogen bonds destroying capability. Thanks to these properties, a pretreatment involving ionic liquids requires mild reaction conditions and is expected to decrease sugar degradation, inhibitor formation, processing costs, and capital investments tanks to the recycling opportunity associated with ionic liquids. Nevertheless, the presence of LCCs could not be avoided due their intrinsic nature that is a covalent bond connecting a polysaccharide chain to a lignin moiety. Indeed, whereas a fairly large lignin fraction could definitely be solubilized and

removed from the lignocellulosic substrate (*10-12*), polysaccharides are regenerated from the ionic liquid solution after the addition of an antisolvent such as water or ethanol (*14*). Even if the regenerated lignocellulosic material possesses a relatively homogeneous and amorphous morphology which contributes to the enhanced enzymatic digestibility, it is still clear the need for an experimental methodology able to describe the extent of connection between lignin and polysaccharides. Such information would be of considerable importance in the choice of the most appropriate pretreatment in order to maximize the yield in fermentable sugars while minimizing processing time and cost. Recently, Zoia et al. (*15*) reported a methodology based on comparative GPC analyses of benzoylated intact wood and correspondent benzoylated holocellulose and lignin fractions. Valuable information could be achieved by means of this approach, but a preliminary processing of the examined substrate, aimed at its fractionation, could not be avoided.

In this work we propose a straightforward chromatographic method for the detection of LCCs based on the acetylation and benzoylation of the whole lignocellulose specimen. Extensively ball-milled samples of four herbaceous plants (rice husk, wheat straw, *Arundo donax*, and *Miscanthus sinesis*) were dissolved in the ionic liquid 1-allyl-3-methylimidazolium chloride ([amim]Cl) and then reacted with benzoyl chloride or acetyl chloride in the presence of pyridine under mild conditions. Both the highly substituted lignocellulosic esters exhibited an enhanced solubility in tetrahydrofuran (THF), but developing a different instrumental response when submitted for GPC-UV analysis. Specifically, benzoylated specimens enabled the UV-detection of the whole substrate components - cellulose, hemicellulose, and lignin - regardless of possible chemical connection among them, whereas acetylated specimens accounted for the sole contribution of LCCs and of course possibly free lignin due to the lack of UV-chromophores in the

unbound polysaccharide portion. The GPC-UV analyses of each cellulosic and hemicellulosic fraction offered a valuable method for the assessment of the LCC-bound polysaccharide nature. Moreover, the method allowed to venture a purely qualitative evaluation of the LCCs molecular weight and composition in terms of hemicellulose to lignin ratio. As a completion of this work, an exhaustive chromatographic and spectroscopic characterization of each extracted lignin is provided as a preliminary investigation.

4.2 Experimental results

4.2.1 Lignins characterization

Acidolysis lignin specimens extracted from rice husk, wheat straw, *Arundo donax*, and *Miscanthus sinesis* were thoroughly characterized by means of GPC, 2D-HSQC and ^{31}P-NMR analyses. Results concerning compositional evaluation, GPC, and ^{31}P-NMR characterization are reported in *Table 1*.

	RICE HUSK - AL	ARUNDO DONAX - AL	WHEAT STRAW - AL	MISCANTHUS SINENSIS - AL
Lignin (%)	21.8	29.9	18.6	25.6
Ash (%)	16.0	4.7	9.4	3.1
Holocellulose (%)	62.2	65.4	72.0	71.3
GPC				
M_n (g/mol)	10200	15000	10200	9600
M_w (g/mol)	41000	81800	57500	36000
M_p (g/mol)	5100	6400	4900	5500
I	4.0	5.5	5.6	3.7
^{31}P NMR				
Aliphatic -OH, tot (mmol/g)	2.89	4.35	3.42	3.47
Aliphatic -OH, β-O-4 $^{(A)}$ (mmol/g)	1.27	1.74	1.31	1.69
Cond PhOH $^{(L)}$ + S-OH $^{(D)}$ (mmol/g)	0.21	0.32	0.29	0.27
G-OH $^{(F)}$ (mmol/g)	0.61	0.61	0.67	0.58
P-OH $^{(H)}$ (mmol/g)	0.66	0.53	0.43	0.77
COOH (mmol/g)	0.22	0.15	0.29	0.17

Table 1. Compositional evaluation, GPC, and ^{31}P-NMR data for acidolysis lignin specimens extracted from rice husk, *Arundo donax*, wheat straw, and *Miscanthus sinensis*. ^{31}P-NMR quantitative data are expressed as mmol per gram of extracted lignin. Chemical structures of each assigned NMR signal are reported in *Figure 2*.

Similar results were obtained for each sample. The isolated lignins were a p-hydroxyphenyl : guaiacyl : syringyl lignin typical of herbaceous species, with

each of the three main constituent units well represented. GPC analysis also confirmed a similar molecular weight distribution for every lignin.

As a consequence of the development of bioethanol production platforms, large amounts of lignin are produced as side stream. Uniform chemical features in lignin process streams are therefore profitable and desired properties as they could be utilized as a feedstock for green chemicals, offering a significant opportunity for enhancing the operation of a lignocellulosic biorefinery regardless of the origin of the feeding material.

Results from qualitative 2D-HSQC-NMR analyses are reported in *Table 2*. β-arylether subunits (β–O–4) are the major interunit structure of lignins, followed by phenylcoumaran (β–5) and pinoresinol (β-β) units. 2D-HSQC-NMR analyses also provide a qualitative assessment of the presence of p-coumarates and ferulates (*16*), particularly abundant in herbaceous plants and involved in lignification, crosscoupling with lignin monomers and possibly oligomers.

	RICE HUSK - AL	**ARUNDO DONAX - AL**	**WHEAT STRAW - AL**	**MISCANTHUS SINENSIS - AL**
2D-HSQC-NMR Sidechains Region				
β-O-4 [(A)]	+ + +	+ + +	+ + +	+ + +
β-5 [(B)]	+ +	+ +	+	n.d.
β-β [(C)]	n.d.	+ +	+	+
2D-HSQC-NMR Aromatic Region				
S-OH [(D)]	+ + +	+ + +	+ + +	+ + +
S-OH, α-ketone [(E)]	n.d.	n.d.	+ +	n.d.
G-OH [(F)]	+ + +	+ + +	+ + +	+ +
Ferulate [(G)]	n.d.	+	+	n.d.
P-OH [(H)]	n.d.	+ +	+ + +	+ +
p-Coumarate [(I)]	+ + +	+ + +	+ + +	+ + +

Table 2. 2D-HSQC-NMR data for acidolysis lignin specimens extracted from rice husk, *Arundo donax*, wheat straw, and *Miscanthus sinensis*. Outcomes are reported as relative abundance and differentiated in sidechain and aromatic region absorptions. Chemical structures of each assigned NMR signal are reported in *Figure 2*.

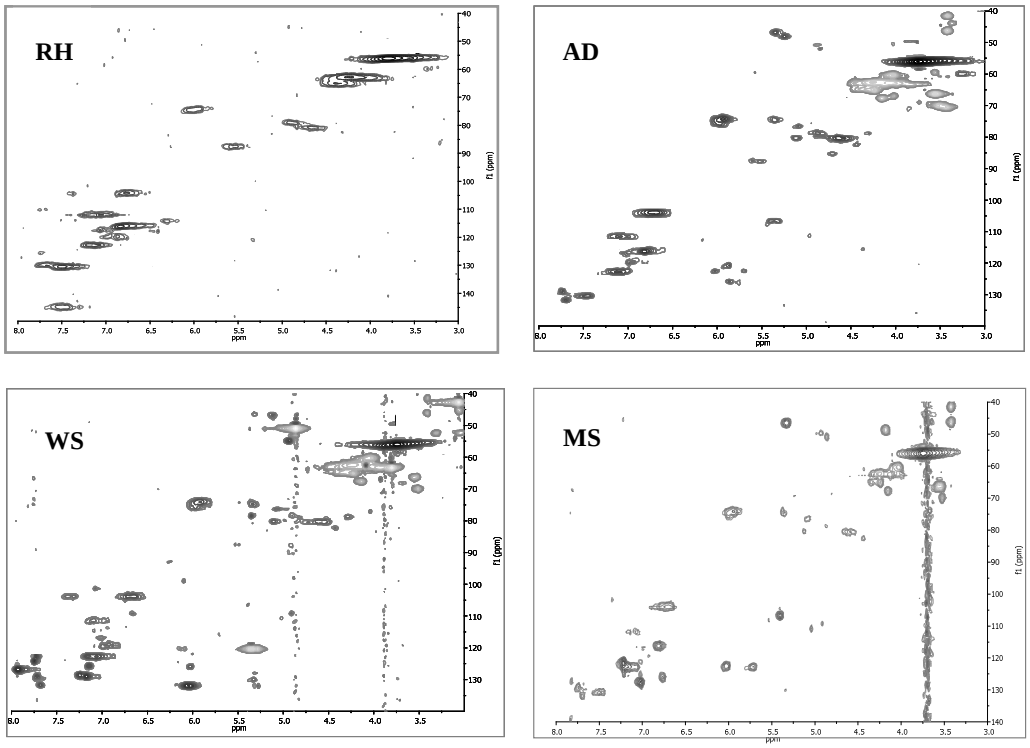

Figure 1. 2D-HSQC-NMR spectra of extracted lignins. Clockwise: rice husk, *Arundo donax*, *Miscanthus sinensis*, and wheat straw. Side chain region $^{13}C/^{1}H$ correlation area: 40-90/3-6. Aromatic region $^{13}C/^{1}H$ correlation area: 100-140/6-8.

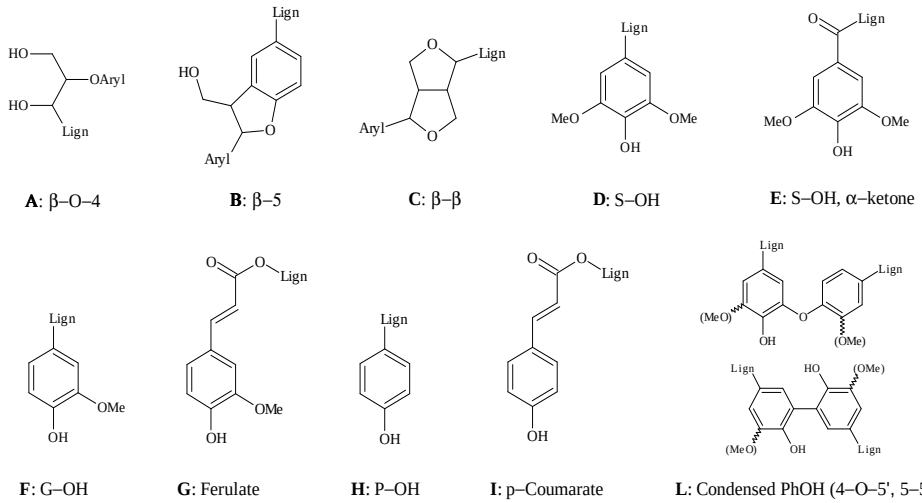

A: β–O–4 **B**: β–5 **C**: β–β **D**: S–OH **E**: S–OH, α–ketone

F: G–OH **G**: Ferulate **H**: P–OH **I**: p–Coumarate **L**: Condensed PhOH (4–O–5', 5–5')

Figure 2. Intermonomeric (A, B, C), phenolic (D, F, H, L), and other aromatic units (E, G, I) detected by 2D-HSQC-NMR and ^{31}P-NMR spectroscopy.

All grasses have lignins that are acylated by p-coumaric acid. NMR work on grasses (*17,18*) showed that the acylation is exclusively at the γ-position, implicating enzymatic processes in the formation of the ester. The DFRC (Derivatization Followed by Reductive Cleavage) method, which leaves such γ-esters intact, further established the γ-acylation and indicated that p-coumarates were predominantly on syringyl units (*19*). This was recognized as the reason why both syringyl and p-coumarates units were so well represented in the HSQC spectra of all four herbaceous substrates.

Cross-coupling of ferulates with lignin monomers (and possibly oligomers) incorporates ferulates intimately into lignin in a variety of structures and results in lignin-polysaccharide cross-linking (*20,21*). Moreover, there is growing evidence that ferulates act as nucleation sites for lignification in grasses *(22*). Even if ferulate is not one of the three accepted monolignols constituting lignin, it behaves like a monomer, radically cross-coupling with monolignol radicals and fully and inextricably incorporating into the phenylpropanoid polymer. In grasses, it is likely that most lignin molecules have ferulate incorporated into them. Ferulates incorporated this way therefore analyze as lignin and there is no way to isolate or separate lignins from them. Therefore, it has been suggested that ferulates are a natural component of lignins in grasses (*23*). Their full incorporation into the polymer network could justify the lower amount of ferulates units detected by the HSQC experiment if compared to p-coumarates.

4.2.2 Set up of the chromatographic method

In order to set up the chromatographic system for the detection of LCCs, UV spectra of acetylated and benzoylated samples of cellulose and lignin extracted from rice husk were acquired between 230 and 430 nm. The spectra of acetylated and benzoylated lignin, and benzoylated cellulose showed different absorption bands between 240 and 280 nm. The two major bands in

these samples were ascribed to the presence of aromatic units (either from lignin itself or the derivatization with benzoyl chloride or both), while the spectrum of acetylated cellulose was not well resolved, with a weak and broad absorbance around 330 nm. *Table 3* reports the extinction coefficients for acetylated and benzoylated lignin and cellulose samples extracted from rice husk, calculated from the absorbance values measured at 240 and 280 nm.

	Concentration (mg/ml)	**ε 240 nm (ml/mg*cm)**	**ε 280 nm (ml/mg*cm)**
Cellulose acetylated	0.1	4.00	0.96
Cellulose benzoylated	0.1	30.37	9.43
Lignin acetylated	0.1	25.65	19.13
Lignin benzoylated	0.1	34.12	16.07

Table 3. Results of UV-Vis analyses of acetylated and benzoylated cellulose and lignin samples extracted from rice husk. The extinction coefficient was calculated according to the Lambert-Beer law, A=[ ]*d*ε, where A is the measured absorbance, d the path length (cm), [ ] the concentration (mg/mL) and ε the extinction coefficient (mL/mg*cm) at the given wavelength.

When analyzed at 240 nm, benzoylated cellulose and benzoylated lignin presented similar, large ε values (30.37 *versus* 34.12). Instead, when analyzed at 280 nm, acetylated cellulose showed a really low ε, with an instrumental response 20 times lesser than lignin (0.96 *versus* 19.13). On the basis of these results, we decided to choice 240 nm as recording wavelength for GPC analysis of benzoylated samples in order to maximize their instrumental response, and 280 nm as recording wavelength for GPC analysis of acetylated samples to minimize the contribution of free polysaccharides while benefitting of the natural high absorbance intensity of the polyphenol moiety. The GPC analyses of acetylated and benzoylated cellulose and lignin (concentration 1 mg/mL) are reported in *Figure 3*.

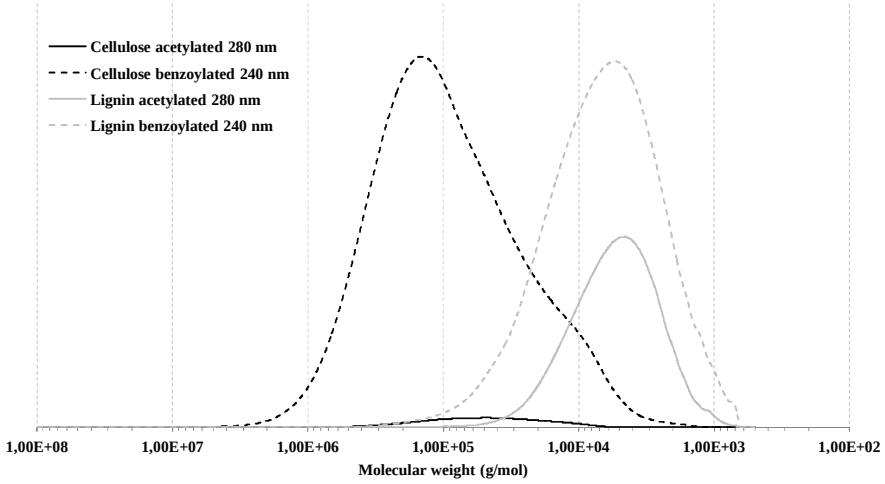

Figure 3. Overlapped GPC-UV profiles of cellulose and lignin, both acetylated and benzoylated.

As expected, the chromatograms highlighted that after benzoylation both cellulose and lignin are readily detected with a similar instrumental response, while after acetylation lignin showed a much higher response respect to the acetylated cellulose. This is related to the lack of strong chromophores in the polysaccharide fraction after acetylation and represented the key point for the recognition of LCCs in native substrates. Any absorbance of acetylated native material should therefore be related to the presence of aromatic compounds. Any polysaccharide, if bound to these natural chromophores, as is the case of LCCs, will give a UV response leading to a particular molecular weight distribution accounting for these high molecular weight fractions. Residual absorbance of cellulose after acetylation was ascribed to the presence of by-products arising from the reaction of cellulose groups with pyridine or ionic liquid. Benzoylated specimens, otherwise, enable the UV-detection of the whole substrate components that are cellulose, hemicellulose, and lignin, regardless of possible chemical connection among them.

4.2.3 GPC analysis of the annual plants: native materials

Extensively ball-milled samples of the four herbaceous plants were dissolved in the ionic liquid 1-allyl-3-methylimidazolium chloride ([amim]Cl) and then reacted with benzoyl chloride or acetyl chloride in the presence of pyridine under mild conditions. These benzoylated and acetylated samples were then analyzed by GPC-UV at 240 nm and 280 nm respectively to maximize their analytical response. It is worth to point out again that acetylated sample chromatograms should exclusively account for the molecular weight distribution of those lignocellulosic fractions which naturally contain aromatic groups (LCCs and free lignin), due to the higher instrumental response observed for lignin than for free polysaccharides. Acetylated and benzoylated chromatograms were overlapped for each herbaceous substrate; the result is reported in *Figure 4*.

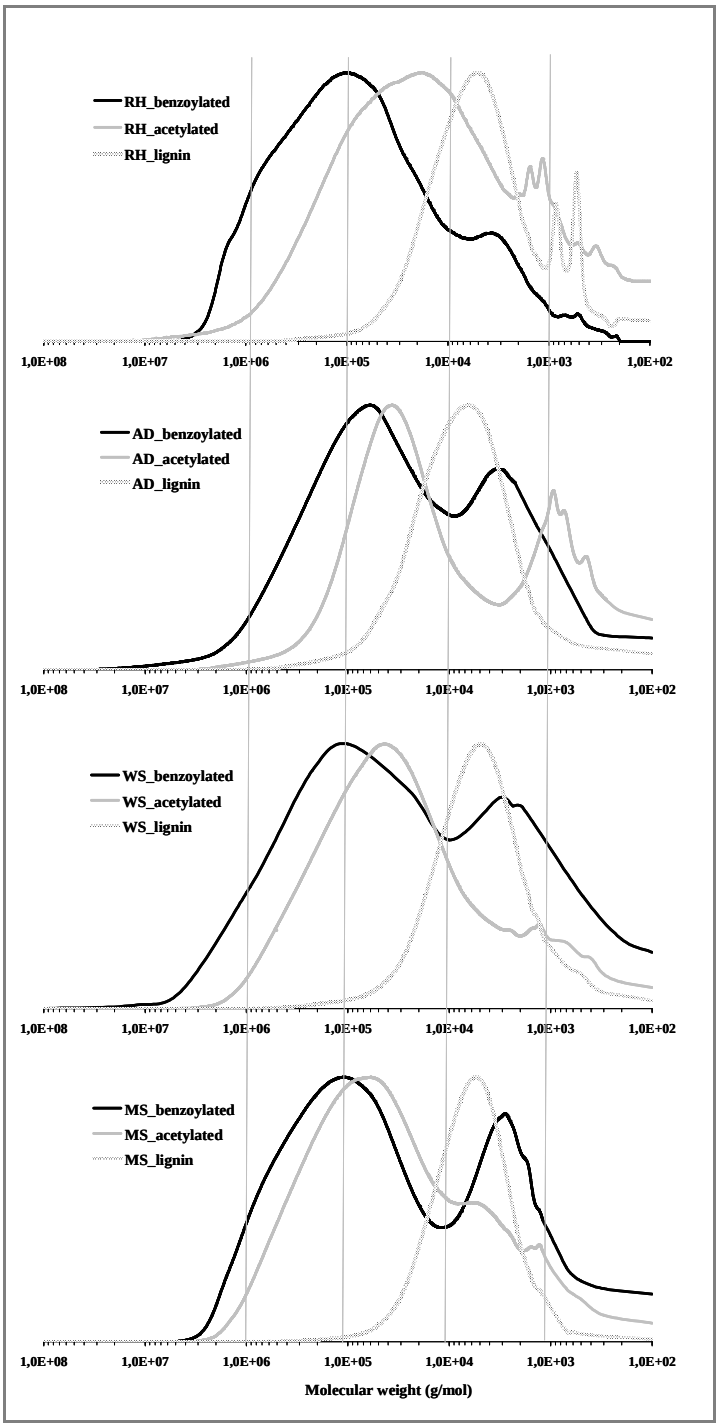

Figure 4. Overlapped GPC profiles of benzoylated (black line) and acetylated (gray line) milled native samples (top to bottom: rice husk - RH, *Arundo donax* - AD, wheat straw - WS; and *Miscanthus sinensis* - MS). Chromatograms of acidolysis lignin samples (acetylated, dotted line) are also reported as reference signals.

For all the analyzed samples (RH, AD, WS and MS), the benzoylated chromatograms showed a more or less pronounced shoulder in the higher molecular weight region than the acetylated ones, supporting the presence of free polysaccharides of considerable molecular weights. The profile of acetylated samples showed the presence of macromolecules with a larger molecular weight with respect to the corresponding extracted lignin specimen. These components, detected at 280 nm, could be associated with the presence of polysaccharides connected to aromatic compounds. On account of these relative comparison among GPC profiles of benzoylated and acetylated native grasses it seems likely to recognize two situations. Rice husk and *Arundo donax* are characterized by pretty different benzoylated and acetylated GPC profiles, which may presumably suggest the presence of LCCs of low molecular weight. When wheat straw and *Miscanthus sinensis* are concerned, the two chromatograms are quite similar – especially in the case of *Miscanthus sinensis* - giving the impression to be in presence of medium to high molecular weight LCCs. The GPC technique herein developed was not able to discern the nature of the aromatic compounds covalently bounded to the polysaccharide fraction. They may be ascribed either to lignin (aromatic polymer) or to p-coumaric and ferulic acids (aromatic compounds), known to be connected by ester bonds to hemicellulose (*24*). Moreover, the presence of different peaks in the lower molecular weights region, noticed in all the benzoylated and acetylated chromatograms, could be explained by the presence of free hemicellulose (detectable only after benzoylation at 240 nm) and free lignin (detectable in any instrumental configuration).

4.2.4 GPC analysis of the annual plants: fractionation products

Afterwards, the main lignocellulosic fractions (i.e., cellulose, hemicellulose and lignin) of all the four herbaceous samples were isolated and derivatized

in IL. They were then subjected to GPC analysis with the aim to rationalize composition and components distribution in each chromatogram describing the whole derivatized samples. The results are reported in *Figure 5* and *Figure 6*. Pure cellulose and hemicellulose samples were both acetylated and benzoylated. In the case of cellulose samples, *Figure 5* reports only benzoylated chromatograms due to the low instrumental response obtained from acetylated ones, according to the experimental results discussed in section *5.2.2*. When hemicellulose was concerned, both acetylated and benzoylated specimens were detectable by GPC-UV, giving a similar molecular weight distribution. Such observation itself may be considered as an evidence of LCCs occurrence, and may be justified by the presence of any aromatic compound bounded to the hemicellulose structure and not removed by the preliminary oxidative step involving NaClO. For the purposes of this study, *Figure 6* compares only the acetylated chromatograms of hemicellulose to the acetylated chromatograms acquired after the derivatization of the whole materials. It is worth noticing that residual aromatic compounds bounded to the hemicellulose fraction could not affect the molecular weight distribution due to their limited contribution to the polymer molecular weight.

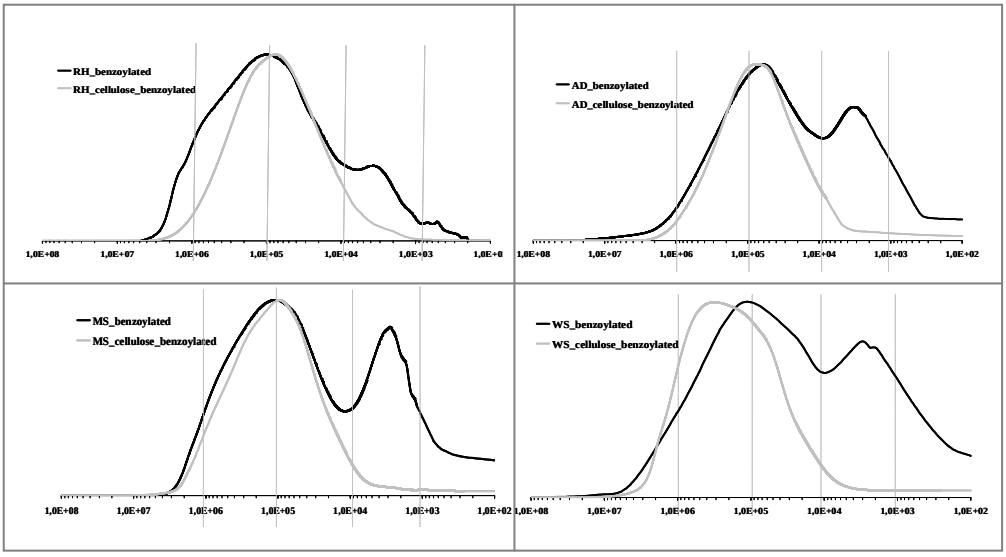

Figure 5. Identification of the main polysaccharide components in the UV-detected fractions of benzoylated native samples (Clockwise: rice husk - RH, *Arundo donax* - AD, wheat straw - WS; and *Miscanthus sinensis* - MS). Overlapped GPC profiles of benzoylated native material (black line) and benzoylated extracted cellulose (gray line).

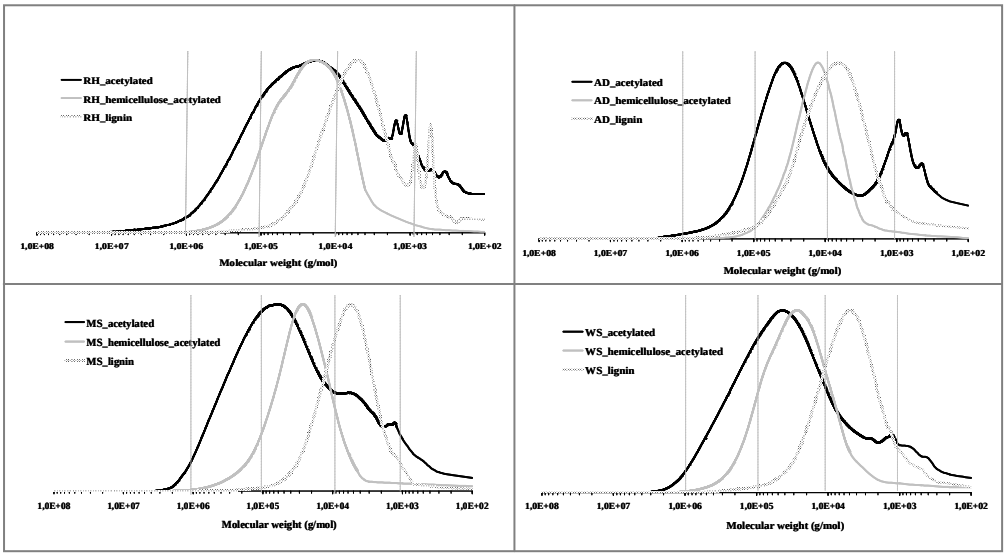

Figure 6. Identification of the main polysaccharide components in the UV-detected fractions of acetylated native samples (Clockwise: rice husk - RH, *Arundo donax* - AD, wheat straw - WS; and *Miscanthus sinensis* - MS). Overlapped GPC profiles of acetylated native material (black line), acetylated extracted hemicellulose (gray line), and acetylated acidolysis lignin (dotted line).

With regard to the benzoylated chromatograms in *Figure 5*, where is reported the comparison between the entire native materials and the corresponding extracted cellulose, it was possible to verify a significant overlapping of the two GPC profiles in the higher molecular weight area, thus confirming that the polysaccharide describing the higher molecular weight fractions of all the examined samples ought to be identified with cellulose. Only for rice husk is observed a slight difference with the higher molecular weights of the native material not fully represented by the cellulosic fraction. This mismatch was accounted as a possible result of additional chemical interaction among rice husk components, which is known to be an outstandingly recalcitrant material.

On the contrary, *Figure 6* showed a substantial disagreement between the chromatograms of acetylated native materials and the corresponding extracted hemicellulose.

Comprehensively, it is like a fraction in the higher molecular weight region is missing in all the acetylated chromatograms: this fraction was interpreted as the LCCs area. The fractionation process cleaved away the lignin polymer by a progressive oxidation, thus leaving a missing contribution in the higher molecular weight that could be explained only taking into account a chemical connection between hemicellulose and lignin.

Other valuable informations could be achieved further analyzing these four distributions. Indeed, the extracted hemicellulose specimens were described by almost the same M_p but a less polydispersed peak for RH and WS, while in the case of AD and MS the distributions were sharper and completely shifted toward lower molecular weight with respect to the corresponding native material. In the case of RH and WS, the slight differences in the overlapped chromatograms may be rationalized assuming that hemicellulose is mainly bounded to small polyphenolic fragments (either oligomers or monomers in the form of p-coumaroyl and feruloyl esters) resulting in low

molecular weight LCCs. Instead, differences in the molecular weight distributions of acetylated AD and MS native specimens and related extracted hemicelluloses could be justified presuming that the hemicellulose fraction is mainly bounded to large lignin fragments. As long as rice husk, wheat straw, and *Miscanthus sinensis* are concerned, these hypotheses are also confirmed by the conclusions reached in the previous section (*5.2.3*). The contradictory results obtained for *Arundo donax* (low molecular weight LCCs as supposed in section *5.2.3 vs* hemicellulose linked to large lignin fragments, i.e., LCCs of high molecular weight, here) may be explained by a limited amount of LCCs, resulting in a low absorbance in the higher molecular weight region of the acetylated native material even if hemicellulose is conceived as bound to large lignin fragments.

4.2.5 Applications

In order to apply the developed GPC system to detect any significant change in the material composition after a harsh physical treatment, specimens of steam-exploded wheat straw and *Arundo donax* were subjected to GPC-UV analysis after being acetylated and benzoylated. Results are reported in **Figure 7** and **Figure 8** .

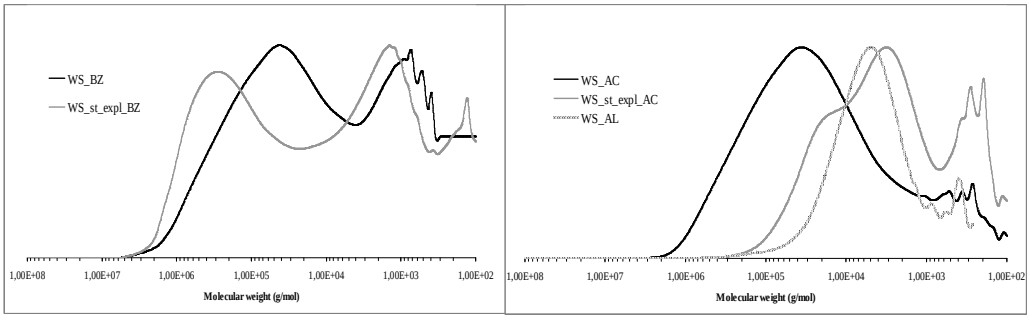

Figure 7. Left: overlapped GPC profiles of benzoylated native wheat straw (black line) and benzoylated steam-exploded wheat straw (gray line). Right: overlapped GPC profiles of acetylated native wheat straw (black line) and acetylated steam-exploded wheat straw (gray line). The chromatogram of acetylated acidolysis lignin is also reported as reference signal.

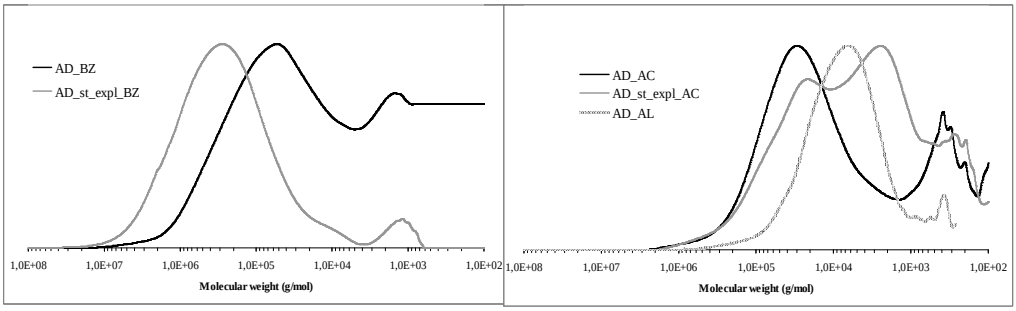

Figure 8. Left: overlapped GPC profiles of benzoylated native *Arundo donax* (black line) and benzoylated steam-exploded *Arundo donax* (gray line). Right: overlapped GPC profiles of acetylated native *Arundo donax* (black line) and acetylated steam-exploded *Arundo donax* (gray line). The chromatogram of acetylated acidolysis lignin is also reported as reference signal.

Both the benzoylated chromatograms of steam-exploded wheat straw and *Arundo donax* had their principal peak, or at least its maximum, shifted toward higher molecular weights. This difference in the UV response could be regarded as a consequence of the fiber separation which possibly resulted in the removal/solubilization of low molecular weight cellulose chains.

The acetylated chromatograms of steam-exploded specimens showed that a large portion of the hemicellulose fraction was hydrolyzed, resulting in a bimodal GPC profiles, consistent with a lignin-enriched sample. The removal of hemicellulose was really effective for wheat straw, which lost almost all this polysaccharide fraction. Concerning *Arundo donax,* it seemed that the steam explosion process was not as much effective. Otherwise, these experimental results may be deemed as an agreement with the hypothesis of a low LCCs content previously discussed (*section 5.2.4*).

4.3 Conclusions

The opportunity for a plain investigation of the presence and amount of lignin-carbohydrate complexes (LCCs) in renewable feedstocks is a major issue in the choice of the most appropriate pretreatment strategy. In this

study, extensively milled lignocellulosic materials from Rice husk, *Arundo donax*, wheat straw, *Miscanthus sinensis*, and their fractionation products (cellulose, hemicellulose, and lignin) have been characterized by means of GPC-UV. The acetylation and benzoylation of the milled native substrates in ionic liquid media, and the systematic comparison between their GPC-UV chromatograms has revealed itself as a straightforward technique in the detection of LCCs. The comparison between acetylated hemicellulosic fractions and corresponding acetylated native substrates proved a more or less pronounced connectivity between lignin (or any other aromatic compounds) and the hemicellulosic moiety. Moreover, the method allowed to venture an assessment of the LCCs molecular weight and composition in terms of hemicellulose to lignin ratio, demonstrating its reliability even if based on purely qualitative evaluations. On the other hand, the comparison between benzoylated cellulosic fractions and corresponding benzoylated native substrates demonstrated that cellulose was a substantially unbound moiety, accounting for the sample composition at higher molecular weights. Moreover, extracted lignin specimens were completely characterized revealing a similar structure for all the materials under examination.

References

1. Salanti, A.; Zoia, L.; Tolppa, E.L.; Orlandi, M. Chromatographic Detection of Lignin-Carbohydrate Complexes in Annual Plants by Derivatization in Ionic Liquid Media. *Biomacromolecules, accepted for publication.*
2. Kim, S.; Dale, B.E. Global potential bioethanol production from wasted crops and crop residues. *Biomass Bioenergy* **2004**, *26*, 361-375.
3. Clark, J. H. Green chemistry for the second generation biorefinery - sustainable chemical manufacturing based on biomass. *J Chem. Technol. Biotechnol*. **2007**, *82*, 603-609.
4. Zhang, Y. H. P.; Ding, S. Y.; Mielenz, J.R.; Cui, J. B.; Elander, R. T.; Laser, M.; Himmel, M. E.; McMillan, J, R.; Lynd, R. L. Fractionating recalcitrant lignocellulose at modest reaction conditions. *Biotechnol. Bioeng*. **2007**, *97 (2)*, 214-223.
5. Ragauskas, A.J.; Williams ,C. K.; Davison, B. H.; Britovsek, G.; Cairney, J.; Eckert, C.A.; Frederick, W.J. Jr; Hallett, J.P.; Leak, D.J.; Liotta, C.L. The path forward for biofuels and biomaterials. *Science*, **2006**, *311(5760)*, 484-489.
6. Arantes, V.; Saddler, J. N. Access to cellulose limits the efficiency of enzymatic hydrolysis: the role of amorphogenesis. *Biotech. Biofuels*, **2010**, *3 (4)*,156-168.
7. Berlin, A.; Balakshin, M.; Gilkesa, N.; Kadla, J.; Maximenko, V.; Kubo, S.; Saddler, J. Inhibition of cellulase, xylanase and β-glucosidase activities by softwood lignin preparations *J. Biotechnol*. **2006**, *125 (2)*, 198-209.
8. Balan, V.; da Costa Sousa, L.; Chundawat, S. P. S.; Marshall, D.; Lansing, E.; Sharma, L. N.; Chambliss, C. K.; Dale, B. E. Enzymatic Digestibility and Pretreatment Degradation Products of AFEX-Treated Hardwoods (Populus nigra). *Biotechnol. Prog*., **2009**, *25 (2)*, 365-375.
9. Galbe, M.; Zacchi, G. Pretreatment of lignocellulosicmaterials for efficient bioethanol production. *Adv. Biochem. Eng. Biotechnol*. **2007**, *108*, 41-65.
10. Lee, S. H.; Doherty, T. V.; Linhardt, R. J.; Dordick, J. S. Ionic liquid-mediated selective extraction of lignin from wood leading to enhanced enzymatic cellulose hydrolysis. *Biotechnol. Bioeng*. **2009**, *102 (5)*, 1368-1376.
11. Tan, S. S. Y.; MacFarlane, D. R.; Upfal, J.; Edye, L. A.; Doherty, W. O. S.; Patti, A. F.; Pringle, J. M.; Scott, J. L. Extraction of lignin from lignocellulose at atmospheric pressure using alkylbenzenesulfonate ionic liquid. *Green Chem*., **2009**, *11*, 339-345.
12. Fu, D.; Mazza, G.; Tamaki, Y. Lignin extraction from straw by ionic liquids and enzymatic hydrolysis of the cellulosic residues. *J. Agric. Food Chem*. **2010**, *58 (5)*, 2915-2922.

13. Li, B.; Asikkala, J.; Filpponen, I.; Argyropoulos, D. S. Factors affecting wood dissolution and regeneration of ionic liquids. *Ind. Eng. Chem. Res.* **2010**, *49 (3)*, 2477-2484.
14. Swatloski, R. P.; Holbrey, J. D.; Spear, S. K.; Rogers, R. D. Ionic Liquids for the dissolution and regeneration of cellulose. In: Molten Salts XIII, Proceedings of the thirteenth international symposium on molten salts. De Long, H. C.; Bradshaw, R. W.; Matsunaga, M.; Stafford, G. R.; Truelove, P. C. eds. 2002, 155-165.
15. Zoia, L.; King A. W. T.; Argyropoulos, D. S. Molecular weight distributions and linkages in lignocellulosic materials derivatized from ionic liquid media. *J. Agric. Food Chem.* **2011**, *59 (3)*, 829-838.
16. Kim, H.; Ralph, J. Solution state 2D NMR of ball-milled plant cell wall gels in DMSO-d6/pyridine-d5. *Org. Biomol. Chem*. **2010**, *8(3)*, 576-591.
17. Crestini, C.; Argyropoulos, D.S. Structural analysis of wheat straw lignin by quantitative 31P and 2D NMR spectroscopy. The occurrence of ester bonds and α-O-4 substructures. *J. Agric. Food Chem*., **1997**, *45*, 1212-1219.
18. Ralph, J.; Marita, J.M.; Ralph, S.A.; Hatfield, R.D.; Lu, F.; Ede, R.M.; Peng, J.; Quideau, S.; Helm, R.F.; Grabber, J.H.; Kim, H.; MacKay, J.J.; Sederoff, R.R.; Chapple, C.; Boudet, A.M. Solution-state NMR of lignins. In: Progress in Lignocellulosics Characterization, Argyropoulos, D.S. Eds., TAPPI press, Atlanta, GA, 1999, 55-108.
19. Ralph, J.; Kim, H.; Peng, J.; Lu, F. Arylpropane-1,3-diols in lignins from normal and CAD-deficient mutant pines. *Organic Lett*., **1999**, *1*, 323-326.
20. Ralph, J.; Helm, R.F.; Quideau, S.; Hatfield, R.D. Lignin-feruloyl ester cross-links in grasses. Part 1. Incorporation of feruloyl esters into coniferyl alcohol dehydrogenation polymers. *J. Chem. Soc., Perkin Trans*., **1992**, *1*, 2961-2969.
21. Ralph, J.; Hatfield, R.D.; Grabber, J.H.; Jung, H.G.; Quideau, S.; Helm, R.F. Cell wall cross-linking in grasses by ferulates and diferulates. In Lignin and Lignan Biosynthesis, ed. Lewis, N.G. & Sarkanen, S. American Chemical Society, Washington, DC, 1998, 209-236.
22. Ralph, J.; Grabber, J.H.; Hatfield, R.D. Lignin-ferulate crosslinks in grasses: active incorporation of ferulate polysaccharide esters into ryegrass lignins. *Carbohydr. Res*., **1995**, *275*, 167-178.
23. Ralph, J. Lignin structure: recent developments. In: Proceedings of the 6th Brazilian Symposium Chemistry of Lignins and Other Wood Components, Guaratingueta, Brazil, 1999, 97–112

5. RICE HUSK LIGNIN RECOVERY AND ITS EFFECT AS A FILLER ON THE THERMAL BEHAVIOUR OF POLY(3-HYDROXYBUTYRATE)-BASED BIOCOMPOSITE (*1,2*) [DEVELOPED IN COLLABORATION WITH SCCP AND ISMAC CNR]

5.1 Background, objectives, and strategies

5.1.1 Rice husk lignin extraction

A suitable renewable feedstock for the chemical and energy industry is extremely important for the sustainable development of society. Nowadays, the current prosperity of chemical is based on cheap and steady feedstock supply, especially non-renewable fossil resources as crude oil, coal and natural gas. At present, renewable matter such as lignocellulosic materials, the most abundant biomass resource in the world, are foreseen as principal alternatives to fossil resources. The lignocellulosic biomass, which represents about 50% of the global biomass, has an annual production estimated in 10-50 billion of tons (*3*) and is predominantly originated by low-cost agricultural and forestal wastes. The main chemical components of lignocellulosic materials are cellulose, hemicellulose, lignin and phenolic extractives, with a minor amount of other compounds such as ashes, proteins, starch, terpenes, waxes, resins, fatty acids and other extractives (*4*, *5*).

In recent years, herbaceous plants are receiving increasing attentions for two primary reasons: annual renewability and large annual biomass stock (1550 million tons/year worldwide) (*6*). Among others, rice is one of the most cultivated crops in the world with a global production of about 680 million tons/year (www.fao.org FAOSTAT Database, 2008). Italy produces approximately 1.4 million tons/year of rice, with the 90% of this production concentrated in the Northern Italy, mostly of which in Lombardy and Piedmont (www.politicheagricole.gov.it). Rice husk, the outer cover of rice grain, is among the principal processing side-products of the rice milling industry and accounts for about 20% by weight of rice. Averagely, rice husk

is composed by 22% of lignin, 38% of cellulose, 18% of hemicelluloses and 2% of extractives and 20% of ashes (*7*) but its chemical composition may differ since disparate variables (geographic area, climatic conditions, type of paddy, soil chemistry, fertilizers) are involved in the crop growth. Rice husk does not possess a remarkable commercial interest and its price is very low (30-40 €/ton in Italy, www.enterisi.it). Because of the elevated ashes and lignin content, rice husk is not appropriate as animal feed raw material. Therefore, it is for the most part addressed to serve as animal litter, soil fertilizer or combustible for the production of electricity and heat, creating environmental pollution. Recently, many efforts have been done trying to valorize rice husk by exploiting its characteristics as an abrasive surface or as a high ash containing material. Recent studies have demonstrated that rice husk can be burnt under controlled conditions to obtain a large amount of silica (about 95% of the total ashes content) which may find application in a variety of end products such as building materials, adsorbents phase for the treatment of wastewaters, solid phase for supported enzymes, and fillers (*8, 9*). Moreover, the polysaccharide fraction has been suggested for various applications, such as adhesives, films and biofuel production (*10, 11*).

On the contrary, despite its widespread availability, industrial applications of lignin and phenolic extractives from rice husk are rather limited, and it has been reckoned that only 1-2% of it is addressed to the development of innovative bio-based products (*12*). The aim of the present study is to increase this percentage, exploiting agro-industrial lignin wastes as a renewable feedstock to substitute synthetic additives and fillers in adhesives, resins, thermoplastics and composites (*13, 14*).

In this work, lignin and extractives from rice husk were isolated and characterized. Rice husk extractives have been already proved to possess antioxidant activity (*15, 16*). Three solvents (water, ethanol and acetone) were tested in different extractions with the aim to isolate extractives in a

different solubility range. The extractives thus recovered were assayed for their antioxidant activity by means of a DPPH radical scavenging test.

With regard to the lignin isolation, two different extraction procedures were tested: the acidolysis and the alkaline enzymatic. The acidolysis method has been taken into account as a simple and well-defined procedure for the isolation of a representative and pure lignin sample. The alkaline enzymatic method has been envisaged as an economic and industrial applicable extraction procedure. Both the procedures were investigated to recognize the best experimental conditions for the maximization of yield and purity. Afterwards, the different lignins were fully characterized by means of gravimetric, chromatographic (GPC) and nuclear magnetic resonance analyses (^{31}P NMR and 2D-HSQC-NMR). Alkaline Enzymatic Lignin (AEL) and Acidolysis Lignin (AL) samples were also subjected to DPPH colorimetric assay to assess their radical scavenging activity.

5.1.2 Biocomposites analysis

In recent years, agricultural by-products have been tested as fillers for the production of polymer matrix composites (*17,18*). These fillers are not only inexpensive but also able to minimize the environmental pollution. Moreover, biodegradable lignocellulosic fillers possess several advantages compared to inorganic additives, such as greater deformability, lower density and reduced cost. Depolymerization and chemical modifications aimed at the introduction of lipophylic chains represent potential approaches to enhance the affinity of lignocellulosic materials towards polymeric systems. The increasing social environmental awareness and the forecast of oil shortage that will endanger the production of conventional plastics in the future have prompted the attention on biopolymers. Nowadays, the biopolymer sector still represents only a very limited share of the global market, but it is expected to have a huge potential for the future, due to the countless applications that polymers

have gained in our society (*19-21*). Poly(3-hydroxybutyrate) (PHB) is accumulated by a wide variety of micro-organisms as an intracellular storage source of organic carbon and chemical energy. PHB has attracted much attention as a biocompatible and biodegradable thermoplastic polymer but its application has often been limited by its brittleness. PHB was blended with several synthetic polymers to improve its thermal and mechanical properties (*22-25*). Biocomposites are novel materials obtained by compounding a biodegradable polymer with biodegradable fillers (*26*). In recent years, fillers from renewable source, such as lignocellulose fibers, have been increasingly used in the preparation of PHB-based biocomposites (*27-29*). The presence of lignin gives particular properties to the composite. It can act as a stabilizer preventing polymer ageing due to its antioxidant activity (*30-33*). Lignin is also able to produce a large amount of char residue upon heating at elevated temperature in an inert atmosphere; this feature is a basic aspect of flame retardant additives, since char reduces the combustion heat and heat release rate of polymeric materials (*34-36*). Moreover, lignin can behave as a nucleating agent during the crystallization of different thermoplastic polymers and interfere on their supramolecular structure (*37,38*). Recent papers reported about the influence of lignin on the properties of PHB-based composites prepared by melt mixing (*39,40*).

In the present work, PHB and acetylated lignin biocomposites were prepared by casting from chloroform solution to enable interactions at molecular level between lignin and biopolymer matrix. Results from preliminary thermal analysis showed that the interference of the AL on PHB thermal stability and crystallization behaviour is stronger than that of the AEL. Therefore, a second part of the study was dedicated to the structural and morphological characterization of PHB-AL composites and to the evaluation of the influence of lignin content on the thermal properties of PHB-AL composites

with the aim to establish a relationship between the biocomposite properties and the ligno-derivatives characteristics.

5.2 Experimental results: rice husk lignin

5.2.1 Radical scavenging activity of water, ethanol and acetone extractives

Plenty of studies have demonstrated that several plant extracts, mainly composed of phenolic structures, possess interesting antioxidant (*41*,*42*) and antimicrobial properties (*43*). On the basis of these studies, three different solvents (water, ethanol and acetone) were tested in the isolation of extractives from rice husk in order to cover a solubility range and appreciate if the antioxidant ability changed depending on the extraction solvent. To test the radical scavenging ability of the extracts was chosen a DPPH radical scavenging test, since the oxidation is often initiated by a free radical attack. Moreover, the DPPH method is rapid, simple, sensitive, reproducible and does not require special instrumentation. The antioxidant activity of rice husk extractives was compared to that of commonly used antioxidants of both natural (quercetin, rutin) and synthetic origin (BHT, BHA).

Table 1 summarizes the calculated IC_{50} values.

	IC_{50} (µg/ml)	**PhOH (mmol/g)**	**IC_{50} (nmol PhOH/ml)**
Rice husk extractives			
Water	82.9	0.59	48.9
Ethanol	112.4	1.02	114.6
Acetone	195.2	1.22	238.1
Reference			
Quercetin	1.9	16.54	31.4
Rutin	4.1	6.55	26.9
BHA	6.8	5.55	37.7
BHT	8.6	4.54	39.0

Table 1. Radical scavenging activity of water, ethanol and acetone extractives from rice husk, IC_{50} concentration expressed both as a function of the weight (first column) and the phenolic content (third column). Values referred to methanolic solutions.

Despite the lower phenolic content (estimated by quantitative ^{31}P-NMR analysis for the three different extractives types), among the others water-soluble extractives were found to be the most powerful radical scavenger. If the same data are regarded as a function of the total phenolic moiety, the IC_{50} values for water extractives and reference antioxidants were found to be quite similar, proving a close relationship between number of phenolic functionalities and scavenged DPPH radicals. Though the solubility properties may play a crucial role with regard to the chemical characteristics of the isolated products, it is not clear the reason why ethanol and acetone extractives showed a much higher IC_{50} value having a large phenolic content nevertheless. According to other studies (*44,45*), it seems that a direct correlation between the content of the main antioxidant compounds (total polyphenols) and the total antioxidant potential should not be taken for granted. Moreover, common phenols released as a consequence of lignin degradation such as coumaric acid, vanillin, and vanillic acid are proved to react very poorly with the DPPH free radical with a slow kinetic reaction (*46*).

5.2.2 Compositional evaluation of rice husk

A preliminary characterization of native rice husk highlighted the following composition: 4.7% of extractives (sum of water 3.5%, and ethanol 1.2% extractives), 26% of lignin (sum of acid insoluble 23.3% and acid soluble 2.7% lignin), 16.8% of ash, and 52.6% of carbohydrates. In the sample no proteins were detected. It is noteworthy the considerable amount of lignin and the large amount of ash content (ash content in wood is generally comprised between 3-5%), constituted by around 85% - 90% of amorphous silica (*7*). These percentages reflect the biological function of rice husk, which is a physical protection of rice grains from external damages caused by environmental conditions, parasites and herbivores. The output of this

compositional estimation is close to literature data (*7*), taking into account that slight differences may be related to different environmental and cultivating conditions as well as to the rice plant species.

5.2.3 Lignin extraction: screening and identification of the most suitable methods

The isolation of lignin from rice husk was performed following different procedures, either chemical or/and enzymatic, in order to evaluate the better extraction strategies among different approaches. A first method was based on an acid hydrolysis with HCl 0.1 M in dioxane/water, followed either by lignin precipitation in HCl 0.01 M (named acidolysis type 1) or by flocculation in an acetic acid/water solution (named acidolysis type 2). As an alternative approach, was investigated a cellulolytic treatment of the rice husk. Others procedures tested comprehended: an alkaline hydrolysis with NaOH 0.2 M, followed by lignin precipitation in HCl 0.5 M, and an enzymatic hydrolysis/acidolysis lignin (EAL) obtained from a cellulolytic sample further extracted according to the acidolytic (type 1) method.
Table 2 displays an overview of the obtained results.

	Acidolytic-1 (HCl 0,01 M)	**Acidolytic-2 (CH3COOH)**	**Cellulolytic lignin**	**EAL**	**Alkaline**
Milling time (h)	20	15	20	30	blended
Lignin yield (%)	46,3	30,0	-	40,5	27,5
Klason lignin (%)	86,0	79,0	32,0	86,0	75,0
Ashes (%)	< 2	< 2	24,0	< 2	< 2

Table 2. Rice husk lignin – sample composition: lignin yield (normalized on Klason lignin content), content values of Klason lignin, and ashes varying the extraction procedure.

The best results were identified in the acidolytic (type 1) and EAL samples, which showed an appreciable lignin recovery, high purity, low ash content and a reduced percentage of residual carbohydrates. Since a double

purification would represent a time-consuming strategy and no additional improvements are noticed, the most useful approach was recognized in the acidolytic (type 1) extraction.

Even if the extracted lignin there from was contaminated by a large amount of residual polysaccharides, the alkaline method represents an economic and industrial feasible extraction procedure. Therefore, the alkaline lignin extraction was chosen as a second approach to be fully investigated. With the aim to improve the outcome reducing the residual carbohydrates content, it was decided to perform a cycle of enzymatic purification on the extracted lignin before proceeding in any characterization of the sample.

5.2.4 Lignin isolation: acidolysis lignin (AL)

Besides the extractives isolation, some biomass treatments allow to recover a quite pure lignin fraction which may also find a huge industrial feedback (*47*), being the major lignocellulosic biomass component after carbohydrates.

As discussed above, a first approach investigated for lignin isolation was an acidolytic extraction, performed on rice husk samples subjected to different milling periods. The acidolytic method has been used in order to isolate a pure lignin fraction to be used as a reference specimen for the characterization of rice husk. *Table 3* reports yields and composition of the various acidolysis lignin samples (AL). All of them were also characterized by GPC analyses, in order to identify any significant variation in the molecular weight distributions, and by means of quantitative ^{31}P-NMR spectroscopy to determine the amount of aliphatic hydroxyls, condensed and syringyl phenolic moieties (S-OH + Cond. PhOH), guaiacyl units (G-OH), p-coumaryl alcohols (P-OH), and carboxylic acid functionalities (COOH) as well.

Milling Time (h)	**0**	**5**	**10**	**15**	**20**	**30**
Yield (%)	16.0	26.8	34.0	31.2	46.3	41.9
Purity (Klason %)	> 85	> 85	> 85	> 85	> 85	> 85
Ashes (%)	< 2	< 2	< 2	< 2	< 2	< 2
GPC						
M_n (g/mol)	9000	7900	8300	9900	10200	9300
M_w (g/mol)	31500	30300	29500	37200	41000	36300
M_p (g/mol)	4800	4700	5100	5400	5100	4900
I	3.5	3.8	3.5	3.8	4.0	3.9
^{31}P NMR						
Aliphatic -OH (mmol/g)	3.08	2.89	3.40	2.98	3.03	2.88
S-OH + Cond. PhOH (mmol/g)	0.23	0.21	0.34	0.27	0.23	0.31
G-OH (mmol/g)	0.47	0.61	0.70	0.61	0.65	0.60
P-OH (mmol/g)	0.66	0.66	0.74	0.65	0.65	0.63
COOH (mmol/g)	0.23	0.22	0.23	0.22	0.27	0.23

Table 3. Yields, purity, ashes content, average molecular weight indexes and labile hydroxyls composition of acidolysis lignin extracted from differently milled rice husk samples.

The overlap of the GPC profiles (not shown) displayed an appreciable overlay of the different chromatograms, with the more extensively milled rice husk lignin sample (15, 20, 30 hours) being the richer in high molecular weights. This qualitative observation is confirmed by the average molecular weights calculation (M_n, M_w, M_p), reported in *Table 3*. Though extraction carried out on larger particle may be supposed to result in the isolation of a lower molecular weight lignin fraction, as observed in wood lignin (*48*), the GPC profiles and the average molecular weight indexes demonstrated an overall uniformity in the morphological properties of the examined samples. This observation could account for a lignification process which is not discriminating among different regions of the husk. The homogeneity of the extracted acidolysis lignins is furthermore supported by the ^{31}P-NMR analyses, which showed similar chemical features in terms of aliphatic hydroxyls, phenols and acidic functionalities content value for all the

examined specimens. These results demonstrated that the milling time, thus the lignocellulosic powder granule size, had no influence on the morphological and chemical characteristics of lignin whereas the extraction yield was greatly affected.

5.2.5 Lignin isolation: optimization of alkaline-enzymatic lignin (AEL) extraction

In the last few years, experimental endeavors have been directed toward the exploitation of lignocellulosic materials by non-conventional methods which are more concerned for the environment and the industrial applicability than those used on a laboratory scale. The use of NaOH solution is a common method to process wood and lignocellulosic non-woody materials to remove lignin (*49*). Moreover, it is worth noticing that, besides lignin, the alkaline treatment is able to solubilize other lignocellulosic components such as hemicelluloses, residual extractives and ashes. Often, the acidic precipitation is not sufficient to remove all contaminants, mainly polysaccharides as hemicelluloses which co-precipitate along lignin. Some of these carbohydrates could be hydrolyzed by means of an enzymatic treatment, improving lignin purity.

Therefore, a second part of the study was dedicated to the optimization of the alkaline extraction conditions for rice husk lignin. In order to reduce the residual polysaccharides content, all the alkaline lignin specimens were subjected to an enzymatic digestion as a further purification step. A mild alkaline treatment was chosen to avoid potential modifications in the lignin structure due to drastic conditions. The experimental conditions under investigation were: the extraction time, the reaction temperature, and the concentration of NaOH. If not otherwise specified, extraction time, temperature and NaOH concentration were set at 4 hours, 90 °C, and 0.2 M. The effects of the various processing conditions on yield, purity,

morphological features (GPC), and labile hydroxyls composition (^{31}P-NMR) on rice husk alkaline lignin were investigated (*Table 4*).

	Reaction Temperature (°C)			**NaOH Concentration (M)**		
	70	**80**	**90**	**0.1**	**0.2**	**0.3**
Yield (%)	11.2	15.3	22.3	11.2	22.3	29.1
Purity (Klason %)	65.2	65.2	74.3	49.7	74.3	77.9
Ashes (%)	< 2	< 2	< 2	< 2	< 2	< 2
GPC						
M_n (g/mol)	11300	12300	12000	7400	12000	13600
M_w (g/mol)	106000	113000	96300	39000	96300	115000
M_p (g/mol)	4200	4600	4600	3800	4600	4500
I	9.4	9.2	8.0	5.4	8.0	8.4
^{31}P NMR						
Aliphatic -OH (mmol/g)	1.23	0.86	2.58	0.77	2.58	3.71
S-OH + Cond. PhOH (mmol/g)	0.06	0.06	0.18	0.05	0.18	0.13
G-OH (mmol/g)	0.14	0.10	0.34	0.09	0.34	0.38
P-OH (mmol/g)	0.15	0.07	0.23	0.08	0.23	0.14
COOH (mmol/g)	0.27	0.20	0.62	0.16	0.62	0.59

Table 4. Optimization of the alkaline lignin extraction: effect of different reaction temperatures and NaOH concentrations on yields, purity, and morphological and chemical features. If not otherwise specified: reaction period, NaOH concentration, and reaction temperature set at 4 h, 0.2 M, and 90°C.

Yields and purities of the examined samples were almost all comprised between 15% and 25%, and 65% and 75% respectively. Only a slight increment in yield and purity was detected increasing the extraction time (data not reported), whereas a raise in both the reaction temperature and the NaOH molarity resulted in the extraction of a larger and purer lignin fraction (*Table 4*). For all the set of conditions tested were noticed particularly high M_w values with respect to those found for the acidolytic extraction. Otherwise, M_n and M_p values were found to be almost equal for both the procedures, suggesting the presence of residual polysaccharides chains linked to the lignin macromer which might have lowered the polymer retention time.

Results from quantitative ^{31}P-NMR analyses led to more interesting conclusions. The variable "extraction time" did not seem to be an important affecting factor since the only consequence of its increment was an otherwise expected heighten in the oxidation degree (data not shown). When the variables "reaction temperature" and "NaOH concentration" (*Table 4*) were concerned, pretty low values of aliphatic hydroxyls, phenolic moieties and acidic functionalities were detected at 70°C, 80°C, and 0.1 M, probably on account of an especially limited solubility and purity of these samples related to excessively mild extraction conditions. If the temperature was raised to 90°C or, otherwise, the concentration of NaOH was brought to 0.2 M or 0.3 M, aliphatic alcohol and phenolic moieties content values moved upward, as well as the carboxylic acid content as a consequence of a major oxidation. In the effort to found the best compromise among yield and purity, the optimum extraction conditions were recognized in the following: 4 hours, 90°C and 0.3 M.

5.2.6 Comparison between AL and AEL Samples

Table 5 displays an overview of the obtained results for both the optimized acidolysis lignin, AL (20 h of ball milling) and the optimized alkaline enzymatic lignin, AEL (4 hours, 90°C and 0.3 M NaOH + cellulase). The best results with regard to gravimetric analyses (yield, purity, ashes) were identified in the AL sample (46.3%, 86%, <2%), which showed an appreciable lignin recovery, high purity, a reduced carbohydrates fraction, and low ash content. However, considering the absence of milling, the result from the AEL protocol should be deemed as competitive (29.1%, 77.9%, <2%).

	AL	AEL
Milling time (h)	20	blended
Yield (%)	46.3	29.1
Purity (Klason %)	86.0	77.9
Ashes (%)	< 2	< 2
Carbohydrate (%)	12.0	20.0
GPC		
M_n (g/mol)	10200	13600
M_w (g/mol)	41000	115000
M_p (g/mol)	5100	4500
I	2.8	8.4
^{31}P NMR		
Aliphatic -OH (mmol/g)	3.03	3.71
Cond. PhOH + S-OH (mmol/g)	0.23	0.13
G-OH (mmol/g)	0.65	0.38
P-OH (mmol/g)	0.65	0.14
COOH (mmol/g)	0.27	0.59

Table 5. Comparison among yields, compositional evaluation, and morphological and chemical features of rice husk lignin specimens AL and AEL by gravimetric, GPC and ^{31}P NMR analyses.

The average molecular weight indexes, along with the overlapped GPC profiles of AL and AEL specimens (not shown), provide the evidence of an AEL sample characterized by a molecular weight distribution notably represented by high molecular weight fractions if compared to the acidolytic one, maybe due to the presence of residual carbohydrate despite the enzymatic purification. The samples were also characterized by means of quantitative ^{31}P-NMR spectroscopy. *Figure 1*, along with *Table 5***,** shows that rice husk lignin is mainly formed by guaiacyl and p-hydroxyphenyl units, not depending by the applied extraction procedure. A higher content of aliphatic hydroxyls and acidic functionality, along with a modest amount of phenolic moieties, was observed for the alkaline extraction. The higher content of aliphatic alcohol, along with the presence of several resolved peaks between 145 and 150 ppm (the aliphatic alcohol range) in the ^{31}P-NMR spectrum of AEL, was related to the presence of carbohydrates impurities likely

connected to the lignin fraction. This observation is in agreement with the GPC result, and it could also explain the lower value of free phenols: part of them could be involved in lignin-carbohydrate bond that the alkaline treatment is not able to cleave. Moreover, the lower value of P-OH in the AEL sample could be related to the alkaline cleavage of p-coumaroyl ester bonds, also observed for wheat straw (*50*).

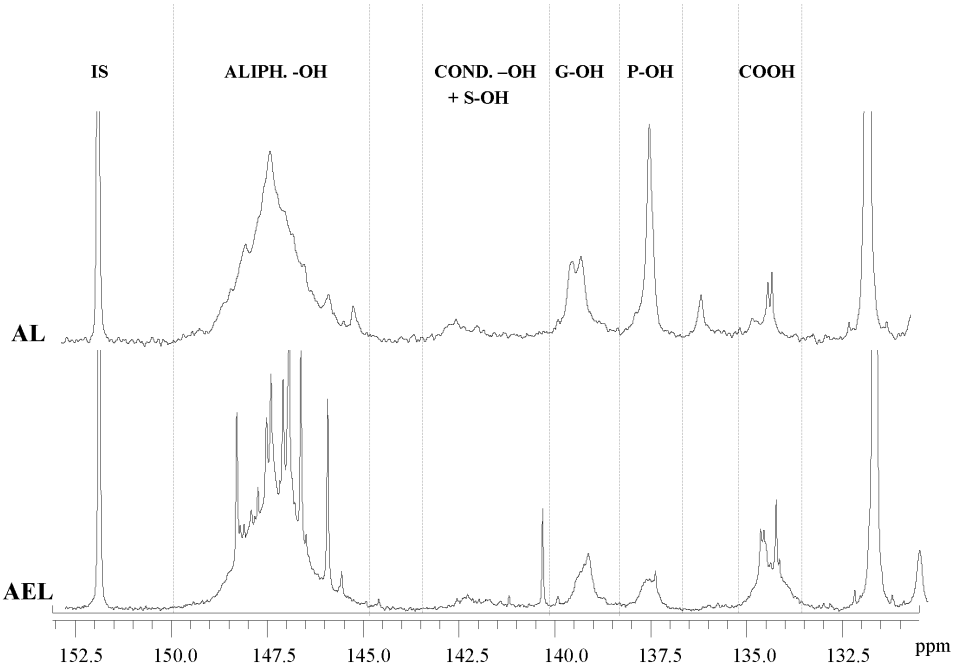

Figure 1. Comparison between ^{31}P-NMR spectra of AL and AEL samples. Approximative integration ranges included for: aliphatic hydroxyls (Aliph -OH), syringyl and condensed phenolic units (Cond.-OH + S-OH), guaiacyl phenols moieties (G-OH), p-coumaryl units (P-OH), and carboxylic acid functionalities (-COOH).

AL and AEL specimens were further analyzed by 2D-HSQC-NMR spectroscopy to identify the principal intermonomeric bonds and to evaluate any significant differences in the two polyphenols connectivity. The main intermonomeric units in lignin include: arylglycerol-β-arylether (β-O-4), phenylcoumaran (β-5), pinoresinol (β-β), and dibenzodioxocine (5-5'-O-4). The spectra, reported in *Figure 2*, highlighted that both the lignins contain

arylglycerol-β-arylether units (β-O-4) as the most representative interunit. Cross-peaks relating to other principal intermonomeric bonds (β-5, β-β) were also identified. Concerning the AEL specimen, an abundant presence of intense correlation signal at δ_C/δ_H ~ 70-75, 5.0-5.5 (oval shape) is noted. These signals were related to partially oxidized residual carbohydrates.

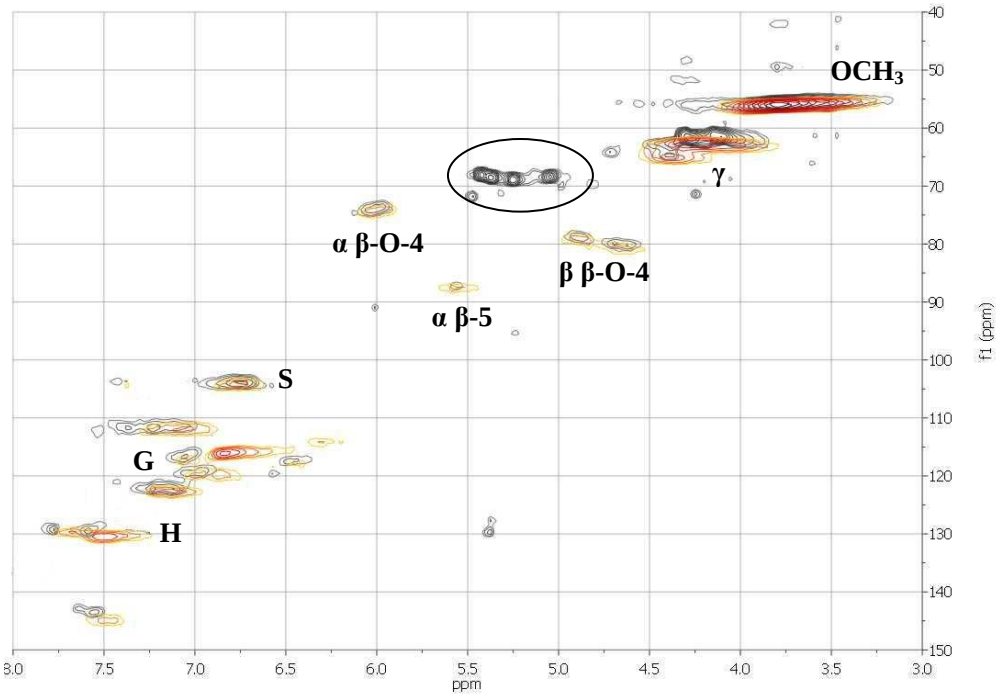

Figure 2. Overlapped 2D-HSQC-NMR spectra of acetylated AL (red scale) and AEL (gray scale) samples from rice husk, showing the aliphatic side chain, $^{13}C/^{1}H$ 40-90/3-6 (β-O-4, β-5), the aromatic region, $^{13}C/^{1}H$ 100-140/6-8 (S syringyl, G guaiacyl, and H p-coumaryl), and signals assigned to partially oxidized residual carbohydrate (circled).

Comprehensively, gravimetric and spectroscopic analyses were consistent with an AEL sample still rich in carbohydrates, even after the cellulolytic treatment, and also containing a large amount of oxidized functionalities, originated either by cellulose degradation or lignin side chains oxidation (or both).

5.2.7 Radical scavenging activity of AL and AEL

In recent years, agricultural by-products have been tested as fillers for the production of polymer matrix composites (*17*, *18*). These fillers are not only inexpensive but also able to minimize the environmental pollution. Moreover, biodegradable lignocellulosic fillers possess several advantages compared to inorganic additives, such as improved mechanical properties and reduced cost. It has been demonstrated that lignin can improve both biodegradability and physical and mechanical properties when added to these materials; moreover, due to its antioxidant activity it can also act as a stabilizer, preventing polymer ageing (*33*). On the basis of these studies, a DPPH radical scavenging test was performed on the AL and AEL samples and their IC_{50} values were compared to that of reference antioxidants (quercetin, rutin, BHA, BHT) (*Table 6*).

	IC_{50} (µg/ml)	**PhOH (mmol /g)**	**IC_{50} (nmol PhOH/ml)**
Rice husk lignin			
AL	37.2	1.53	56.8
AEL	52.6	0.65	32.6
Reference			
Quercetin	1.8	16.54	30.4
Rutin	4.3	6.55	28.3
BHA	4.5	5.55	24.7
BHT	10.4	4.54	47.4

Table 6. Radical scavenging activity of AL and AEL specimens, expressed as IC_{50} concentration as a function of both the weight (first column) and the phenolic content (third column). Values referred to dioxane:water solutions (9:1).

When the radical scavenging activity was expressed as a function of the total phenolic content, lignins and references IC_{50} values were found to be overall similar, demonstrating a close relationship between number of phenolic functionalities and scavenged DPPH radicals.

Chemical modifications aimed at the introduction of lipophylic chains represent potential approaches that may enhance the affinity of lignocellulosic fillers toward polymeric systems. The next section of this work is dedicated to the study of the thermal behaviour of poly(3-hydroxybutyrate) based ecocomposites containing functionalized AL and AEL as filler.

5.3 Experimental results: biocomposites analysis

5.3.1 Screening: thermal stability of AL and AEL

The thermal decomposition of lignins was determined by thermogravimetric analysis under inert atmosphere and oxidative atmosphere. Before TGA run, the samples were maintained at 110°C for 60 min to eliminate the physically adsorbed water (*51*). *Figure 3* shows the TGA and DTG curves of AL and AEL samples under air atmosphere.

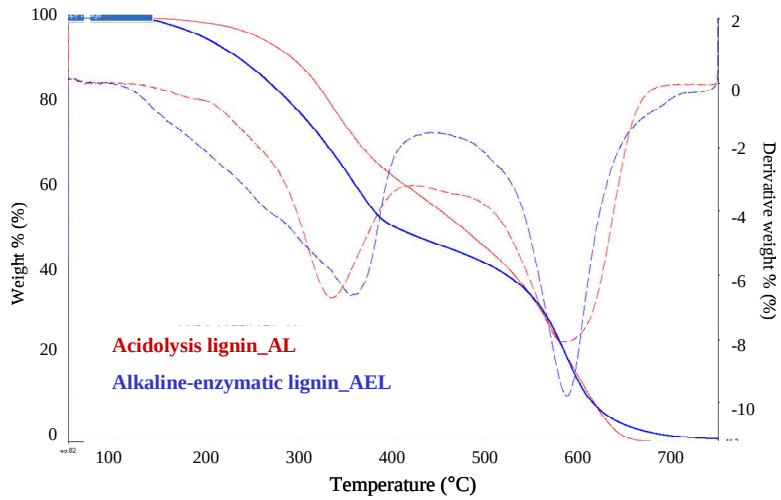

Figure 3. TGA (dashed line) and DTG (straight line) curves in air atmosphere of AL (red line) and AEL (blue line).

In general, the AL sample is found to be more thermally stable than the AEL. The initial degradation temperature corresponding to 5% weight loss ($T_{5\%}$) of

AL sample is marked higher than that of AEL sample, 261 and 201°C, respectively. The main degradation step occurs in the temperature range between 150 and 420°C and is associated with the fragmentation of interunit linkages (*52,53*). Differently from AL, which exhibits a single well-defined peak of degradation centered at 332°C, the TGA trace of AEL sample is characterized by overlapping decomposition events. The multi-stage decomposition with a main peak centered at 351°C and a pronounced shoulder at about 250°C, indicates that the organic substances are released in steps, which reflects that a different mechanism is involved. The presence of a higher carbohydrates content in the AEL sample leads to the differences in the TGA and DTG patterns, being the residual carbohydrate moieties more prone to thermal decomposition (*54,55*). Beyond 420°C both the lignins continue to degrade at a much slower rate. The weight loss registered in this region is attributed to the decomposition of some condensed aromatic structures (*56*). The oxidation of the char residue takes place in the temperature range between 480 and 700 °C, with a DTG maximum at about 580°C, accounting for ca. 50% and 43% of the total weight loss for AL and AEL, respectively. The larger mass loss ascribed to the char oxidation for AL sample is consistent with its higher purity and therefore higher carbon content. The total weight loss for the thermogravimetric run on AL sample was nearly 100%, whereas the AEL sample shows an ultimate residue at 750°C of about 1.5% due to inorganic components.

TGA experiments performed under inert atmosphere pointed out the high thermal stability of AL sample and were characterized by a noticeable non-volatile residue at 750°C, 36% and 31% for AL and AEL, respectively. The residue was almost exclusively due to the formation of highly condensed aromatic structures.

Comprehensively, the TGA experimental data evidenced significant differences in the thermal degradation behaviour of the investigated lignins.

These results are ascribed to the differences in their preparation as well as in detailed chemical structure.

5.3.2 Screening: thermal properties of PHB-AL and PHB-AEL composites

Thin films of PHB/AL and PHB/AEL composites with different composition were prepared by casting from chloroform. The lignin features, i.e. the lignin purity, the molecular weight distribution and the amount of chemical functional groups, could play an important role in the final biocomposite properties. The thermal stability and the crystallization behaviour of PHB-based composites was therefore analyzed and compared by means of TGA experiments carried out under oxidative conditions. Thermograms of pure PHB, and AL and AEL biocomposites containing 15% of lignin load are reported in *Figure 4*.

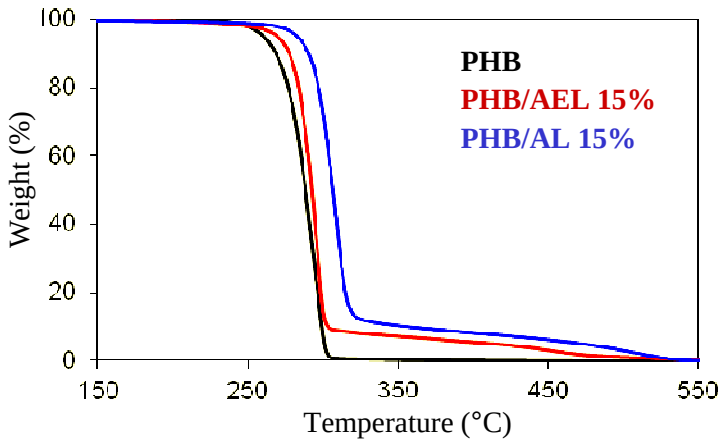

Figure 4. TGA curves in air atmosphere of PHB (black line), PHB-AEL 15% (red line), and PHB-AL 15% (blue line).

On heating at 20°C/min, pure PHB volatilizes completely in a single narrow step from 220 to 320°C with a maximum rate of 1.5 mg/min at 293°C. Compared to the polymer matrix, both PHB-based composites show differences in the values of the onset degradation, identified with the

temperature at which 5% degradation occurs, and maximum rate degradation temperature (T_{max}). PHB-AEL 15% composite showed an increase of 8°C in onset temperature ($T_{5\%}$) compared to pure PHB, while PHB-AL 15% presented a higher increase, 12°C. PHB and PHB-AEL 15% composite showed similar T_{max} values, whereas the T_{max} of PHB-AL 15% was markedly better, around 17°C higher. Summarizing, the weight loss is slowed down in both biocomposites and the PHB-AL composite presents the higher stabilization effect on the thermoxidative degradation of the polymer matrix. The remarkable improvement in the thermal stability is due to a physical barrier effect of the char yield. Indeed, the char acts as a barrier to heat and mass transfer, hindering the diffusion of the oxygen from the gas phase to the polymer matrix and, at the same time, the out-diffusion of the volatile decomposition products.

The DSC analysis of PHB and related biocomposites containing 5% of lignin is reported in *Figure 5*, where successive scans are displayed. The choice of appropriate melting conditions is a key point for the analysis of crystallization kinetics of PHB because of its low resistance to thermal degradation (*57,58*). With the aim to delete previous thermal history and to minimize the degradation of the macromolecules chains, the melting was carried out at 190°C for 3 min. During the cooling step, the PHB sample shows an exothermic peak of crystallization with a maximum at about 74°C (*Figure 5*, black line). A similar trend is observed for the PHB-AEL 5% cooling scan, where the crystallization peak is shifted to 68°C (*Figure 5*, blue line). Differently, the PHB-AL 5% biocomposite does not show exothermic peak when cooled from the melt, while an exothermal crystallization event, peaked at 52°C, occurs during the heating step, corresponding to the cold crystallization from the amorphous state (*Figure 5*, red line).

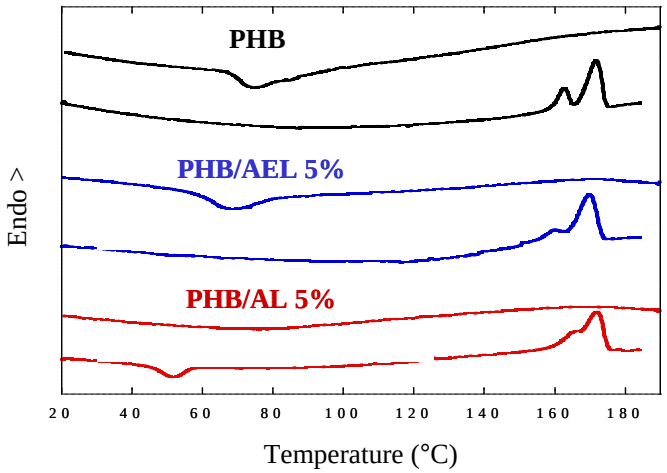

Figure 5. DSC cooling and heating scans of PHB (black line), PHB/AEL 5% (blue line), and PHB/AL 5% (red line) samples melted at 190°C for 3 min.

Thus, the non-isothermal crystallization kinetics of PHB is influenced by the presence of the lignin and the biocomposite containing AL showed a more marked interference on the crystallization behaviour of the PHB.

Pure PHB displays characteristic double melting peaks at 163 and 171°C (*Figure 5*). The first peak is due to the melting of the crystals formed during the primary crystallization and the second transition is assigned to the melting of the crystals formed as a result of recrystallization on heating (*59,60*). Likewise, these features are evidenced in both PHB-based composites, even if less pronounced.

Altogether, the above reported results demonstrated that the interference of the acidolysis lignin on PHB thermal stability and crystallization behaviour is stronger than that of the alkaline-enzymatic one. Therefore, a second part of the study was devoted to the structural and morphological characterization of PHB/AL composites and to the evaluation of the influence of lignin content on their thermal properties.

5.3.3 Thermal stability of different PHB-AL composites

The thermal degradation behaviour of the PHB-AL samples, with lignin content varying from 2.5% to 15%, was investigated by TGA measurements carried out under air flow, and compared to that of reference PHB.

A first general observation is that the TGA and DTG curves progressively shift towards higher temperature with the increase in the amount of AL in the sample. *Table 7* summarizes the characteristic temperatures of active degradation, i.e. $T_{5\%}$, a measure of the decomposition onset, $T_{50\%,}$ the mid-point of the degradation process, T_{max}, the temperature of maximum degradation rate, and the fraction of residual material at different temperatures.

Sample	$T_{5\%}$ (°C)	$T_{50\%}$ (°C)	T_{max} (°C)	R_{350} (%)	R_{400} (%)	R_{450} (%)	R_{500} (%)
PHB	261	288	293	0.3	0	0	0
PHB/AL 2.5%	271	296	300	2	1	0	0
PHB/AL 5%	279	303	306	4	3	2	0
PHB/AL 10%	283	307	310	7	5	3	0.5
PHB/AL 15%	283	308	310	10	8	6	3

Table 7. TGA data under air atmosphere for PHB/AL biocomposites. $T_{5\%}$, decomposition onset; $T_{50\%,}$ mid-point of the degradation process; T_{max}, temperature of maximum degradation rate; R, percentage of residual material at different temperatures.

It is observed that in the biocomposites the initial weight loss takes place at higher temperature than in pure PHB and the $T_{5\%}$ value progressively increases as the AL content is raised. Analogously, as the amount of AL increases, $T_{50\%}$ and T_{max} values increase. In general, the enhancement of the thermal stability of the composites depends on the obtainment of an effective dispersion of the filler into the polymer matrix. TGA results indicate that at AL content up to 10%, the presence of charring lignin strongly interferes increasing the thermal stability of the composite. Indeed, a progressive

accumulation of carbonaceous residue, efficient in air shielding, takes place on the polymer surface. When the lignin amount reaches 15%, the characteristic T-values result to be similar to those of the PHB/AL 10% sample, thus suggesting that the thermal stability of the PHB-AL composites is not proportional to the AL fraction. In contrast, the amount of non-volatile material is strictly related to the AL amount in the biocomposites.

Therefore, AL content of 10% seems to represent the optimal concentration in delaying the thermo-oxidative degradation of the PHB matrix.

5.3.4 Kinetics of crystallization

Isothermal crystallizations were performed at 117°C by DSC. The weight fraction of the material crystallized at time *t*, X_t , was calculated by the relation:

$$X_t = \int_0^t (dH/dt)dt \Big/ \int_0^\infty (dH/dt)/dt$$

where the first integral is the heat generated between the beginning of crystallization and time *t*, and the second is the total heat generated at complete crystallization.

Figure 6 reports the X_t values as a function of crystallization time for pure PHB and PHB/AL biocomposites.

It can be seen that characteristic sigmoid curves shift to the right with increasing the AL content. From these crystallinity curves, the half-time of crystallization, $t_{1/2}$, defined as the elapsed time from the onset until the crystallization reaches 50% of the whole crystallization event, was derived (*Table 8*). The presence of AL causes an increase in the crystallization time and a decrease in the crystallization rate. The more the lignin content the more this effect is enhanced.

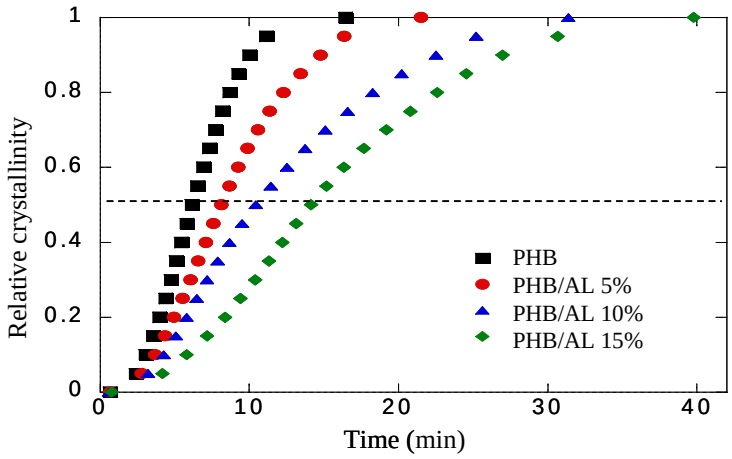

Figure 6. Development of relative crystallinity with time for isothermal melt crystallization of PHB (full black square), PHB/AL 5% (full red circle), PHB/AL 10% (full blue triangle), and PHB/AL 15% (full green rhombus).

The isothermal crystallization kinetics of pure PHB and PHB/AL composites is described by the well-known Avrami equation (*61*):

$$1- X_t = \exp (-K_n t^n)$$

where K_n and n, i.e. the overall crystallization rate constant and the Avrami index, respectively, are parameters depending on the type of nucleation and on the geometry of the growing crystals.

Table 8 collects the values of n and K_n determined from the slope and the intercept, respectively, of the straight lines obtained by plotting $\log[-\ln(1-X_t)]$ versus log t. For all samples, a straight line with a good correlation was observed over a wide range of conversion (X_t values included between 0.05 to 0.95) and Avrami index close to 2 was obtained. n-values around 2 are typical of a bi-dimensional growth of crystalline units, developed by heterogeneous nucleation (*23*). The crystallization rate parameter K_n decreases by increasing the AL content in the composite.

Sample	$t_{1/2}$ (min)	n	K_n (min^{-n})
PHB	6.1	2.2	0.0127
PHB/AL 2.5%	7.3	2.2	0.0078
PHB/AL 5%	8.1	2.1	0.0077
PHB/AL 10%	10.4	2.0	0.0066
PHB/AL 15%	14.1	2.0	0.0033

Table 8. Kinetics parameters for isothermal crystallization.

From the Avrami analysis, it is clear that the crystallization of PHB, in its pure state as well as in the biocomposites, is characterized by the same *n* value. Thus, although the overall crystallization rate decreases, the nucleation mechanism and geometry of crystal growth into the PHB phase are not affected by the presence of AL.

Figure 7 shows the POM images of pure PHB and PHB/AL 15% composite taken during crystallization from the melt. The PHB crystallizes in a typical spherulitic morphology. The well distribution of AL microparticles or aggregate of particles is displayed as an uniform texture. The morphological characterization by SAXS and WAXS (not reported) pointed out the presence of AL particles having dimensions ranging from some tens of nm to some μm, confirming the accomplishment of an effective dispersion of the filler into the polymer matrix.

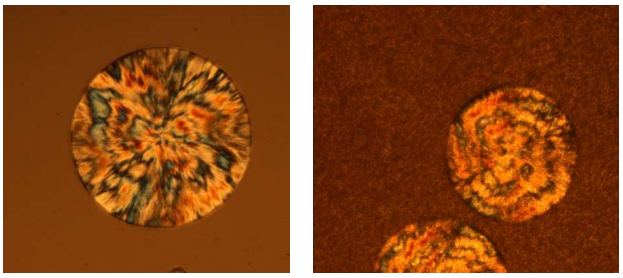

Figure 7. Polarizing optical photomicrograph of pure PHB (left) and PHB/AL 15% composite (right).

According to Chen and Chung (*62*), the spherulite growth rate *G* can be estimated by taking the first derivative of the plot of the spherulite radius (*r*) vs the temperature (*T*), at each experimental point, when the crystallization is performed at constant cooling rate:

$$dr/dT = (dr/dt)\,(dt/dT)$$

where *dr/dt* is the radial growth rate and *dt/dT* is the reciprocal of the cooling rate.

Figure 8 reports the *G* value for PHB/AL 15% composite and reference PHB as a function of temperature. A decrease of *G* values was observed for the ecocomposite into the whole temperature range.

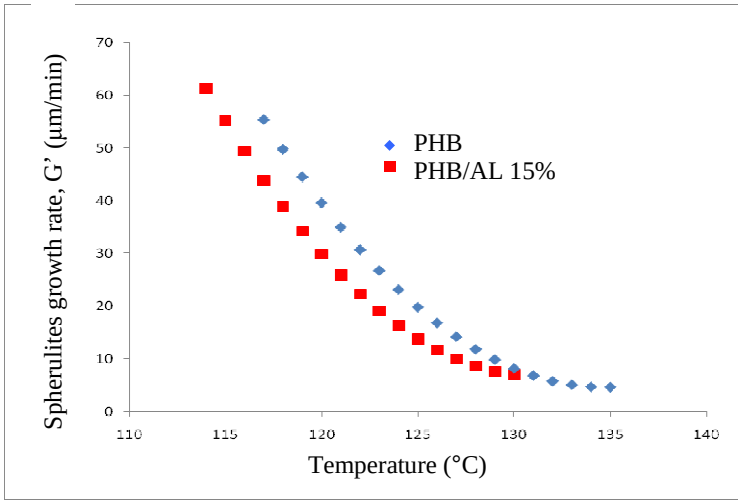

Figure 8. Spherulite radial growth rate of pure PHB (full blue rhombus) and PHB/AL 15% composite (full red square).

The kinetics data showed that the addition of AL causes a decrease of the overall crystallization rate and the spherulite radial growth of PHB. Taking into account that the PHB/AL 15% composite is constituted by two separated phases, the interference on the crystallization kinetics is not attributable to a diluent effect of the AL component. The depression of the crystallization rate is ascribed to the increase of energy related to the transport of the PHB

macromolecules through the melt, caused by the presence of lignin domains (*63*). Hence, the presence of lignin domains interferes in the movement and aggregation of macromolecules through the melted polymer.

5.4 Conclusions

Rice husk lignin was isolated by means of acidolytic or alkaline enzymatic extraction procedure. The isolation methods lead to lignin samples characterized by significant differences among their molecular, thermal and chemical features. The AEL sample showed a lower molecular weight and a higher content of carbohydrates, even after the cellulolytic treatment; whereas the AL sample presented a high purity. A different behaviour was also evidenced in the thermal stability as well as in the char formation.

The lignin characteristics gave rise to a different affinity between the polymer matrix and the lignin component, thus determining dissimilar final properties of the PHB-based biocomposites. The AL evidenced a marked interference on the thermo-oxidative degradation and the crystallization behaviour of the PHB. The PHB-AL biocomposite showed an enhancement of the thermal resistance, being the thermal degradation process shifted to higher temperatures. The increase of thermal stability was observed as a function of the lignin amount in PHB-AL biocomposite series. The addition of AL caused a decrease of the overall crystallization rate and the spherulite radial growth of the PHB. The interference of the separated non-crystallizable AL domains on the PHB kinetics properties was ascribed to the heighten of the energy required for the motion of the macromolecules through the melt.

References

1. Salanti, A.; Zoia, L.; Orlandi, M.; Zanini, F.; Elegir, G. Structural characterization and antioxidant activity evaluation of lignins from rice husk. *J. Agric. Food Chem*., **2010**, *58*, 10049-10055.
2. Bertini, F.; Canetti, M.; Cacciamani, A.; Elegir, G.; Orlandi, L.; Zoia, L. Effect of lingo-derivatives on thermal properties and degradation behaviour of poly(3-hydroxybutyrate)-based biocomposites. *Polym. Degrad. Stab. Submitted.*
3. Sanchez, C. Lignocellulosic residues: biodegradation and bioconversion by fungi. *Biotech. Adv.* **2009**, *27*, 185-194.
4. Ralph, J.; Lundquist, K.; Brunow, G.; Lu, F.; Kim, H.; Schatz, P.F.; Marita, J.M.; Hatfield, R.D.; Ralph, S.A.; Christensen, J.H.; Boerjan, W. Lignins: natural polymers from oxidative coupling of 4-hydroxyphenylpropanoids. *Phytochem. Rev*. **200**4, *3*, 29-60.
5. Feldman, D. Wood - chemistry, ultrastructure, reactions, by Fengel, D. and Wegener, G. Walter de Gruyter Ed: Berlin and NewYork, 1984, 613 pp. J. Polym. Sci.: Polym. Lett. Ed, 1985, 23 (11), 601-602.
6. Kim, S.; Dale, B.E. Global potential bioethanol production from wasted crops and crop residues. *Biomass Bioenergy* **2004**, *26*, 361-375.
7. Chandrasekhar, S.; Satyanarayana, K.G.; Pramada, P.N.; Raghavan, P.; Gupta, T.N. Processing, properties and applications of reactive silica from rice husk-an overview. *J. Mater. Sci*. **2003**, *38*, 3159-3168.
8. Krishnani, K.K.; Meng, X.; Christodoulatos, C.; Boddu, V.M. Biosorption mechanism of nine different heavy metals onto biomatrix from rice husk. *J. Hazard. Mater***. 2008**, *153*, 1222-1234.
9. D'Souza, S.F.; Godbole, S.S. Immobilization of invertase on rice husk using polyethylenimine. *J. Biochem. Biophys. Methods* **2002,** *52*, 59-62.
10. Saha, B.C.; Iten, L.B.; Cotta, M.A.; Wu, Y.W. Dilute acid pretreatment, enzymatic saccharification, and fermentation of rice hulls to ethanol. *Biotechnol. Prog*. **2005**, *21*, 816-822.
11. Yu, J.; Zhang, J.; He, J.; Liu, Z.; Yu, Z. Combinations of mild physical or chemical pre-treatment with biological pre-treatment for enzymatic hydrolysis of rice hull. *Bioresour. Technol*. **2009**, *100*, 903-908.
12. Lora, J.H.; Glasser, W.G. Recent industrial applications of lignin: a sustainable alternative to non-renewable materials. *J. Polym. Environ*. **2002**, *10*, 39-48.
13. Thielemans, W.; Can, E.; Morye, S.S.; Wool, R.P. Novel applications of lignin in composites materials. *J. Appl. Polym. Sci*. **2002**, *83*, 323-331.
14. Stewart, D. Lignin as base material for materials applications: Chemistry, application and economics. *Ind. Crops Prod*. **2008**, *27*, 202-207.
15. Asamarai, A.M.; Addis, P.B.; Epley, R.J.; Krick, T.P. Wild Rice Hull Antioxidants. *J. Agric. Food Chem*. **1996**, *44*, 126-130.

16. Butsat, S.; Weerapreeyakul, N.; Siriamornpun, S. Changes in phenolic acids and antioxidant activity in thai rice husk at five growth stages during grain development. *J. Agric. Food Chem*. **2009**, *57*, 4566-4571.
17. Avella, M.; Rota, G.L.; Martuscelli, E.; Raimo, M.; Sadocco, P.; Elegir, G. Poly(3-hydroxybutyrate-co-3-hydroxyvalerate) and wheat straw fibre composites: thermal, mechanical properties and biodegradation behaviour. *J Mater. Sci.*, **2000**, *35*, 829-836
18. Kim, H.S.; Kim, H.J.; Lee, J.W.; Choi, I.G. Biodegradability of bio-flour filled biodegradable poly(butylene succinate) bio-composites in natural and compost soil. *Polym. Degrad. Stab*., **2006**, *91*, 1117-1127
19. Mohanty, A.K.; Misra, M.; Hinrichsen, G. Biofibres, biodegradable polymers and biocomposites: an overview. *Macromol Mater Eng*, **2000**, *276-277*, 1-24.
20. Mohanty, A.K.; Misra, M.; Drzal, L.T. Sustainable bio-composites from renewable resources: opportunities and challenges in the green materials world. *J Polym Environ* **2002**, *10*, 19-26.
21. Luckachan, G.E.; Pillai, C.K.S. Biodegradable polymers. A review on recent trends and emerging perspectives. *J Polym Environ* **2011**, *19*, 637-76.
22. Greco, P.; Martuscelli, E. Crystallization and thermal behaviour of poly(D(-)3-hydroxybutyrate) - based blends. *Polymer* **1989**, *30*, 1475-83.
23. Dubini Paglia, E.; Beltrame, P.L.; Canetti, M.; Seves, A.; Marcandelli, B.; Martuscelli, E. Crystallization and thermal behaviour of poly(D(-)3-hydroxybutyrate)/poly(epichlorohydrin) blends. *Polymer* **1993**, *34*, 996-1001.
24. Gassner, F.; Owen, A.J. Physical properties of poly(p-hydroxybutyrate)-poly(ε-caprolactone) blends. *Polymer*, **1994**, *35*, 2233-2236.
25. Avella, M.; Martuscelli, E.; Orsello, G.; Raimo, M.; Pascucci, B. Poly(3 hydroxybutyrate)/poly(methyleneoxide) blends: thermal, crystallization and mechanical behaviour. *Polymer*, **1997**, *38*, 6135-43.
26. Le Digabel, F.; Avérous, L. Properties of biocomposites based on lignocellulosic fillers. *Carbohyd Polym*, **2006,** *66*, 480-93.
27. Shanks, R.A.; Hodzic, A.; Wong, S. Thermoplastic biopolyester natural fiber composites. *J Appl Polym Sci* **2004**, *91*, 2114-21.
28. Grillo Fernandes, E.; Pietrini, M.; Chiellini, E. Bio-based polymeric composites comprising wood flour as filler. *Biomacromolecules* **2004**, *5*, 1200-5.
29. Barkoula, N.M.; Garkhail, S.K.; Peijs, T. Biodegradable composites based on flax/polyhydroxybutyrate and its copolymer with hydroxyvalerate. *Ind Crop* **2010**, *31*, 34-42.
30. Pouteau, C.; Dole, P.; Cathala, B.; Averous, L.; Boquillon, N. Antioxidant properties of lignin in polypropylene. *Polym Degrad Stab* **2003**, *81*, 9-18.

31. Pucciariello, R.; Villani, V.; Bonini, C.; D'Auria, M.; Vetere, T. Physical properties of straw lignin-based polymer blends. *Polymer*, **2004**, *45*, 4159-69.
32. Gregorova, A.; Košíková, B.; Moravcik, R. Stabilization effect of lignin in natural rubber. *Polym Degrad Stab*, **2006**, *91*, 229-33.
33. Gregorova, A.; Košíková, B.; Staško, A. Radical scavenging capacity of lignin and its effect on processing stabilization of virgin and recycled polypropylene. *J Appl Polym Sci* **2007,** *106*, 1626-31.
34. Li, J.; Li, B.; Zhang, X.; Su, R. The study of flame retardants on thermal degradation and charring process of manchurian ash lignin in the condensed phase. *Polym Degrad Stab*, **2001**, *72*, 493-8.
35. Canetti, M.; Bertini, F.; De Chirico, A.; Audisio, G. Thermal degradation behaviour of isotactic polypropylene blended with lignin. *Polym Degrad Stab* **2006**, *91*, 494-8.
36. Song, P.; Cao, Z.; Fu, S.; Fang, Z.; Wu, Q.; Ye, J. Thermal degradation and flame retardancy properties of ABS/lignin: effects of lignin content and reactive compatibilization. *Thermochimica Acta* **2011**, *518*, 59-65.
37. Canetti, M.; De Chirico, A.; Audisio, G. Morphology, crystallization and melting properties of isotactic polypropylene blended with lignin. *J Appl Polym Sci* **2004,** *91*, 1435-42.
38. Canetti, M.; Bertini, F.; Supermolecular structure and thermal properties of poly(ethyleneterephthalate)/lignin composites. *Compos Sci Technol* **2007,** *67*, 3151-7.
39. Weihua, K.; He, Y.; Asakawa, N.; Inoue, Y. Effect of lignin particles as a nucleating agent on crystallization of poly(3-hydroxybutyrate). *J Appl Polym Sci*, **2004,** *94*, 2466-74.
40. Mousavioun, P.; Doherty, W.O.S.; George, G. Thermal stability and miscibility of poly(hydroxybutyrate) and soda lignin blends. *Ind Crop Prod* **2010,** *323*, 656-61.
41. Dudonné, S.; Vitrac, X.; Coutière, P.; Woillez, M. ; Mérillon J. Comparative study of antioxidant properties and total phenolic content of 30 plant extracts of industrial interest using DPPH, ABTS, FRAP, SOD, and ORAC assays. *J. Agric. Food Chem***. 2009**, *57*, 1768-1774.
42. Diouf, P.N.; Stevanovic, T.; Cloutier, A. Antioxidant properties and polyphenol contents of trembling aspen bark extracts. *Wood Sci. Technol.* **2009**, *43*, 457-470.
43. Cruz, J.M.; Domínguez, J.M.; Domínguez, H.; Parajó J.C. Antioxidant and antimicrobial effects of extracts from hydrolysates of lignocellulosic materials. *J. Agric. Food Chem.* **2001**, *49*, 2459-2464.
44. Yu, L., Haley, S., Perret, J., Harris, M., Wilson, J., & Qian, M. Free radical scavenging properties of wheat extracts. *J. Agric. Food Chem.* **2002**, *50*, 1619-1624.

45. Gorinstein, S.; Zachwieja, Z.; Katrich, E.; Pawelzik, E.; Harvenkit, R.; Trakhtenberg, S.; Martin-Belloso O. Comparison of the contents of the main antioxidant compounds and antioxidant activity of white grapefruit and his hybrid. *Lebensm. - Wiss. u. - Technol***. 2004**, *37*, 337-343.
46. Brand-Williams, W.; Cuvelier, M.E.; Berset, C. Use of a free radical method to evaluate antioxidant activity. *Lebensm. - Wiss. u. - Technol*. **1995**, *28*, 25-30.
47. Lora, J. H.; Glasser, W.G. Recent Industrial Applications of Lignin: A Sustainable Alternative to Nonrenewable Materials. *Journal of Polymers and the Environment*, **2002**, *10 (1/2)*, 39-49.
48. Anderson, G.; Filpponen, I.; Lucia, A. L.; Saquing, C.; Baumberger, S.; Argyropoulos, D. S. Toward a Better Understanding of the Lignin Isolation Process from Wood. *J. Agric. Food Chem*. **2006,** *54*, 5939-5947.
49. Iglesias, G.; Bao, M.; Lamas, J.; Vega, A. Soda pulping of Miscanthus sinensis. Effects of operational variables on pulp yield and lignin solubilization. *Bioresour. Technol*. **1996**, *58*, 17-23.
50. Crestini C.; Argyropoulos D.S. Structural Analysis of Wheat Straw Lignin by Quantitative 31P and 2D NMR Spectroscopy. The Occurrence of Ester Bonds and β-O-4 Substructures. *J. Agric. Food Chem.* **1997**, *45*, 1212-1219.
51. El Saied, H.; Nada, A.M.A. The thermal behaviour of lignins from wasted black pulping liquors. *Polym Degrad Stab* **1993**, *40*, 417-21.
52. Sun, R.C.; Tomkinson, J.; Lloyd Jones, G. Fractional characterization of ash-AQ lignin by successive extraction with organic solvents from oil palm EFB fibre. *Polym Degrad Stab* **2000**, *68*, 111-9.
53. Tejado, A.; Pena, C.; Labidi, J.; Echeverria, J.M.; Mondragon, I. Physico-chemical characterization of lignins from different sources for use in phenol-formaldehyde resin synthesis. *Bioresour Technol* **2007**, *98*, 1655-63.
54. Chauvette, G.; Heitz, M.; Rubio, M.; Khorami, J.; Chornet, E.; Menard, H. TG/DTG as a rapid method for the characterization of solid residues derived from liquefaction of lignocellulosics. *Thermochimica Acta* **1985,** *84*, 1-5.
55. Raveendran, K.; Ganesh, A.; Khilar, K.C. Pyrolysis of biomass and biomass components. *Fuel* **1996,** *75*, 987-98.
56. Sun, R.C.; Fang, J.M.; Rowlands, P.; Bolton, J. Physicochemical and thermal characterization of wheat straw hemicelluloses and cellulose. *J Agric Food Chem* **1998**, *46*, 2804-9.
57. El-Hadi, A.; Schnabel, R.; Straube, E.; Müller, G.; Riemschneider, M. Effect of melt processing on crystallization behavior and rheology of poly(3-hydroxybutyrate) (PHB) and its blends. *Macromol Mater Eng* **2002,** *287*, 363-72.

58. Di Lorenzo, M.L.; Sajkiewicz, P.; Gradys, A.; La Pietra, P. Optimization of melting conditions for the analysis of crystallization kinetics of poly(3-hydroxybutyrate). *e-Polymers*, **2009**, *27*.
59. de Koning, G.J.M.; Scheeren, A.H.C.; Lemstra, P.J.; Peeters, M.; Reynaers, H. Crystallization phenomena in bacterial poly[(R)- 3-hydroxybutyrate]: 3. Toughening via texture changes. *Polymer* **1994**, *35*, 4598-605.
60. Gunaratne, L.M.W.K.; Shanks, R.A.; Amarasinghe, G. Thermal history effects on crystallisation and melting of poly(3-hydroxybutyrate). *Thermochimica Acta* **2004**, *423*, 127-35.
61. Avrami, M. Kinetics of phase change, I. General theory. *J Chem Phys* **1939**, *7*, 1103-12.
62. Chen, M.; Chung, C.T. Analysis of crystallization kinetics of poly(ether ether ketone) by a nonisothermal method. *J Polym Sci Polym Phys* **1998,** *36*, 2393-9.
63. Cimmino, S.; Iodice, P.; Martuscelli, E.; Silvestre, C. Poly(3-D(-)hydroxybutyrate)/atactic poly(methylmethacrylate) blends: morphology, miscibility and crystallization relationships. *Thermochimica Acta* **1998,** *321*, 89-98.

6. ARCHAEOLOGICAL WATERLOGGED WOODS CHARACTERIZATION

6.1 Background, objectives, and strategies

Archaeological wooden artifacts can survive better in wet environments where microbial and fungal activity is limited, as is the case of underwater shipwrecks. In aquatic environments anaerobic bacteria are primarily responsible for the depletion of wood carbohydrates, leaving a porous and unstable residual structure mainly consisting of lignin (*1*,*2*) which can easily collapse during drying and needs specific consolidation treatments. During this process lignin can also be degraded or altered to some extent but very little is known about its chemical decay, although it is believed to be limited compared to the degradation undergone by cellulose and hemicellulose (*3*).

The main chemical components in wood are cellulose, hemicellulose, lignin and extractives. Cellulose is a homo-polymer of β-1,4-glucose units with a highly regular H-bonded network between its layers, especially in the case of crystalline cellulose, while hemicellulose is a carbohydrate hetero-polymer consisting of different monomers. Lignin is an irregular, cross-linked polymer network, which is composed of randomly cross-linked phenylpropanoid units, basically derived from coniferyl alcohol in softwoods, and from both coniferyl alcohol and sinapyl alcohol in hardwoods.

High-resolution nuclear magnetic resonance (NMR) spectroscopy has been one of the most important analytical techniques for 40 years in the field of organic and polymeric chemistry. Nevertheless, the number of NMR contributions in the field of archaeological wooden materials characterization *(4-6*) has been very limited whereas NMR has been well developed in the paper industry and related fields of applications *(7,8).* Recently, high-resolution nuclear magnetic resonance of ^{13}C, developed in the field of geochemistry to characterize fungal degraded wood and to evaluate lignin in organic matter (*9*) and sediments (*10*), has been intensively used to

characterize and elucidate the chemical structure of archaeological wood samples. The best results achieved in the elucidation of archaeological woods structure has been summarized in an exhaustive overview about the most promising ^{13}C high-resolution solid-state NMR techniques recently published by Bardet (*11*). Anyway, the solid state ^{13}C-NMR is not sensitive enough for a comprehensive characterization and quantification of all the intermonomeric bonds which are representative of the lignin structure. Furthermore, this technique is not able to detect and quantify important functional groups such as carboxylic and alcoholic moieties. In order to gain a complete picture of lignin chemical features (*12-14*), liquid NMR analytical tools such as qualitative and quantitative heteronuclear single quantum coherence (2D-HSQC), quantitative ^{13}C-NMR and ^{31}P-NMR analysis, have been adopted. The limit of this approach is that the diagnostic of archaeological wooden objects is still based on lignin isolation which may result in some extent of chemical and structural modification, even if mild conditions are applied to the extraction procedure.

The three-dimensional lignin network that binds lignocellulosic components together makes it practically impossible to dissolve wood in its native form in conventional molecular solvents. Thus, it is important to find a non-derivatizing solvent to provide efficient dissolution and stability to varius reagent in order to achieve an homogeneous reaction environment to preserve the native structure of wood. Ionic liquids (ILs) have arisen as such solvent. In recent years, there have been lots of reports on dissolution of cellulose in ILs and its application but solubilization of native lignocellulosic materials is far more complicated due to their complex structure from the three-dimensional lignin network.

In ILs, both the cation and the anion of the salt play a crucial role in the dissolution of cellulose. The most promising cations are butyl or allyl

derivatives of imidazolium salts whereas counter chloride anion is usually the most effective due to its hydrogen bonds destroying capability.

ILs such as [amim]Cl can provide an homogenous reaction medium for wood-based lignocellulosic materials. Highly substituted lignocellulosic esters can be obtained under mild conditions by reacting wood dissolved in ionic liquid with either acetyl chloride or benzoyl chloride in the presence of pyridine**.** Alternatively, the lignocellulosic material can be phosphytilated by reaction with 2-chloro-4,4,5,5-tetramethyl-1,3,2-dioxaphospholane in the presence of pyridine as well. As a result, the functionalized wood develops an enhanced solubility in molecular solvents, allowing for a complete characterization by means of spectroscopic and chromatographic techniques.

Nowadays, the most important goal in elucidating wood structure is the preservation of informations about the presence and the extent of any additional interaction between lignin and different biopolymer found in wood. Both GPC (*15*) and ^{31}P NMR analyses may provide evidence about the presence of elusive lignin carbohydrate complexes (LCCs) (*16,17*) that may be altered to some extent during chemical modifications. In this study is investigated the chemical alteration of archaeological woods samples, along with the corresponding extracted lignin, collected from the archaeological site of the Ancient Ships of San Rossore (Pisa, Italy), where over the last 10 years 31 Roman shipwrecks dating between the 2nd century BC and the 5th century AD have been discovered (*18*). The *taxa* of the examined woods were: *Arbutus unedo* (Strawberry tree) and *Quercus* (Oak). The adopted analytical approach integrated nuclear magnetic resonance spectroscopic techniques such as bidimensional heteronuclear single quantum coherence (2D-HSQC-NMR) and phosphorous-31 nuclear magnetic resonance (^{31}P-NMR) with gel permeation chromatography (GPC) to determine chemical features and molecular weight distributions for wood and the corresponding extracted lignin.

6.2 Experimental results

6.2.1 GPC analysis of extracted lignins

The ageing effects on the structure of archaeological waterlogged wood were at first evaluated by GPC analyses in order to detect possible increase/decrease in the average molecular weights of the extracted lignin (*Figure 1*).

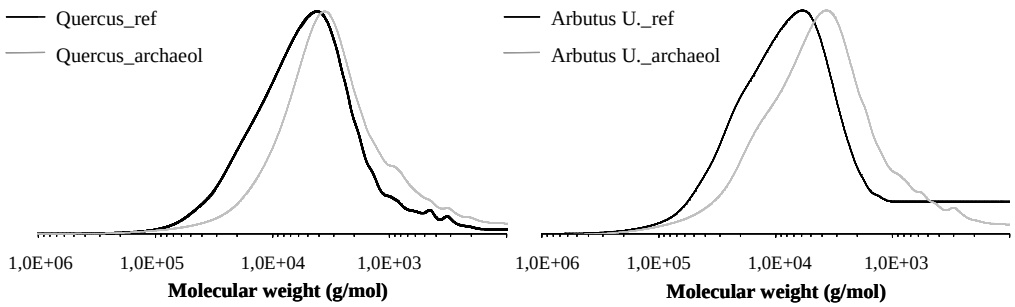

Figure 1. Overlapped GPC profiles of reference (black line) and archaeological (gray line) acetylated lignin extracted from *Quercus* (left) and *Arbutus unedo* (right).

Both the archaeological lignins underwent a limited delignification process since no sensible shift towards low molecular weights is observed with regard to reference lignin specimen. Assuming the reference sound sample representativity, it seems that *Quercus* lignin has been subjected to a depolymerization process which mainly affected the high molecular weight fraction while *Arbutus Unedo* lignin underwent a comprehensive consumption.

6.2.2 NMR analysis of extracted lignins

Lignin samples extracted from both archaeological and reference sound woods were further analyzed by 2D-HSQC-NMR spectroscopy to identify the principal intermonomeric bonds and to evaluate any significant changes in the polyphenol chemical structure. The main intermonomeric units in

lignin include: arylglycerol-β-arylether (β-O-4), phenylcoumaran (β-5), pinoresinol (β-β), and dibenzodioxocine (5-5'-O-4).

The analyses, reported in *Figures 2* and *Figure 3*, highlighted that all the examined lignins were rich in arylglycerol-β-arylether units (β-O-4). Cross-peaks relating to other principal intermonomeric bonds (β-5, β-β) were also identified. These results confirmed and reinforced Bardet's and Colombini conclusion (*20*): in ancient waterlogged woods the chemical structure of lignin is not heavily modified by the ageing process, and the principal intermonomeric linkages are still represented.

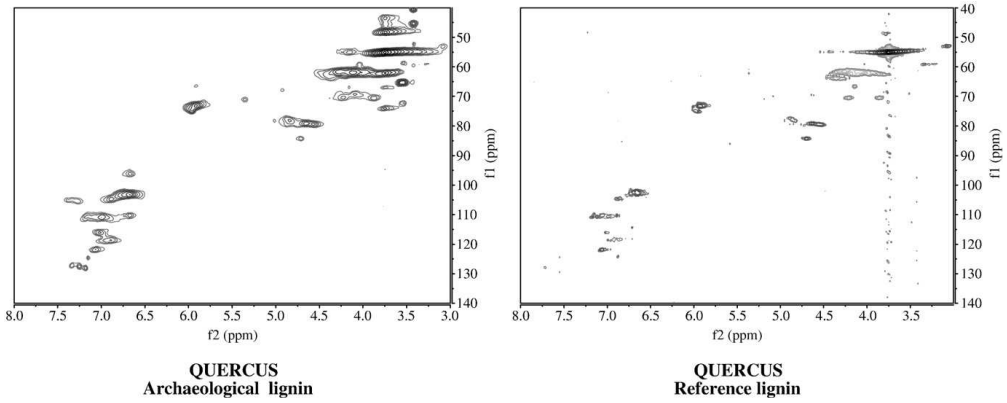

Figure 2. 2D-HSQC-NMR spectra of acetylated lignin extracted from archaeological (left) and reference sound (right) *Quercus* wood.

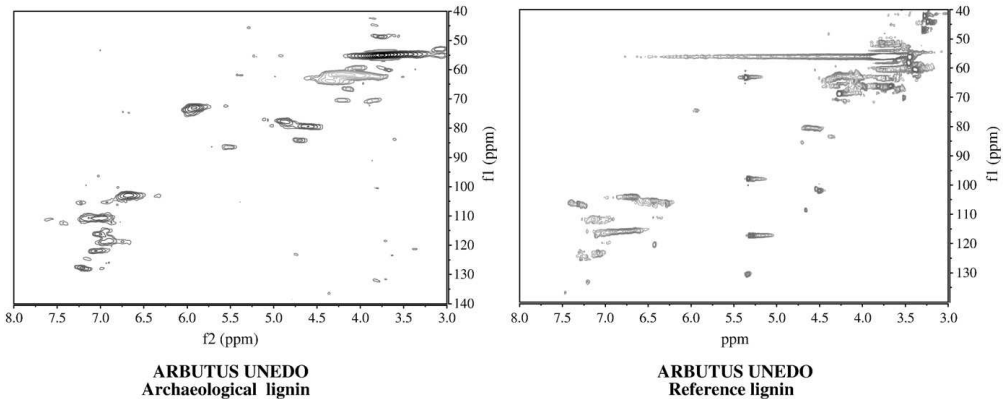

Figure 3. 2D-HSQC-NMR spectra of acetylated lignin extracted from archaeological (left) and reference sound (right) *Arbutus Unedo* wood.

The extracted lignins were then characterized by quantitative ^{31}P-NMR spectroscopy in order to detect and quantify p-hydroxycumaryl (P-OH), guaiacyl (G-OH), syringyl (S-OH) and condensed free phenolic units as well as carboxylic acids. *Table 1* reports the ^{31}P-NMR quantification (expressed as mmol/g of lignin) of different phenols and acidic moieties for the extracted lignins. All data were normalized on the Klason lignin content.

	***Quercus* - reference**	***Quercus* - archaeological**	***Arbutus Unedo* - reference**	***Arbutus Unedo* - archaeological**
Condensed Ph-OH (mmol/g)	0,53	0,54	0,50	0,43
S-OH (mmol/g)	0,34	0,64	0,31	0,21
G-OH (mmol/g)	0,61	0,58	0,67	0,68
P-OH (mmol/g)	0,11	0,08	0,08	0,12
COOH (mmol/g)	0,11	0,23	0,24	0,32

Table 1. Extracted lignin – ^{31}P NMR analysis: content values of different free phenols (condensed, syringyl, guaiacyl, p-hydroxyphenyl) and total acidic groups, expressed as mmol/g of lignin. Data normalized on Klason lignin content.

The free phenolic content did not appear notably affected by the ageing process whereas a slight increase in total acidic moieties was observed, according to an oxidative delignification. Such a comprehensive conservation of lignin structure and functionalities was in agreement with literature data (*21*). The random trend of syringyl content was attributed to the limited reliability of the reference specimens.

6.2.3 GPC analysis of unprocessed woods

The development of alternative, strong hydrogen bond destroying solvents as the ionic liquids gave a boost to the investigation of ordinarily unsoluble materials as wood powders. Therefore, GPC analyses were also carried out on benzoylated pulverized woods to facilitate the detection of all wood components by UV detection. The materials recovered after planetary ball

milling were dissolved in ionic liquid, giving an homogeneous phase, and benzoylated with benzoyl chloride in the presence of pyridine.

Figure 4 reports the GPC profiles of the unprocessed reference sound wood (black line) versus the analogue archaeological wood (gray line) for the two wood *taxa* examined. Generally, the molecular weight distributions showed a bimodal trend, due to the contemporary presence of a fraction containing cellulose and lignin carbohydrate complexes (LCCs) and a fraction composed of partially free lignin. For all the ancient samples (grey line) a significant decrease in the wood molecular weight is detected, mostly related to carbohydrates cleavage.

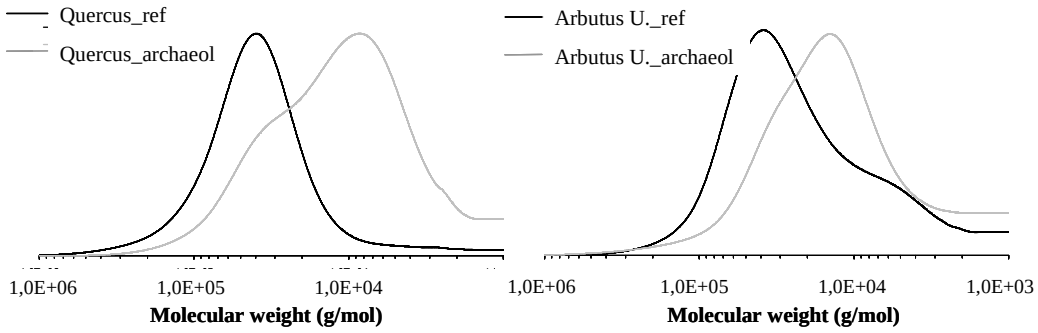

***Figure 4*.** Overlapped GPC profiles of reference (black line) and archaeological (gray line) benzoylated pulverized wood of *Quercus* (left) and *Arbutus unedo* (right).

Quercus sound wood chromatogram (black line) showed a unimodal profile whereas the GPC chromatogram of *Arbutus Unedo* reference wood (black line) highlighted the presence of partially free lignin as a shoulder in the lower molecular weight region. Moreover, *Quercus* archaeological wood (gray line) still exposed a pronounced shoulder related to the residual polysaccharide fraction while *Arbutus Unedo* practically lacked of this signal, according to the higher Klason lignin content (*Table 2*).

Sample	Klason Lignin (%)
Arbutus Unedo - reference	32,5
Arbutus Unedo - ancient	73,9
Quercus - reference	31,4
Quercus - ancient	58,7

Table 2. Klason lignin content in archaeological and sound reference wood**.**

A comparison among these results may account for lignin-carbohydrate complexes (LCC) of different chemical type and strength that could interfere in the degradation process, occurring with different deterioration extent of wood. An extensive network of LCCs or a their pronounced chemical recalcitrance may also account for the moderate carbohydrate consumption observed for *Quercus* wood (*Table 2*). Altogheter, GPC analyses demonstrated a deeper and faster degradation of the polysaccharide matrix compared to a limited delignification process, especially in the case of *Arbutus Unedo* wood, as also clearly conceivable from the Klason lignin data (*Table 2*).

6.2.4 NMR analysis of unprocessed woods

Unprocessed archaeological woods and cellulase-digested reference sound woods were subjected to 2D-HSQC-NMR and quantitative ^{31}P-NMR analyses in order to validate the spectroscopic results gained on lignin specimens. The characterization of lignocellulosic materials in their native form is extremely valuable because, even if mild conditions are applied to the lignin extraction procedure, some extent of chemical and structural modification should be taken into account. Ionic liquid such as [amim]Cl provides an homogenous reaction medium for the esterification of wood-based lignocellulosic materials, allowing for their solubilization into traditional molecular solvents.

HSQC spectra recorded on acetylated *Quercus* and *Arbutus Unedo* archaeological woods (*Figure 5*) displayed the same signals found for the corresponding extracted lignins. Furthermore, also the relative abundance of the principal intermonomeric linkages were comparable, suggesting that the chemical structure of the two lignin specimens was negligibly affected by the adopted extraction procedure. This result confirmed how the acidolytic extraction applied for lignin isolation was mild enough to avoid any significant degradation.

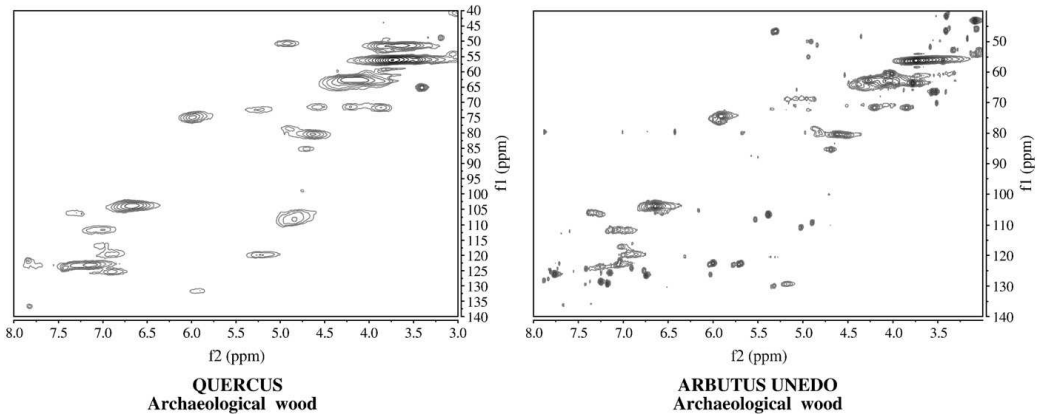

Figure 5. 2D-HSQC-NMR spectra of acetylated archaeological Quercus (left) and Arbutus unedo (right) wood.

In degraded wood the content of cellulose is generally very low compared to lignin, especially after long exposure to wet environments, whereas in reference sound woods the polysaccharide fraction constitutes about 65-70% of the total weight. As a consequence, a comparison between the analyses of archaeological waterlogged wood and sound reference wood can be limited by the presence of polysaccharides which could influence the signal intensity or interfere with the lignin analysis. Therefore, with regards to reference sound woods, an enzymatic purification is needed in order to achieve a sensible spectroscopic characterization of the polyphenolic fraction. ^{31}P-NMR spectra were recorded for unprocessed archaeological woods and

cellulase-digested reference sound woods according to the set of conditions described by King et al. (*22*). The integration values were converted to mmol/g of hydroxyls for a 100% lignin representation.

Table 3 displays the ^{31}P-NMR quantification of free phenols and acidic moieties in archaeological and cellulase-digested reference sound *Quercus* wood. According to the followed experimental procedure, is pointed out a partial insolubility of the cellulase-digested *Quercus* reference wood.

	***Quercus* wood - archaeological**	***Quercus* lignin - archaeological**	***Quercus* wood - reference**	***Quercus* lignin - reference**
Klason lignin (%)	58,7	90,0	31,4	90,0
Condensed + S-OH	0,79	1,18	0,37	0,87
G-OH	0,27	0,58	0,32	0,61
P-OH	n.d.	0,08	n.d.	0,11
COOH	0,44	0,23	0,18	0,11

Table 3. *Quercus*: unprocessed archaeological and cellulase-treated reference sound wood – ^{31}P NMR analysis. Content values of different free phenols (condensed + syringyl, guaiacyl, p-hydroxyphenyl) and total acidic groups, expressed as mmol/g of lignin. Data normalized on Klason lignin percentage.

It is worth noticing that for both archaeological and reference sound Oak wood, the quantification of phenolics moieties showed a substantial dissimilarity if compared to the corresponding lignin data. Specifically, all the data referring to the acidolytic lignin samples were found to be larger than the corresponding integrations on wood specimens. This trend may be due to a high LCCs content which could reduce the number of exposed, available phenolic functionalities because of the presence of covalent bonds between phenols and polysaccharides. This conclusion was also supported by the GPC analyses. The increase in acid moieties for the two wood samples was related to the presence of oxidized carbohydrates.

Table 4 reports the ^{31}P-NMR quantification of free phenols and acidic moieties in archaeological and cellulase-digested reference sound *Arbutus Unedo* wood.

	***Arbutus U.* wood - archaeological**	***Arbutus U.* lignin - archaeological**	***Arbutus U.* wood - reference**	***Arbutus U.* lignin - reference**
Klason lignin (%)	73,9	90,0	32,5	90,0
Condensed + S-OH	0,59	0,64	0,44	0,81
G-OH	0,54	0,68	0,59	0,67
P-OH	0,10	0,12	0,07	0,08
COOH	0,37	0,32	0,33	0,24

Table 4. *Arbutus Unedo*: unprocessed archaeological and cellulase-treated reference sound wood – ^{31}P NMR analysis. Content values of different free phenols (condensed + syringyl, guaiacyl, p-hydroxyphenyl) and total acidic groups, expressed as mmol/g of lignin. Data normalized on Klason lignin percentage.

With regard to the cellulase-treated *Arbutus Unedo* reference wood, the presence of a thick gel precipitate is noted. However, in archaeological and sound reference Strawberry tree wood the phenolics content values were found to be almost equal to the related extracted lignin. This trend was in agreement with the GPC analysis of benzoylated reference wood, which showed a bimodal trend due to the presence of both polysaccharides (either in a free or bounded form, or both) and free lignin, and may be recognized as the proof of a low LCCs content. Again, the slight increase in carboxylic acid functionalities for the two wood samples under examination was related to oxidized polysaccharides.

6.4 Conclusions

Little is known about the chemical transformations of the different wood components during ageing. Under favourable conditions of low temperature and low oxygen, wooden artifacts can survive underwater in a surprisingly good condition.

In this study, archaeological woods and reference sound woods of the same *taxa* (*Quercu*s and *Arbutus Unedo*), along with the corresponding extracted lignin, were fully characterized by means of phosphorus-31 NMR spectroscopy, two dimensional NMR spectroscopy (2D-HSQC-NMR) and GPC analysis. Ionic liquids can provide a homogenous reaction medium for wood-based lignocellulosic materials. Highly substituted lignocellulosic esters and phosphite esters can be obtained under mild conditions by reacting pulverized wood dissolved in ionic liquid with either acyl chlorides or dioxaphospholane in the presence of pyridine. As a result, the functionalized wood develops an enhanced solubility in molecular solvents, allowing for a complete characterization by means of spectroscopic and chromatographic techniques. The samples were collected from the Site of the Ancient Ships of San Rossore (300 BC – 400 AD, Pisa, Italy) and from the Riksapplet shipwreck (1676 AD, Sweden).

The chemical structure of archaeological extracted lignins is still very similar to the chemical structure of lignins specimens isolated from reference sound wood of the same *taxa*. Analyses upon the unprocessed woods pointed out a deeper and faster consumption of the polysaccharide matrix and confirmed a limited degradation of the polyphenolic fraction. Besides, on the basis of this approach it was possible to assess the presence of elusive lignin-carbohydrate complexes which may be altered to some extent during the lignin extraction procedure. Altogether, chromatographic, spectroscopic and Klason analyses demonstrated a severe degradation concerning the archaeological *Arbutus Unedo* wood. Ancient *Quercus* wood, instead, showed an overall recalcitrant behaviour towards chemical and/or biological degradation which could be related to the pronounced LCCs content highlighted by GPC and quantitative ^{31}P NMR analyses for both the archaeological and the reference sound wood.

References

1. Hoffmann, P.;. Jones, M.A. Structure and degradation process for waterlogged archaeological wood. In: Archaeological Wood - Properties, Chemistry and Preservation. Rowell, R.M.; Barbour, R.J. Eds., American chemical Society, American Chemical Society, Washington, 1990, 35–65.
2. Blanchette, R.A. A review of microbial deterioration found in archaeological wood from different environments, *Int. Biodeter. Biodegr*., **2000**, *46*, 189–204.
3. Geoffrey, F.D.; Nilsson, T.; Singh, A.P. Degradation of lignocellulosics by unique tunnelling-forming bacteria. *Can. J. Microbiol*., **1987**, *33*, 943-948.
4. Lambert, J.B.; Shawl, C.E.; Stearns, J.A. Nuclear magnetic resonance in archaeology. *Chem. Soc. Rev*., **2000**, *29*, 175-182.
5. Alesiani, M.; Proietti, F.; Capuani, S.; Paci, M.; Fioravanti, M.; Maraviglia, B. ^{13}C CPMAS NMR spectroscopic analysis applied to wood characterization. *Appl. Magn. Reson*., **2005**, *29*, 177-184.
6. Bardet, M.; Foray, M.F.; Trân, Q.K. High-resolution solid-state CPMAS NMR study of archaeological woods, *Anal. Chem*., **2002**, *74 (17)*, 4386-4390.
7. Ralph, J.; Marita, J.M.; Ralph, S.A.; Hatfield, R.D.; Lu, F.; Ede, R.M.; Peng, J.; Quideau, S.; Helm, R.F.; Grabber, J.H.; Kim, H.; Jimenez-Monteon, G.; Zhang, Y.; Jung, H.J.G.; Landucci, L.L.; MacKay, J.J.; Sederoff, R.R.; Chapple, C.; Boudet, A.M. Solution-state NMR of lignins, in: D.S. Argyropoulos (Ed.), Advances in Lignocellulosics Characterization, TAPPI Press, Atlanta, 1999, pp. 55-108.
8. Canevali, C.; Orlandi, M.; Zoia, L.; Scotti, R.; Tolppa, E.L.; Sipila, J.; Agnoli, F.; Morazzoni, F. Radicalization of lignocellulosic fibers, related structural and morphological changes, *Biomacromolecules*, **2005**, *6*, 1592-1601.
9. Simpson, M.J.; Hatcher, P.G. Determination of black carbon in natural organic matter by chemical oxidation and solid-state ^{13}C nuclear magnetic resonance spectroscopy. *Org. Geochem*., **2004**, *35*, 923-935.
10. Saiz-Jimenez, C.; Boon, J.J.; Hedges, J.I.; Hessels, J.K.C.; De Leeuw, J.W. Chemical characterization of recent and buried woods by analytical pyrolysis. Comparison of pyrolysis data with ^{13}C NMR and wet chemical data, *J. Anal. Appl. Pyrolysis*, **1987**, *11*, 437-450.
11. Bardet M.,; Gerbaud, G.; Giffard, M.; Doan, C.; Hediger, S.; Le Pape, L. ^{13}C high-resolution solid-state NMR for structural elucidation of archaeological woods, *Progress in Nuclear Magnetic Resonance Spectroscopy*, **2009**, 55, 199–214.
12. Colombini, M.P.; Orlandi, M.; Modugno, F.; Tolppa, E.L.; Sardelli, M.; Zoia, L.; Crestini, C. Archaeological wood characterisation by

PY/GC/MS, GC/MS, NMR and GPC techniques. *Microchem. J*., **2007**, *85*, 164-173.
13. Crestini, C.; El Hadidi, N.M.N.; Palleschi, G. Characterisation of archaeological wood: a case study on the deterioration of a coffin. *Microchem. J*., **2009,** *92 (2)*, 150-154.
14. Colombini, M.P.; Lucejko, J.J.; Modugno, F.; Orlandi, M.; Tolpa, E.L.; Zoia, L. A multi-analytical study of degradation of lignin in archaeological waterlogged wood. *Talanta*, **2009**, *80*, 61-70.
15. Argyropoulos, D.S. Opportunities with wood dissolved in ionic liquids, in: M. Orlandi, C. Crestini (Eds.), Proceedings Book of Italic5, Exorma, Roma, 2009, pp. 81-84.
16. Kilpelainen, I.; Xie, H.; King, A.; Granstrom, M.; Heikkene, S.; Argyropoulos, D.S. Dissolution of wood in ionic liquids. *J. Agric. Food. Chem*., **2007**, *55*, 9142-9148.
17. Xie, H.; King, A.W.T.; Kilpelainen, I.; Granstrom, M.; Argyropoulos, D.S. Thorough chemical modification of wood-based lignocellulosic materials in ionic liquids. *Biomacromolecules*, **2007**, *8*, 3740-3748.
18. Giachi, G.; Bettazzi, F.; Chimichi, S.; Staccioli, G. Chemical characterisation of degraded wood in ships discovered in a recent excavation of the Etruscan and Roman harbour of Pisa. *J. Cult. Heritage*, **2003**, *4*, 75–83.
19. Salanti, A.; Zoia, L.; Tolppa, E.L.; Giachi, G.; Orlandi, M. Charactreization of waterlogged wood by NMR and GPC techniques. *Microchem. J*., **2010**, *95*, 345-352.
20. Bardet, M.; Foray, M.F.; Tran Q. K. High-resolution solid-state CP MAS NMR study of archaeological woods. *Anal. Chem*., **2002**, *74*, 4386-4390.
21. King, A.W.T.; Zoia, L.; Filpponen, I.; Olszewska, A.; Xie, H.; Kilpelainen, I.; Argyropoulos, D.S. In situ determination of lignin phenolics and wood solubility in imidazolium chlorides using ^{31}P NMR. *J. Agric. Food Chem.*, **2009**, *57*, 8236-8243.

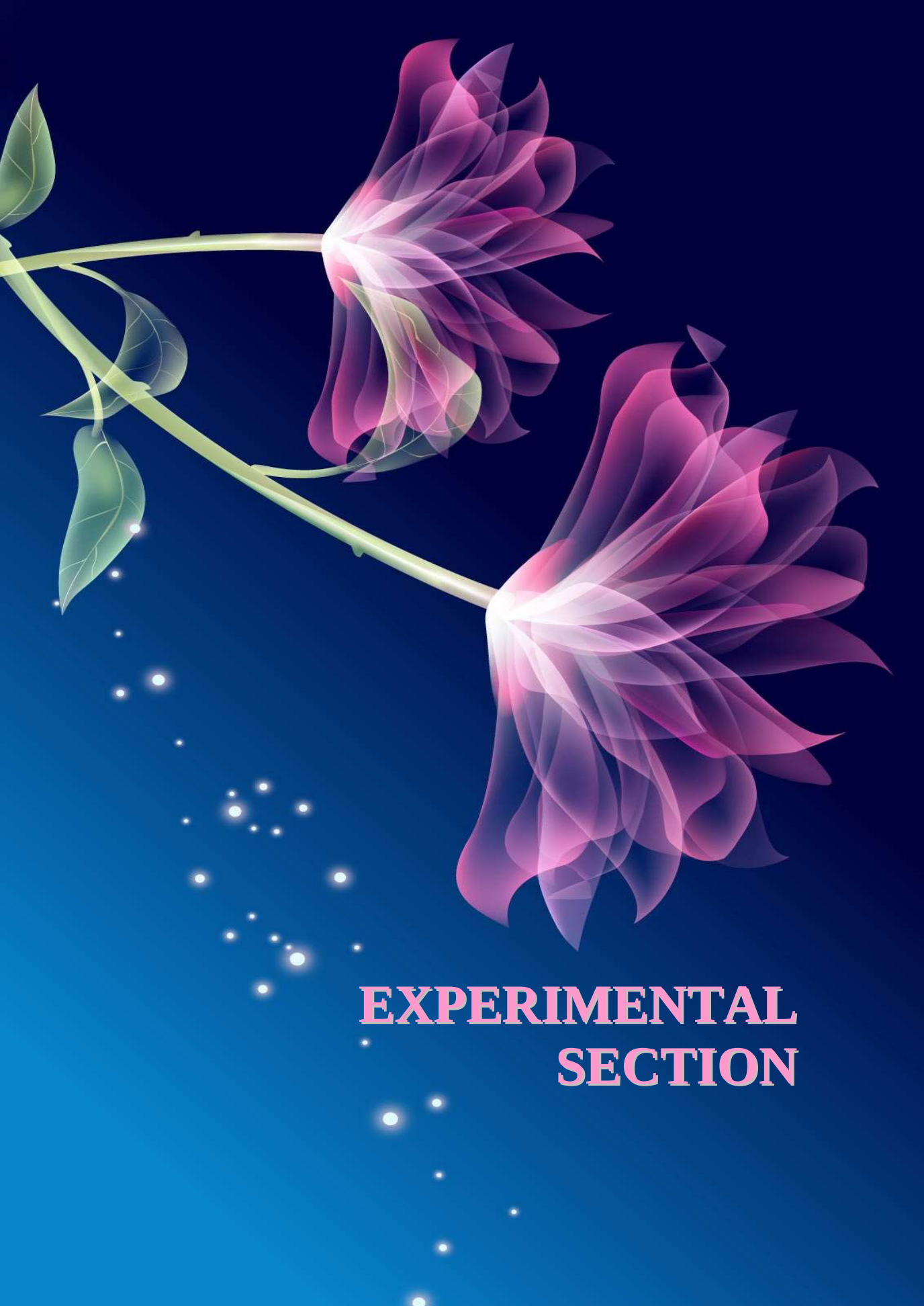

EXPERIMENTAL SECTION

GENERAL EXPERIMENTAL PROCEDURE

A comprehensive view of the experimental procedure applied in this thesis is reported below. This general protocol has been followed with slight differences within each project.

The first scheme comprises a state-of-the-art protocol for the material compositional evaluation and lignin characterization. The second scheme has been for the most part developed, implemented, and integrated during the three years of the PhD by our research group.

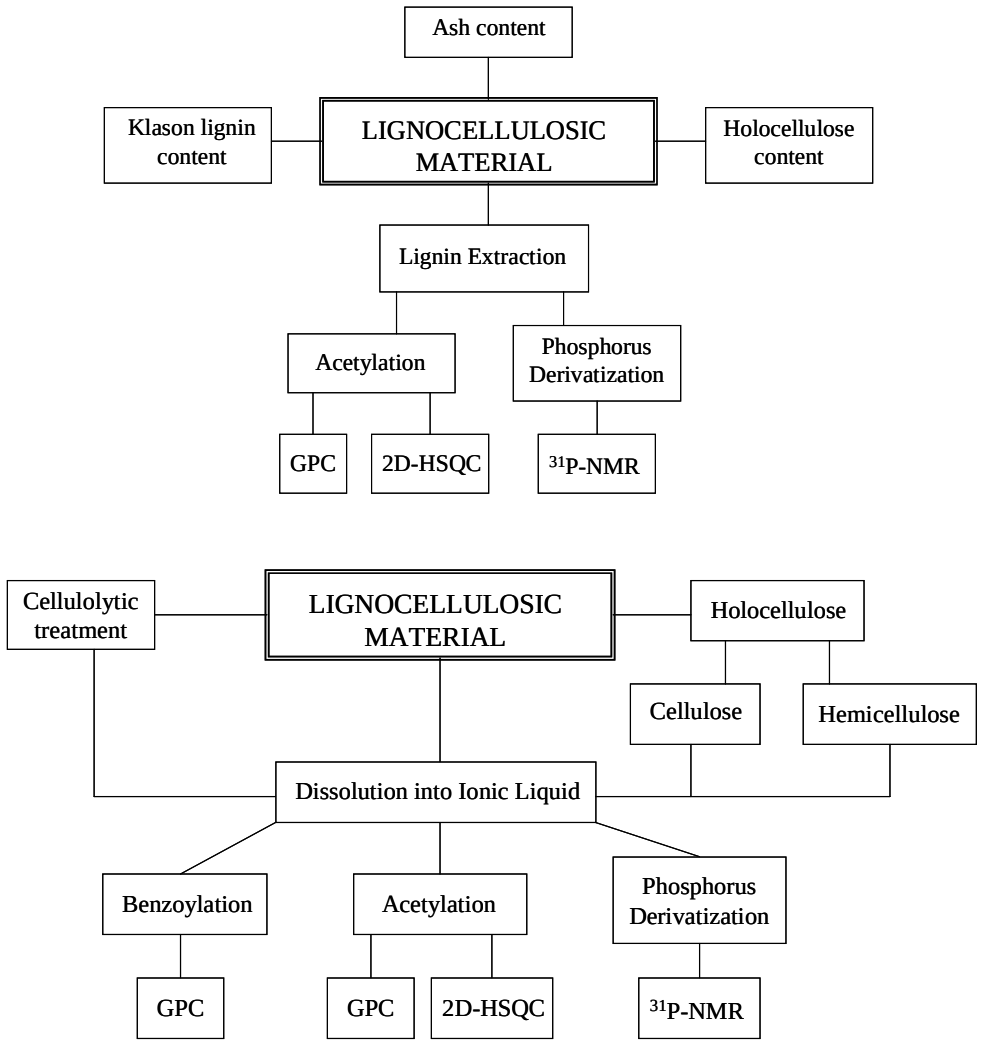

7. MATERIALS

7.1 Reagents and materials

All reagents and solvents (ACS grade) were purchased from Sigma-Aldrich and used as received without further purification.

Rice husk was kindly provided by a local factory, Gariboldi S.p.A.; *Arundo donax* and wheat straw, along with corresponding steam-exploded samples were supplied by a local factory; *Miscanthus sinensis* was gently provided during COST action FP0901.

Alkaline-enzymatic lignin was prepared by SCCP (Italian Pulp and Paper Research Institute, Milan) within a joined research activity (LIGNOPLAST project 2009-2011, financed by Fondazione Cariplo) of the University of Milano-Bicocca, SCCP and ISMAC CNR (Milan).

The poly(3-hydroxybutyrate) investigated was a commercial Biopol® sample (M_w = 134500 g/mol, M_w/M_n = 2.9) provided by ICI as a fine white powder.

Two fragments of archaeological waterlogged wood from the excavation of the San Rossore Roman Harbor (Pisa) were provided by the Archaeological Superintendence of Tuscany. Sound references wood were furnished from IVALSA CNR (Florence).

7.2 Materials preparation

7.2.1 Herbaceous plants

The four herbaceous substrates (rice husk, *Arundo donax*, wheat straw, *Miscanthus sinensis*, 10 g) were crushed in a blender for 5 minutes and passed through a 1 mm screen. The ground materials thus obtained were Soxhlet extracted with c.a. 250 mL of acetone for 24 hours. The dry, extractives-free samples (3 g) were milled in a planetary ball mill for 20 hours at 300 rpm, using a 100 mL zirconium-grinding bowl (zirconium dioxide 95%) in the presence of 6 zirconium balls (10 mm in diameter each).

In the case of rice husk also different milling periods were run (5, 10, 15, 30 h).

7.2.2 Wood

Fragments of archaeological waterlogged woods (10 g) and reference woods were washed with deionized water, freeze-dried and ground in a mortar. The wood powders thus obtained were Soxhlet extracted with c.a. 250 ml of an acetone-water solution (9:1) for 48 h. Afterwards they were submitted to an alkaline extraction with (0.075 mol/L) NaOH for 1 h (liquid-to-wood ratio 50:1) to remove tannins and then dried in an oven at 50°C until a constant weight was reached. The dry, extractives-free pulverized woods were then milled in a planetary ball mill for 24 h at 75 rpm, using a 100 ml zirconium-grinding bowl (zirconium dioxide 95%) in the presence of 6 zirconium balls (10 mm in diameter each).

7.3 Lignin content

The amount of total lignin was calculated as the sum of the acid-insoluble (Klason lignin) and acid soluble lignin content, measured according to the methodology reported by Yeh et al. (*1*). The values reported are the average of 3 analyses ±1.0% (P=0.05, n=3).

7.4 Ashes Content

Accurately weighed and dried samples (100 mg) were put in tared, well desiccated porcelain crucibles and placed in a muffle furnace set at 550°C for 3 hours. The crucibles were then stored in a desiccator until room temperature was reached. The ash content was determined gravimetrically. The values reported are the average of 3 analyses ±1.0% (P=0.05, n=3).

7.5 Biocomposites preparation

Different amounts of acetylated lignin samples were solubilized in chloroform. PHB was also dissolved in chloroform. Then the two solutions were mixed and dried in rotavapor and in vacuum pump, in order to obtain PHB/AL and PHB/AEL biocomposites with weight ratios of 97.5/2.5, 95/5, 90/10, and 85/15.

Pure PHB processed under identical conditions was prepared as reference material. The casting procedure does not modify the polymer molar mass (M_w = 133100 g/mol, M_w/M_n = 3.1).

7.6 Enzymatic hydrolysis

Approximately 1 g of reference sound milled wood was dispersed in 35 ml of acetate buffer (pH 4.5) in an Erlenmeyer flask. After the addition of the cellulase enzyme (40 FPU per gram of milled-wood, cellulase activity ~130 FPU), the flask was covered and placed in a shaker set at 40°C for 48h. The insoluble material remained after enzymatic hydrolysis was collected by centrifugation (3500 rpm, 30 min), washed with acidified deionized water (pH 2) and freeze-dried.

8. EXTRACTION PROCEDURES

8.1 Acidolysis lignin

The lignin extraction was performed according to a modification of the milled wood method developed by Holmbom and Stenius (*2*). The pulverized material (1 g) was refluxed under nitrogen atmosphere for 2 hours in a 0.1 M HCl dioxane-water solution (30 ml, 85:15) and then allowed to cool to room temperature. The insoluble material left after lignin solubilization was collected by centrifugation (3000 rpm, 15 min). The supernatant was added dropwise into a 0.01 M HCl aqueous solution (250 mL) which was then kept at +4 °C overnight to allow for a complete lignin precipitation. The

precipitate was collected by centrifugation (3000 rpm, 15 min), washed with acidified distilled water (pH 2) and freeze-dried.

8.2 Alkaline-enzymatic lignin (prepared by SCCP)

Dry rice husk was treated for 4 hours in 0.3 M NaOH at 90°C under mechanical stirring. After cooling the solid residue was separated from the black liquor and washed with a 0.3 M NaOH solution. Black liquor and washing solution were combined and lignin was precipitated by adding 5 M HCl to reach pH 3. The precipitate was recovered by centrifugation, washed and freeze-dried. In order to clean lignin from carbohydrates contamination, the sample was then subjected at two hydrolysis steps with a crude cellulase from *T. reesei* ATCC 26921 (50 U/g per step).

8.3 Extractives isolation for DPPH colorimetric assay.

Extractives isolation was performed by means of solvents possessing different polarity in order to cover a solubility range. Each extraction was performed in duplicate. Dried ground rice husk (2.5 g) was subjected to a Soxhlet extraction for 6 hours with 170 ml of either water or ethanol or acetone. After the extraction, the solutions were oven dried at 105 °C and weighted. Thereafter, each residue was resuspended in 5 mL of methanol, filtered on a tared 0.45 μm GHP filters and centrifuged in tared centrifuge tube (11000 rpm, 2 min) to eliminate methanol insoluble materials. The new concentration of the extractives was calculated and all the methanolic solutions were kept at + 4 °C until needed for the DPPH colorimetric assay.

8.4 Preparation of holocellulose

Holocellulose was prepared according to a modification of the method outlined by Chang et al (*3*). Approximately 2 g of severely blended substrate was placed in a 250 mL Erlenmeyer flask and let soak in 60 mL of water.

Afterwards, 60 mL of a NaClO aqueous solution (10-15% available chlorine) were added and 25 mL of glacial acetic acid were slowly incorporated under stirring. After being covered with a smaller inverted Erlenmeyer, the mixture was heated at 90°C. After 2 hours of oxidation, the solid residue left, i.e., holocellulose was filtered in a sintered glass crucible and oven-dried.

8.5 Extraction of Hemicellulose and α-Cellulose (*4*)

About 1 g of holocellulose was transferred in a 3 wide-mouth 250 mL round bottom flask. Using a dropping funnel, 50 mL of 5% aqueous potassium hydroxide solution and 0.014 g of $NaBH_4$ were added under nitrogen atmosphere at constant stirring for the extraction of hemicellulose A. After 2 hours, the mixture was filtered off through a sintered funnel and the filtrate acidified with glacial acetic acid until pH 5-6 was reached. The solid residue recovered was then treated in the same way for the extraction of hemicellulose B but 24% aqueous potassium hydroxide was used instead. The acidified filtrate was then joined to the previously recovered hemicellulose A solution. After the addition of ethanol (200 mL), the solution was kept at +4°C overnight to allow for hemicellulose precipitation. The exceeding supernatant liquor was removed with a vacuum assisted pipette. The precipitate was then recovered by centrifugation (3000 rpm, 15 min), washed with ethanol and freeze-dried. The insoluble residue left, designated as α-cellulose, was thoroughly washed with deionized water, ethanol, and dried with diethyl ether.

9. DERIVATIZATION PROCEDURES

9.1 Lignin acetylation

Approximately 60 mg of extracted lignin was acetylated in 2 ml of an acetic anhydride : pyridine solution (1:1, v/v) kept overnight at 40 ºC. After stripping with ethanol, toluene and chloroform (15 ml x 3 times each), the

sample was dried in vacuum and solubilized in THF or DMSO-d_6 for GPC and 2D-HSQC-NMR analysis, respectively.

9.2 Benzoylation in ionic liquid

Ionic Liquid, 1-allyl-3-methylimidazolium chloride ([amim]Cl, 950 mg), was added to the pulverized lignocellulose (50 mg) in a 8 mL dried sample bottle equipped with a mechanical stirrer, vortexed and heated at 80^{o}C until the solution was clear (18 hrs, overnight). Pyridine (230 μL, 2.6 mmol) was added; the solution was vortexed until homogeneous and allowed to cool to room temperature. Then benzoyl chloride (280 μL, 2.4 mmol) was added in one portion and vortexed until a homogeneous paste was formed. The sample was kept under magnetic stirring at room temperature for 2 hours. To precipitate the benzoylated product, a deionized water-ethanol solution (1:3 v/v, 20 mL) was added and the mixture vigorously shaken and vortexed for 5 min. The solid was filtered off through a sintered funnel (grade 3), washed with further ethanol and purified with methanol. Benzoylated samples were solubilized in THF and passed through a 0.45 μm GHP Acrodisc syringe filter for GPC analysis.

9.3 Acetylation in ionic liquid

Ionic Liquid, 1-allyl-3-methylimidazolium chloride ([amim]Cl, 950 mg), was added to the pulverized lignocellulose (50 mg) in a 8 mL dried sample bottle equipped with a mechanical stirrer, vortexed and heated at 80^{o}C until the solution was clear (18 hrs, overnight). After the addition of pyridine (400 uL, 5 mmol) the solution was vortexed until homogeneous and allowed to cool to room temperature. Acetyl chloride (300 uL, 4.2 mmol) was added in one portion and the mixture vortexed until a homogeneous yellow paste was formed. Afterwards, $CHCl_3$ was added in two portions (250 μL each) and the mixture vortexed. Further $CHCl_3$ (two portions, 1 mL each) was included and

the sample heated at 40 °C for 30 min, giving a dark, clear solution. The sample was transferred in a 100 ml round bottom flask with additional $CHCl_3$ to ensure complete recovery of the entire sample; $CHCl_3$ was then removed under rotary evaporation. Then a deionized water-ethanol solution (1:3, 20 ml) was added to induce the product precipitation and the mixture was vigorously shaken and vortexed for 2 minutes. The solid was filtered off through a sintered funnel (grade 3), washed with further ethanol and purified with methanol. Acetylated herbaceous specimens were solubilized in THF, filtered through a 0.45 μm GHP Acrodisc syringe filter and subjected to GPC analysis. Acetylated archaeological wood samples were solubilized in DMSO-d_6 (800 μl) to run 2D-HSQC-NMR analyses.

9.4 ^{31}P NMR Derivatization

9.4.1 Lignin

Accurately weighted samples (30 mg) were dissolved in a pyridine-deuterated chloroform solution (1.6:1 v/v ml, 800 μL) containing 1 mg/mL of chromium(III) acetylacetonate, [$Cr(acac)_3$] as relaxation agent. Then 100 μL of endo-N-hydroxy-5-norbornene-2,3-dicarboximide (e-HNDI) solution (121.5 mM, $CDCl_3$/pyridine 4.5:0.5) was added, along with 100 μL of 2-chloro-4,4,5,5-tetramethyl-1,3,2-dioxaphospholane as the derivatizing agent (*5*) to quantitate the amount of different labile hydroxyl groups (aliphatics, phenolics and acidic). Furthermore, the same procedure was employed for the specific determination of aliphatic hydroxyls derived from β-O-4 moieties in herbaceous plants, using 100 μL of 2-chloro-1,3,2-dioxaphospholane as the phosphorous derivatizing agent instead (*6*). ^{31}P-NMR spectra were recorded on 800 μl samples.

9.4.2 Wood

Accurately weighted wood powder (40 mg, about 1 mmol of free hydroxyl groups) was stirred in [amim]Cl (500 mg) for 18 h at 80 ºC in a 10 ml screw-top glass sample bottle. Pyridine (200 µl, 2.50 mmol) was added in one portion and the sample vortexed until visibly homogeneous (~20 s). The sample was allowed to cool to room temperature. Then 2-chloro-4,4,5,5-tetramethyl-1,3,2-dioxaphospholane (300 µl, 1.89 mmol) was added in one portion and vortexed until a cream-paste was formed. A deuterated chloroform stock solution of $Cr(acac)_3$ (1 mg/ml, 500 µl) was added in 4 portions (125 µl each) vortexing between each addition. Finally, an e-HNDI solution (121.5 mM, $CDCl_3$/pyridine 4.5:0.5, 200µl) was added in and the solution vortexed. Further dilutions with the $Cr(acac)_3/CDCl_3$ solution were necessary to reach complete solubility of the sample (required optimum dilution: 2000 µl). ^{31}P-NMR spectra were recorded on 800 µl samples.

10. METHODS

10.1 GPC analysis

The analyses were performed on a Waters 600 E liquid chromatography connected to a HP1040 ultraviolet UV detector. The injection port was a Rheodyne loop valve equipped with a 20 µL loop. The GP-column system was composed by a sequence of an Agilent PL gel 5 µm, 500 Å and an Agilent PL gel 5 µm, 10^4 Å. The solvent used was tetrahydrofuran (Fluka 99.8%). PL Polymer Standards of Polystyrene from Polymer Laboratories were used for calibration. The PS-calibration curve was tested by means of acetylated dimeric (β-5 and 5,5' lignin substructure) (*7, 8*), tetrameric (9), and hexameric (kindly provided by Prof. Sipila, University of Helsinki, Finland) lignin model compounds. The evaluation of the number-average molecular weight (M_n) and the weight-average molecular weight (M_w) for the extracted

lignin samples was performed according to the methodology developed by Himmel (*10*). The average molar mass of a polydispersed polymer, M, results from several possible methods averaging the different species present, according to the following formula:

$$M = \Sigma N_i M_i^{n+1} / \Sigma N_i M_i^n$$

where N_i is a statistical weight associated to the fraction of molecules possessing molar mass M_i. These averages may be expressed both as M_n (number-average molecular weight, n=0) and as M_w (weight-average molecular weight, n=1). The peak molecular weight M_p is defined as the molecular weight of the species with maximum N_i. Moreover, the ratio $I = M_w/ M_n$, called the Polydispersity Index, was also calculated. The M_n, M_w and M_p values reported are the average of three analyses (M_w: 1000 g/mol; M_n, M_p: 70 g/mol, P = 0.05, n = 3). Acetylated and benzoylated samples were dissolved in THF (1 mg/ml), filtered through a 0.45 μm GHP syringe filter and analyzed at a flow rate of 1 ml/min. Acetylated samples chromatograms were acquired at a wavelength of 280 nm, benzoylated samples at 240 nm.

10.2 2D-HSQC-NMR analysis

2D-HSQC spectra were run in DMSO-d_6 on acetylated samples, to avoid material fractionation before the spectroscopic analysis and to increase both the solubility and the chemical shift dispersion of the side-chain units *(11)*. The inverse detected ^{1}H-^{13}C correlation spectra were recorded on a Bruker Avance 500 MHz instrument at 313K. The spectral width was set at 6 kHz in F2 and 27 kHz in F1. Altogether, 128 transients in 256 time increments were collected. The polarization transfer delay was set at the assumed coupling of 140Hz, and a relaxation delay of 2 s was used. The spectra were processed using Π/2 shifted squared sinebell functions in both dimensions before Fourier transformation. The assignment of predominant signals in 2D-HSQC-

NMR spectra was based on chemical shift data of lignin model compounds and milled wood lignin (MWL), as reported in literature *(12-14).*

10.3 ^{31}P-NMR quantitative analysis

The ^{31}P-NMR spectra were recorded at 333 K on a Bruker Avance 500 MHz instrument. All chemical shifts reported are relative to the reaction product of the internal standard with the chosen dioxaphospholane**,** which has been observed to give a sharp signal in pyridine/CDCl3 at 152 ppm. The spectra were integrated and the precise amount of the different functional groups was calculated as described in literature (*5,6*). The ^{31}P-NMR data reported are the averages of three experiments. The maximum standard deviation of the data was 2×10^{-2} mmol/g, while the maximum standard error was 1×10^{-2} mmol/g.

10.4 Evaluation of the radical scavenging activity of extractives and lignin.

The radical scavenging activity of rice husk extractives, AL, and AEL specimens was determined by means of a spectroscopic assay involving the consumption of the stable free radical originated by DPPH in a methanolic solution. 2 ml of a DPPH methanolic solution (6.1×10^{-5} M, daily prepared) were transferred in a cuvette and the absorbance (A_0) was registered at 515 nm using a Shimadzu UV-2101PC spectrophotometer. Thereafter, different dosages of a 0.5 mg/ml methanolic solution of either water, ethanol, or acetone rice husk extractives (25, 50, 100, 200 μL each) were added. The cuvette was kept in the dark after mixing. When the antioxidant activity of lignins was measured, different dosages of the lignin samples (0.5 mg/ml of either AEL or AL, 100, 300, 400, 500 μL each) were dissolved in a dioxane-water solution (9:1) instead of methanol.

After 15 minutes, the absorbance (A) of the solutions was measured at 515 nm. The inhibition percentage of the free radical DPPH• (% I) was calculated according to the following formula:

$$\% I = [(A_0\text{-}A) / A_0] \times 100$$

Methanolic solutions (dioxane-water 9:1 solutions when the lignins were concerned) of BHA, BHT, quercetin and rutin were tested as reference antioxidants (0.5 mg/ml). The different extractives concentrations tested, expressed as μg/ml, were plotted on a log dose-inhibition curve. The resulting linear calibration curves (water extractives: $R^2 = 0.9926$; ethanol extractives: $R^2 = 0.9898$; acetone extractives: $R^2 = 0.9974$; Acidolysis Lignin: $R^2 = 0.9980$; Alkaline Enzymatic Lignin: $R^2 = 0.9968$) were used to derive the half maximal inhibitory concentration (IC_{50}).

10.5 Thermogravimetric analysis (performed by ISMAC CNR)

Thermogravimetric analyses (TGA) were carried out on a Perkin Elmer TGA-7 instrument with platinum pan. The samples were heated at 20°C/min in air or nitrogen atmosphere under a flow rate of 35 ml/min. TGA and derivate thermogravimetry (DTG) curves were recorded from 50 to 750°C.
The weight of the analyzed samples was 1.5 mg for lignin and 4-5 mg for biocomposites.

10.6 Differential scanning calorimetry (performed by ISMAC CNR)

Differential scanning calorimetry (DSC) measurements were carried out on a Perkin-Elmer Pyris 1 instrument equipped with a liquid subambient device and calibrated with indium standard. The sample was placed in a sealed aluminum pan and melt at 190°C for 3 min. The sample was cooled to 10°C at 10°C/min rate and then heated to 185°C with a scan rate of 10°C/min. The isothermal crystallization kinetics was investigated by DSC using the following standard procedure: the sample was heated up to 187°C and held at

this temperature for 3 min. Then, the sample was cooled at a nominal rate of 500°C min^{-1} to the selected crystallization temperature (T_c). The heat flow evolved during the isothermal crystallization was recorded as a function of time.

10.7 Polarized optical microscopy (performed by ISMAC CNR)

The morphology and the growth rate of PHB spherulites was determined by polarized optical microscopy (POM) using a Nikon Eclipse TE 2000-U microscope equipped with a Mettler FP82 hot stage. Thin sample films were placed between two microscope cover glasses and inserted into the hot stage. In a typical spherulite growth rate determination, the specimen was maintained at 190°C for 3 min and then cooled at room temperature at 2°C/min. Nitrogen gas was purged through the hot stage.

References

1. Yeh, T.F.; Yamada, T.; Capanema, E.; Chang, H.M.; Chiang, V.; Kadla, J.F. Rapid screening of wood chemical component variations using transmittance nearinfrared spectroscopy. *J. Agric. Food Chem*. **2005**, *53*, 3328-3332.
2. Holmbom, B.; Stenius, P. Analytical methods (series editors), papermaking science and technology. In: Forest Products Chemistry; Stenius, P. Ed.; Tappi Press: Atlanta, GA, 2000; Book 3, 105-169.
3. Yokoyama, T.; Kadla, J.F.; Chang, H.M. Microanalytical method for the characterization of fiber components and morphology of woody plants. *J. Agric. Food Chem.* **2002**, *50*, 1040-1044.
4. Pinto, P. Influência da estrutura química dos componentes da madeira no seu desempenho nos processos de produção de pastas celulósicas. Estudo comparativo entre Eucalyptus globulus e outras folhosas. PhD thesis, 2005, University of Aveiro.
5. Argyropoulos, D.S.. Quantitative phosphorus-31 NMR analysis of lignins: a new tool for the lignin chemist. *J. Wood Chem. and Technol.* **1994**. *14 (1)*, 45–63.
6. Granata, A.; D.S., Argyropoulos. 2-Chloro-4,4,5,5-Tetramethyl- 1,3,2-dioxaphospholane a reagent for the accurate determination of the uncondensed and condensed phenolic moieties in lignins. *J. Agric. Food Chem.* **1995**, *43 (6)*, 1538–1544.
7. Himmel, M.E.; Tatsumoto, K.; Oh, K.K.; Grohmann, K.; Johnson, D.K.; Chum, H.L. Molecular weight distribution of aspen lignins estimated by universal calibration. In: Lignin - Properties and Materials; W.G. Glasser, S. Sarkanen Eds., American Chemical Society: Washington, DC, 1989, 82-99.
8. Bruschi, M.; Orlandi, M.; Rindone, B.; Rummakko, P.; Zoia, L. Asymmetric biomimetic oxidations of phenols using oxazolidines as chiral auxiliaries: the enantioselective synthesis of (+)- and (-)-dehydrodiconiferyl alcohol. *J. Phys. Org. Chem*. **2006**, *19*, 592-596.
9. Crestini, C.; Argyropoulos, D.S. The early oxidative biodegradation step of residual kraft lignin models with laccase. *Bioorg. Med. Chem.* **1998,** *6*, 2161-2169.
10. Hyatt, J.A. Synthesis of some tetrameric lignin model compounds containing β-O-4 and 5,5′-interunit linkages, *Holzforschung* **1987**, *41 (6)*, 363-370.
11. Adler, E. Wood chemistry - Past present and future, *Wood Sci. Technol*. **1977**, *11*, 169–218.
12. Ralph, S.A.; Ralph, J.; Landucci, L.L. NMR database of lignin and cell wall model compounds, 2004. Available over Internet at http://www.dfrc.ars.usda.gov/software.html

13. Kilpelaeinen, I.; Sipila, J.; Brunow, G.; Lundquist, K.; Ede, R.M. Determination of two-dimensional NMR spectroscopy to wood lignin structure determination and identification of some minor structural units of hard- and softwood lignins. *J. Agric. Food Chem*. **1994**, *42*, 2790-2794.
14. Kim, H.; Ralph, J. Solution state 2D NMR of ball-milled plant cell wall gels in DMSO-d_6/pyridine-d_5. *Org. Biomol. Chem*. **2010**, *8 (3)*, 576-591.

PAPERS

1. Orlandi, M.; Salanti, A.; Tolppa, E.L.; Zoia, L. Oxidation of Isoeugenol by Salen Complexes with Bulky Substituents. *Int. J. Mol. Sci*. **2010**, *11*, 912-926.

2. Zoia, L.; Salanti, A.; Orlandi, M.; Tolppa, E.L. Characterization of Waterlogged Wood by NMR and GPC Techniques. *Microchem. J.* **2010**, *95*, 345-352.

3. Salanti, A.; Zoia, L.; Orlandi, M.; Zanini, F.; Elegir, G. Structural Characterization and Antioxidant Activity Evaluation of Lignins from Rice Husk. *J. Agric. Food Chem*. **2010**, *58*, 10049-10055.

4. Salanti, A.; Zoia, L.; Tolppa, E.L.; Orlandi, M. Chromatographic Detection of Lignin-Carbohydrate Complexes by Derivatization in Ionic Liquid. *Biomacromolecules, accepted for publication*.

5. Zoia, L, Tolppa, E.L.; Pirovano, L.; Salanti, A.; Orlandi, M.; Gamberini, M.C.; Baraldi, C.; Freguglia, G. 31P-NMR identification and characterization of beeswax in archaeological ointments. *Archaeometry, accepted for publication.*

COMMUNICATIONS

1. Salanti, A.; Zoia, L.; Tolppa, E.L.; Orlandi, M.. Polysaccharides functionalization in ionic liquids. XXXIV *"A. Corbella" Summer School*, June 22-26, **2009** Gargnano (BS), Italy. (*POSTER*)

2. Salanti, A.; Zoia, L.; Tolppa, E.L.; Orlandi, M.. Characterization of archaeological waterlogged woods by nuclear magnetic resonance and gel permeation chromatography. *ITALIC5 – COST FP0602*, September 1-4, **2009,** Varenna (LC), Italy. (*POSTER*)

3. Elegir, G.; Zanini, F.; Causio, J.; Tolppa, E.L.; Salanti, A.; Orlandi, M.. Lignin characterization and recovery from rice husk. *ITALIC5 – COST FP0602*, September 1-4, **2009**, Varenna (LC), Italy. (*POSTER*)

4. Saliu, F.; Salanti, A.; Pirovano, L.; Orlandi, M. HPLC-APCI-MS analysis of tryglycerides in ancient cosmetics and pharmaceutical formulations. *PRIN2007: colors and balms in antiquity*, December 2-3, **2010**, Sansepolcro (AR), Italy. (*POSTER*)

5. Orlandi, M.; Elegir, G.; Zanini, F.; Salanti, A.; Zoia, L. Chemical characterization of lignin from annual plants. Analytical methods for non-wood raw materials and their products and processes. *COST Action FP0901 workshop*, August 19-21, **2010**, Hamburg, Germany. (*ORAL*)

6. Tolppa, E.L.; Zoia, L.; Salanti, A.; Giachi, G.; Orlandi, M. Characterization of archaeological waterlogged woods by nuclear magnetic resonance. *XXXIX Magnetic Resonance Congress (GIDRM*), September 21-24, **2010**, Palermo, Italy. (*ORAL*)

7. Orlandi, M.; Elegir, G.; Zanini, F.; Salanti, A.; Zoia, L. Chemical characterization of lignin from annual plants. Analytical methods for non-wood raw materials and their products and processes. *COST Action FP0901 workshop*, August 19-21, **2010**, Hamburg, Germany. (*ABSTRACT*)

8. Tolppa, E.L.; Zoia, L.; Salanti, A.; Giachi, G.; Orlandi, M. Characterization of archaeological waterlogged woods by nuclear magnetic resonance. *XXXIX Magnetic Resonance Congress (GIDRM*), September 21-24, **2010**, Palermo, Italy. (*ABSTRACT*)

9. Pirovano, L.; Zoia, L.; Tolppa, E.L.; Orlandi, M.; Salanti, A. Caratterizzazione tramite spettroscopia di risonanza magnetica nucleare di unguenti e balsami antichi. *XII Congresso Nazionale di Chimica dell'Ambiente e dei Beni Culturali*, September 26-30, **2010**, Taormina (ME), Italy. (*ABSTRACT*)

10. Zoia, L.; Tolppa, E.E.; Pirovano, L.; Salanti, A.; Orlandi, M.. ^{31}P-NMR identification and characterization of lipids in archaeological unguents. *PRIN2007: colors and balms in antiquity*, December 2-3, **2010**, Sansepolcro (AR), Italy. (*ABSTRACT*)

11. Zanini, F.; Elegir, G.; Salanti, A.; Orlandi, M. Rice husk: a relevant source for a Lombardy based biorefinery scheme. *J. Biotech. Special Abstracts*, **2010**, *150S*, 507-508.

12. Bertini, F.; Cacciamani, A.; Canetti, M.; Salanti, A.; Elegir, G. Renewable lingo-derivatives for poly(3-hydrxybutyrate) based composites. *EUPOC2011*, 29 May-3 June, **2011**, Gargnano (BS), Italy. (*ABSTRACT*)

13. Salanti, A.: Zoia, L.; Tolppa, E.L.; Orlandi, M. Characterization of archaeological waterlogged woods by nuclear magnetic resonance and gel permeation chromatography. *ITALIC5, Proceedings Book*, September 1-4, **2009**, Varenna (LC), Italy. (*EXTENDED ABSTRACT*)

14. Elegir, G.; Zanini, F.; Causio, J.; Tolppa, E.L.; Salanti, A.; Orlandi, M. Lignin characterization and recovery from rice husk. *ITALIC5, Proceedings Book*, September 1-4, **2009**, Varenna (LC), Italy. (*EXTENDED ABSTRACT*)

15. Orlandi, M.; Elegir, G.; Zanini, F.; Salanti, A.; Tolppa, E.L.; Zoia, L. Rice husk lignin characterization. *Proceedings of 11th European Workshop on Lignocellulosic and Pulp (EWPL 2006)*, August 16-19, **2010**, Hamburg, Germany. (*EXTENDED ABSTRACT*)

16. Elegir, G.; Zanini, F.; Orlandi, M.; Tolppa, E.L.; Salanti, A.; Zoia, L. Integrated scheme for rice husk valorization. *Proceedings of 11° European Workshop on Lignocellulosic and Pulp (EWPL 2006)*, August 16-19, **2010**, Hamburg, Germany. (*EXTENDED ABSTRACT*)

17. Zoia, L.; Orlandi, M.; Tolppa, E.L.; Salanti, A. Dilute acid hydrolysis of cellulose hydrogel prepared from its ionic liquid solution. *ITALIC6, Proceedings book*, September 5-8, **2011**, Viterbo, Italy. (*EXTENDED ABSTRACT*)